

Feet First: Developing instrumented insoles to prove association between weight bearing and foot pain

by
Evan Macdonald

B.A.Sc., The University of British Columbia, 2013

Thesis Submitted in Partial Fulfillment of the
Requirements for the Degree of
Master of Applied Science

in the
School of Mechatronic Systems Engineering
Faculty of Applied Sciences

© Evan Macdonald 2019
SIMON FRASER UNIVERSITY
Fall 2019

Copyright in this work rests with the author. Please ensure that any reproduction or re-use is done in accordance with the relevant national copyright legislation.

Approval

Name: Evan Macdonald

Degree: Master of Applied Science

Title: Feet First: Developing instrumented insoles to prove association between weight bearing and foot pain

Examining Committee:

Chair: Helen Bailey
Lecturer

Carolyn Sparrey
Senior Supervisor
Associate Professor

Edward Park
Supervisor
Professor

Michael Ryan
Supervisor
Adjunct Professor
Biomedical Physiology and Kinesiology

Carlo Menon
Internal Examiner
Professor

Date Defended/Approved: December 6, 2019

Ethics Statement

The author, whose name appears on the title page of this work, has obtained, for the research described in this work, either:

- a. human research ethics approval from the Simon Fraser University Office of Research Ethics

or

- b. advance approval of the animal care protocol from the University Animal Care Committee of Simon Fraser University

or has conducted the research

- c. as a co-investigator, collaborator, or research assistant in a research project approved in advance.

A copy of the approval letter has been filed with the Theses Office of the University Library at the time of submission of this thesis or project.

The original application for approval and letter of approval are filed with the relevant offices. Inquiries may be directed to those authorities.

Simon Fraser University Library
Burnaby, British Columbia, Canada

Update Spring 2016

Abstract

It is commonly thought that more time spent weight bearing at work increases the risk of developing plantar fasciitis, a condition causing pain on the bottom of the foot. This link is not recognized by workers compensation boards because the methods used by researchers to determine workers activities lack sufficient objectivity. This work aimed to solve this problem by developing a prototype of a low-cost smart shoe insole capable of accurately recording workplace activities. This device was implemented in a variety of workplaces to collect information about 34 worker's activities over the course of 3-5 days. An algorithm was developed to classify sitting, standing and walking with an accuracy of 99.3% and analysis showed the time spent standing throughout the workday was correlated with the presence of foot pain. This work lays the foundation for a large population study to provide the objective results needed to change workplace policies.

Keywords: Activity Classification; Machine Learning; Force Sensors; Plantar Fasciitis; Smart Insole; Workplace Injury

Table of Contents

Approval.....	ii
Ethics Statement.....	iii
Abstract.....	iv
Table of Contents.....	v
List of Tables.....	viii
List of Figures.....	ix
List of Acronyms.....	xii
Executive Summary	xiii
Chapter 1. Introduction.....	1
1.1. Background and Motivation.....	1
1.2. Anatomy of the Foot.....	2
1.2.1. Bony Structures.....	4
1.2.2. Musculature and Connective Tissue	5
1.2.3. Arches.....	6
1.3. Biomechanics of Foot Loading.....	7
1.3.1. Foot Loading and the Gait Cycle.....	7
Stance Phase of Gait.....	7
Swing Phase of Gait	8
1.3.2. Measuring Gait and Ambulation.....	8
1.3.3. Shock Absorption and Load Distribution	9
1.3.4. Plantar Tissue Loading	11
1.4. Monitoring Workplace Activities	12
1.4.1. Self-Report Data	12
1.4.2. Accelerometer Based Activity Trackers	13
1.4.3. Insole Based Activity Trackers	14
1.5. Problem and Need:	17
1.6. Hypothesis	18
1.7. Objectives	18
1.8. Scope of the Thesis	19
Chapter 2. Posture Differentiating Insole (PDI) Prototype Development.....	21
2.1. Introduction	21
2.2. Posture Differentiating Insole Design.....	22
2.2.1. Design Criteria	22
2.2.2. Component Selection.....	23
Sensor selection	23
Microcontroller	26
Battery	27
2.2.3. Sensor Locations	27
2.2.4. Final Design - Hardware	31
Instrumented Insole	32

Electronics Case	33
2.2.5. Final Design - Software	34
2.2.6. Synchronization of Data	36
2.2.7. In-lab Performance Evaluation	37
2.3. Results	38
2.3.1. Design verification	38
2.3.2. Participant Feedback on Design	40
2.4. Discussion	41
2.4.1. Hardware Durability	41
2.4.2. Sensor Calibration	43
2.5. Future Work	43
Chapter 3. Classification of Activities from PDI Data	45
3.1. Introduction	45
3.2. Methods	46
3.2.1. Participants	46
3.2.2. Raw Data	48
3.2.3. Data Synchronization	48
3.2.4. Calibration Data	49
3.2.5. Feature Generation	51
3.2.6. Algorithms	52
3.2.7. Classification Accuracy	53
3.2.8. Sensor Reduction	54
3.3. Results	55
3.3.1. Raw data	55
3.3.2. Activity Classification Accuracy	57
3.3.3. Sensor Reduction	59
3.3.4. Activity Specific Sensitivity and Specificity	65
3.3.5. Leave-One-Out Cross-Validation	66
3.3.6. Activity Misclassification	67
3.3.7. Algorithm Resource Intensity	70
3.3.8. Impact of Incorrect Synchronization	70
3.3.9. One Insole vs. Two Insoles	71
3.3.10. Impact of Sampling Frequency	71
3.4. Discussion	72
3.4.1. Impact of Classification Accuracy	74
3.4.2. Are Accelerometers Necessary?	74
3.4.3. Additional Considerations	75
3.5. Future Work	76
Chapter 4. Workplace Postures	78
4.1. Introduction	78
4.2. Methods	79
4.2.1. Participants	79
4.2.2. Data Collection and Analysis	80

4.2.3.	Device Validation	80
4.2.4.	Comparison of PDI Results to Self-report Data	80
4.3.	Results	81
4.3.1.	Participant Demographics	81
4.3.2.	Workplace Activities	82
4.3.3.	Out-of-lab PDI Design Validation	84
4.3.4.	Classification Error	85
4.4.	Discussion	89
4.4.1.	Implication for Research and Policy Decisions	91
4.4.2.	Limitations	92
4.4.3.	Natural Environment Validity	93
4.5.	Future Work	96
Chapter 5.	Effects of Workplace Standing on Plantar Foot Pain.....	97
5.1.	Introduction	97
5.2.	Methods	98
5.2.1.	Activity Classification.....	98
5.2.2.	Pain Measurement	99
5.2.3.	Data analysis.....	99
5.2.4.	Statistical Methods	100
5.3.	Results	100
5.3.1.	Participants	100
5.3.2.	Averaged Days.....	101
5.3.3.	Highest Exposure Day	104
5.4.	Discussion.....	106
5.4.1.	Limitations	107
5.5.	Future Work	108
Chapter 6.	Contributions and Conclusions	110
6.1.	Contributions	110
6.2.	Limitations of the Research.....	111
6.3.	Future Research Directions	111
6.4.	Significance.....	112
References.....		114
Appendix A.	Standard Trial Procedure.....	123
Appendix B.	Insole Fabrication Procedure	129
Appendix C.	PDI Code.....	143
Appendix D.	FADI Form	153
Appendix E.	Participant Questionnaire	155

List of Tables

Table 1 - Comparison of shoe insoles developed for activity classification	15
Table 2 – Comparison of commercially available pressure sensing insoles	16
Table 3 - Results of PDI design verification	39
Table 4 - Maximum FSR value for each location recorded in each participant's calibration data. Maximum values are in bold.....	56
Table 5 - Confusion matrices showing results of both the SVM and MLR algorithms when tested on the test dataset using all sensors	58
Table 6 – Sensitivity and specificity (%) for the SVM algorithm broken down by activity type. Sensors used are per Figure 23.	65
Table 7 - Sensitivity and specificity (%) for the MLR algorithm broken down by activity type. Sensors used are per Figure 25	66
Table 8 - Results of leave-one-out cross-validation (LOOCV). The classification algorithm was trained on all participants except one. Classification accuracy is calculated based on subject's data that was excluded.	67
Table 9 - Results of incorrect synchronization analysis. R offset means data from the right foot was offset by the specified duration. L offset means data from the left foot was offset by the specified duration.....	70
Table 10 - Participant demographics	81
Table 11 – Results of comparison between self-report data and PDI data. All times are in minutes.	86
Table 11 - Results of univariate analysis for an average day showing a comparison of factors between subjects with and without foot pain	102
Table 13 - Results of multivariable logistic regression for the average day with respect to the presence of foot pain.	104
Table 14 - Results of univariate analysis for highest exposure day showing a comparison of factors between subjects with and without foot pain	104
Table 15 - Results of multivariable logistic regression for highest exposure day with respect to the presence of foot pain.	105

List of Figures

Figure 1 - Directional anatomical terms used in reference to the foot.....	3
Figure 2 - Bones and regions of the foot.....	4
Figure 3 - Location and approximate shape of the plantar fascia. Green dots represent attachment points.	5
Figure 4 - Arches of the foot including the medial longitudinal arch (red), lateral longitudinal arch (green) and transverse arch (blue).	6
Figure 5 - Terminology of the phases of the human gait cycle. The cycle is broken into two phases, the stance phase with five positions and the swing phase with three positions. The right leg is the reference leg and is shown in black.	7
Figure 6 - The medial longitudinal arch as a three-bar truss. The top two 'bars' are comprised of the bones of the forefoot, midfoot and hindfoot, the lower 'bar' is the plantar fascia.	10
Figure 7 - The plantar fascia in sitting standing and walking. While sitting (a), the plantar fascia is unstretched and therefore under low tensile load (represented by orange arrows). When force (represented by red arrows) is applied to the foot while standing (b) the plantar fascia experiences a high tensile load to hold the shape of the arch. During the terminal and pre-swing positions of walking (c) the windlass mechanism stretches the plantar fascia over the metatarsal head by dorsiflexing the phalanges. This motion draws the calcaneus towards the forefoot and strengthens the medial longitudinal arch.....	11
Figure 8 - (a) Typical FSR wiring layout, Vin is 3.3V and Vout is connected to an analog pin on the microcontroller. (b) Sample force response curve for the Interlink 402-Short FSR.	25
Figure 9 – Breakdown of the foot into ten anatomical regions per the PRC mask. Region locations depicted on a foot (a), on F-Scan data (b), and with sensor locations overlaid onto the masks (c) (from Merry, 2017)	28
Figure 10 - Developing segmented insole regions roughly corresponding to the PRC mask method. A centerline is drawn based on insole widths at 10% and 66% of insole length measured from the heel (a). Regions are segmented based on percentages of insole length measured from the heel and width(b).....	30
Figure 11 - Segmented insole regions (a), and FSR sensor locations (b)	31
Figure 12 - Photo of a complete PDI insole showing the electronics case, the instrumented insole and the connection cable. The electronics case attaches to the shoelaces and the insole goes inside the participant's shoe.....	31
Figure 13 - A pair of insoles with FSRs and connection wires installed. Wires are all inlaid into the white foam to provide a flat top surface. The black puff foam cover has not yet been added.	32
Figure 14 - Completed assembly of the components inside the electronics case	33
Figure 15 - 3D printed electronics case that attaches to the shoelaces of the user's shoes. Consists of the body (a), the lid (b), and the shoelace clip (c). The	

lid is fastened to the body with screws and the shoelace clip attaches to the bottom of the body (d).	34
Figure 16 - Synchronization method using heel strikes. Red dots represent heel strikes. Data is shifted such that heel strikes on the right foot fall exactly between heel strikes of the left foot.....	37
Figure 17 - Exemplar activity transitions. Time of transition is defined by the red vertical line.....	49
Figure 18 - Data collected with a sensor that has a malfunctioning connection. The line for FSR 7 (pink) should have a smooth curve similar to the other lines, but it instead drops off sharply. This is likely due to a broken wire that intermittently connects when the PDI is loaded or bent in a specific way.	51
Figure 19 – Flow chart showing the process used to train and test the machine learning algorithm.....	53
Figure 20 - Approximate location of FSRs in the PDI insole. Red circles are FSRs and the shape labeled acc is the accelerometer that is located on top of the foot in the electronics case.	54
Figure 21 - Exemplar data from the seven force sensitive resistors in both the left and right shoes of a participant showing sitting, standing and walking	55
Figure 22 - Exemplar data collected from the accelerometer on a participant’s right and left shoe while sitting, standing and walking.....	57
Figure 23 - Results of the backward elimination procedure for the SVM algorithm. A sensor shown in red means that it was included, white or black sensors were digitally removed from the data. The number below the image is the classification accuracy of the SVM algorithm when tested on the test dataset using the sensor configuration depicted above. The confusion matrix below the accuracy displays predicted values on the horizontal axis and true values on the vertical axis.....	61
Figure 24 - Results of the forward selection procedure for the SVM algorithm. A sensor shown in red indicates that it was included, white or black sensors were digitally removed from the data. The number below the image is the classification accuracy of the SVM algorithm when tested on the test dataset using the sensor configuration depicted above. The confusion matrix below the accuracy displays predicted values on the horizontal axis and true values on the vertical axis.....	62
Figure 25 - Results of the backward elimination procedure for the MLR algorithm. A sensor shown in red indicates that it was included, white or black sensors were digitally removed from the data. The number below the image is the classification accuracy of the MLR algorithm when tested on the test dataset using the sensor configuration depicted above. The confusion matrix below the accuracy displays predicted values on the horizontal axis and true values on the vertical axis.....	63
Figure 26 - Results of the forward selection procedure for the MLR algorithm. A sensor shown in red indicates that it was included, white or black sensors were digitally removed from the data. The number below the image is the classification accuracy of the MLR algorithm when tested on the test dataset using the sensor configuration depicted above. The confusion	

matrix below the accuracy displays predicted values on the horizontal axis and true values on the vertical axis.	64
Figure 27 - Activity classification results using the MLR algorithm for SID25.	67
Figure 29 - Activity classification results using the MLR algorithm for SID06	68
Figure 28 - Activity classification results using the SVM algorithm for SID06	68
Figure 31 - Activity classification results using the MLR algorithm for SID09	69
Figure 30 - Activity classification results using the SVM algorithm for SID09	69
Figure 32 - Classification accuracy as a function of decimation. Equivalent sampling frequency shown in parentheses.....	71
Figure 33 - Activity breakdown for each participant averaged over their workweek. Shaded regions represent +/- one standard deviation.....	82
Figure 34 - Plot of the average number of activity changes made throughout the workday for each participant. Participant number is arranged in order from most time spent weight bearing to least time spent weight bearing. The error bars represent the standard deviation in activity changes throughout a participant's workdays.	83
Figure 35 - Bland-Altman plot for standing classification using self-report data and PDI data. All measurements are in minutes. The grey boundary around the mean difference represents the 95% confidence interval of the mean difference value.	87
Figure 36 - Bland-Altman plot for walking classification using self-report data and PDI data. All measurements are in minutes. The grey boundary around the mean difference represents the 95% confidence interval of the mean difference value.	88
Figure 37 - Bland-Altman plot for sitting classification using self-report data and PDI data. All measurements are in minutes. The grey boundary around the mean difference represents the 95% confidence interval of the mean difference value.	89
Figure 38 - Natural environment data recorded from one participant. All 7 FSRs are used in each shoe but no accelerometer is used for this classification. Solutions from the SVM classification algorithm are overlaid on top of the raw FSR signals showing the predicted activity. White is sitting, light grey is standing, and dark grey is walking.	95
Figure 39 - Boxplot including all available data. Each activity is divided into pain and no-pain data and plotted as time spent doing each activity.	101

List of Acronyms

A/P	Anterior / Posterior
BMI	Body Mass Index
FSR	Force Sensitive Resistor
LOOCV	Leave-One-Out Cross Validation
M/L	Medial / Lateral
ML	Machine Learning
MLR	Multinomial Logistic Regression
OSPAQ	Occupational Sitting and Physical Activity Questionnaire
PDI	Posture Differentiating Insole
PF	Plantar Fasciitis
SVM	Support Vector Machine

Executive Summary

Purpose: Plantar fasciitis (PF) is a condition that causes foot pain and sometimes even prevents you from walking. About 2.77 million people per year in the United States report having PF [1]. This costs over \$284 million/yr [2]. The exact cause of PF is still unknown. Research has shown that workers who are on their feet for the majority of the day have an increased risk of foot pain [3]–[5]. However, this work has largely relied on participants self-reporting the amount of time spent standing during the workday. This can lead to large errors as seen in one study where participants misclassified over 3h of activities over 24h [6]. The use of self-report data has produced unreliable results linking PF to common workplace activities [7]. These inconclusive results have made it difficult and highly subjective to judge the merit of workers compensation claims, leading to unreported incidents and a high proportion of rejected claims [8]–[10]. Current technologies capable of objectively measuring workplace activities are either too expensive or too difficult to use. Without improvements in this technology, it is difficult to link foot pain to specific workplace activities.

Research Questions: The questions asked in this study were:

1. Can a low-cost, easy to use, unobtrusive device be made that collects data from a participant in their natural work environment for use in activity classification?
2. Can an algorithm be developed to classify a participant's workplace activities as sitting, standing or walking using the data output from the novel device?
3. Can the device be used in a workplace setting to collect activity data from participants for an extended period of time?
4. How do self-reported activity times compare to the activity times recorded by the device?
5. Is there a relation between the amount of foot pain experienced by a worker and their workplace activities?

Methods: A novel prototype device was designed based on recommendations from existing research and tested in a lab setting to validate functionality. Next, participants both with and without foot pain between the ages of 19-60 with a Body Mass Index (BMI) under 30 were recruited to wear the novel device for a week while at work. A total of 34 participants wore our insoles at work for up to 5 days while they went about their regular

work activities. At the end of each workday participants were asked about their foot pain that day. They were also asked to estimate how much time they spent sitting, standing and walking throughout the day. At one point during the study, each participant was asked to sit, stand and walk a few times in a certain order while being video recorded. This data was used to develop a machine learning algorithm capable of classifying sitting, standing and walking throughout the rest of the participant's work week. The resulting activity data was used to gain insights about workers natural activities in a variety of workplaces and occupations. The relationship between factors related to workplace activities / participant demographics and the presence of foot pain was investigated.

Results: A novel, low-cost instrumented shoe insole called the Posture Differentiating Insole (PDI) was developed using force sensitive resistors (FSRs) and an accelerometer to collect activity data in a workplace setting. This study showed that the PDI can be used in a workplace environment for up to 12 hours per day and up to five days in a row. Participants reported that they mostly forgot they were wearing the insoles indicating that the device was able to record natural activity at work. The machine learning algorithm developed was able to correctly determine the participants activity 99.3% of the time. A few devices experienced malfunctions leading to incomplete data, but the majority worked for the entire study. Data from devices that didn't work correctly was discarded. This left 92 days of data from 29 participants to be analyzed. The time each participant spent sitting, standing and walking each day was determined by the PDI. This data was compared to the times that participant reported at the end of each day. The average time sitting throughout the workday ranged across participants from 34.26% to 95.80% with standard deviations between 0.57% and 20.05%. The average number of activity transitions throughout a participant's workday ranged from 46 to 759. The self-reported data had a classification error of 24%, meaning that participants incorrectly reported an average of 2.3 hours of their workday. Participants usually reported less walking and more sitting and standing than was actually done throughout the day. Comparison of workday activity related factors showed that the total time spent standing throughout the workday is likely to increase the occurrence of foot pain. The time a participant spent doing one activity before switching to a different activity was also investigated. This is something that cannot be measured with self-reported activity times. We found that a

longer time spent standing before changing activities is likely to increase the occurrence of foot pain.

Conclusion: This study has developed a novel device and algorithm capable of objectively classifying workplace activities and shown that the device can be used in a workplace setting to greatly improve on self-reported activity data and provide new analysis methods. This study highlighted multiple factors that are likely to increase the occurrence of foot pain, laying the groundwork for future large population studies.

Interests and Biases: Michael Ryan is a salaried employee of Kintec Footlabs Inc.

Keywords: Plantar Fasciitis, Foot Pain, Self-report Data, Smart Insole, Weight-bearing, Activity Classification, Workplace Injury

Chapter 1.

Introduction

1.1. Background and Motivation

Plantar Fasciitis (PF) is one of the most common causes of chronic foot pain [11], [12]. Over 329,000 people in Canada and 2.79 million people in the United States over the age of 18 suffer from chronic foot pain [1], [13]. It is estimated that approximately 10-24% of the global population will be impacted by foot pain at some point in their lives [14], [15]. Studies have shown that this number rises substantially in individuals subjected to prolonged periods of weight bearing (standing or walking) [3]–[5]. This can be seen in retail workers where 50% have reported foot pain during work [16]. Other occupations where weight bearing is prevalent have reported similar prevalence of foot pain including assembly plant workers (69% [17]), and nurses (55 - 74% [18], [19]). PF has an estimated economic burden in the US of \$284 million per year [2]. However, there is insufficient evidence that prolonged standing is a causal factor for foot pain [7].

PF is often exhibited as pain in the heel or inferior foot and is commonly worst when taking the first few steps after getting out of bed in the morning [14]. This pain has largely been attributed to microtears in the plantar fascia that cause an inflammatory response [2], [11], [12], [14], [20]. The etiology of PF is complex and likely caused by a combination of factors [14]. In approximately 85% of cases the exact etiology is unknown [3]. Tightness of the Achilles tendon [11], and hamstring [21] have been commonly associated with this condition. Other physiological attributes such as arch height, metatarsal pressure, and intrinsic foot muscle tightness have also been associated with PF [3], [12]. Increased BMI is also correlated to the occurrence of PF [4], [22].

While data relating to physiological aspects such as arch height, ankle flexion and BMI is relatively easy to obtain, time spent walking or standing throughout a typical day is much more difficult to accurately measure. Much of the existing research to date has used self-reported workplace activity durations [3], [5], [22]. Research has shown that self-reported measures are not a reliable source of workplace activity durations [6], [23]. The use of self-report data in research regarding risk factors of PF has led to

unreliable results linking PF to common workplace activities [7]. These inconclusive results have made it difficult and highly subjective to judge the merit of workers compensation claims for PF related to workplace exposures. This is evidenced by WorkSafeBC accepting an average of 19 claims per year and rejecting an average of 38 claims per year between 2009 and 2013 [10]. However, these numbers highly underestimate the prevalence of the condition in the workplace as over 80% of workers do not submit claims anticipating that they will be rejected [8], [9]. Each claim accepted cost approximately \$15,000 in lost time [10].

One study investigating factors related to PF did use objective measures of workplace activities including video recordings and step counters [3], however this study only captured snapshots of activity throughout the day, not total activity times. Other studies have used accelerometer-based technologies to categorize activities [24]–[27] but have not been used to investigate PF etiology. In addition, accelerometers are best at distinguishing sitting, standing and walking (common workplace activities) when attached to the user's thigh and waist [28]. This is relatively uncomfortable and difficult to precisely orient, therefore making accelerometers difficult to use in large scale studies. Insole based systems have shown promising results for activity classification [29]; however, at present there are only experimental designs used for academic research [30]–[33] or very expensive commercially available insoles such as the F-scan System (Tekscan Inc., South Boston, MA, USA) which costs approximately \$20,000. There is an immediate need for a low-cost technology capable of accurately determining workplace activities for use in a large-scale study to determine workplace activity factors related to PF.

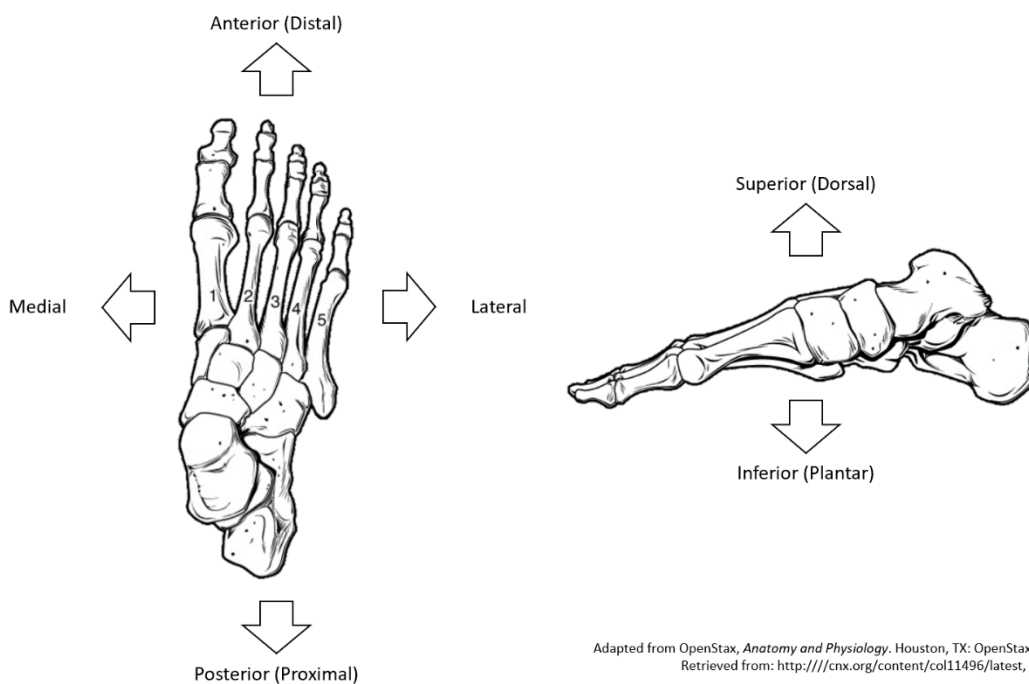
The goal of this thesis is to incorporate previous knowledge about instrumented insole design to develop a useable prototype that can be deployed in a workplace setting. This device will then be used to gather data to train a classification algorithm and begin to investigate correlations between workplace activity data and foot pain, laying the groundwork for population scale research.

1.2. Anatomy of the Foot

To study the forces, loading patterns, and injuries of the foot it is necessary to first understand the basic anatomy of the foot. The following section will give a brief

overview of the foot anatomy including the anatomical terms used throughout this document. The foot is comprised of 26 bones connected with musculature and connective tissue forming three arches. The foot helps to distribute the weight of the body and maintain balance and stability [34].

Specific terms are used to describe anatomical directions, they are as follows (Figure 1). When viewing a foot from the top, the direction towards the front of the foot is the anterior direction, also known as distal, and the direction towards the back of the foot is the posterior direction, also known as proximal. The outside of the foot, furthest away from the other foot, is the lateral direction, and the opposite is the medial direction. When viewing the foot from the side, the top is the superior direction, also known as the dorsal surface, and the bottom is the inferior direction, also known as plantar surface. Toe flexion (downwards) is known as plantarflexion, while toe extension (upwards) is known as dorsiflexion.

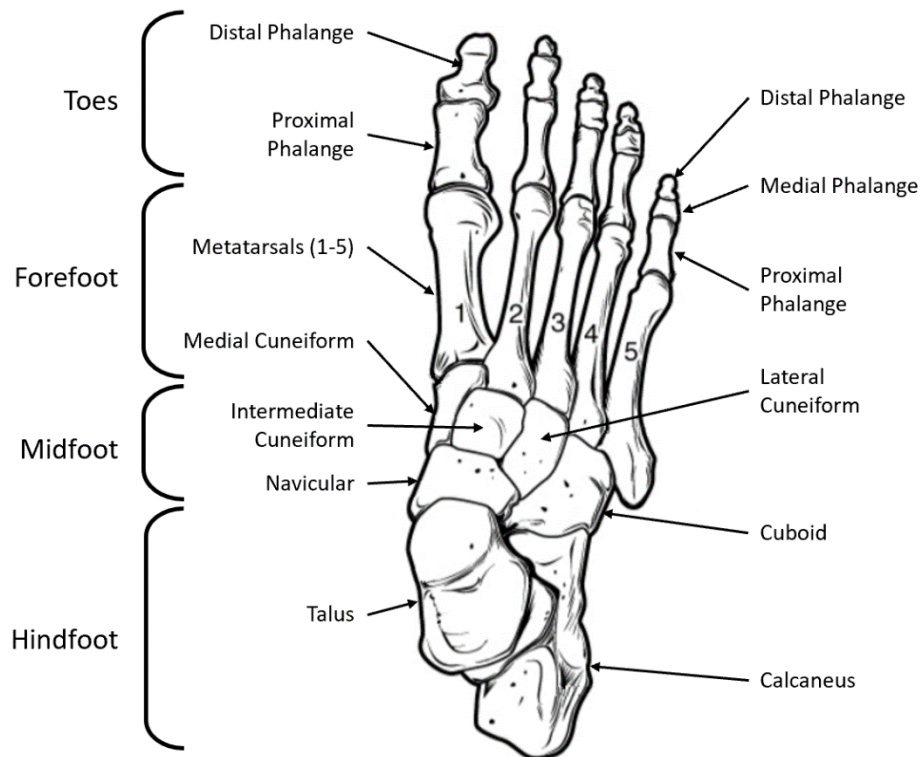


Adapted from OpenStax, *Anatomy and Physiology*. Houston, TX: OpenStax CNX, Retrieved from: <http://cnx.org/content/col11496/latest>, 2013.

Figure 1 - Directional anatomical terms used in reference to the foot

1.2.1. Bony Structures

The bones of the foot are often divided into three sections called the tarsals (talus, calcaneus, cuboid, navicular, and three cuneiform bones), metatarsals (first to fifth metatarsal) and the phalanges (proximal, medial and distal phalanges). The foot can also be divided into three generalized foot regions, the forefoot, midfoot and hindfoot [35]. To provide further clarity, this work has included an additional region, the toes (Figure 2). The bones included in each region are described below.



Adapted from OpenStax, *Anatomy and Physiology*. Houston, TX: OpenStax CNX, Retrieved from: <http://cnx.org/content/col11496/latest>, 2013.

Figure 2 - Bones and regions of the foot

The hindfoot is made up of the talus and the calcaneus. The calcaneus is the furthest posterior bone of the foot. It serves to transmit the majority of the weight of the body to the ground and provides an attachment point for the ligaments from the calf. The talus is located superior to the calcaneus and articulates with the tibia and fibula forming the ankle joint [35].

The midfoot contains the navicular, cuboid, medial cuneiform, intermediate cuneiform and lateral cuneiform. These bones provide an articulating connection

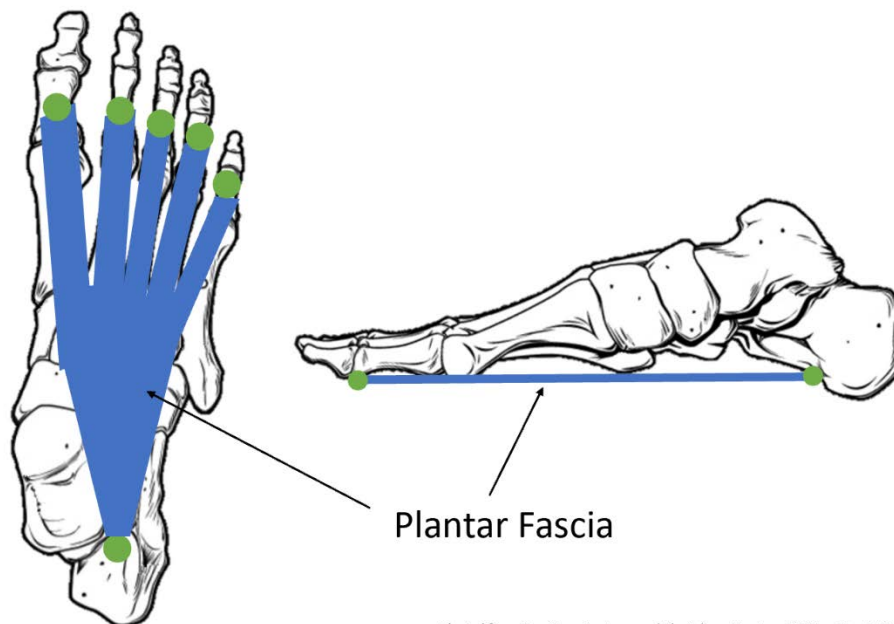
between the calcaneus and talus, and the metatarsals and help make up the medial lateral arch [34].

The forefoot includes the five metatarsal bones. The metatarsal bones are numbered one through five starting at the medial side of the foot.

The toes consist of five proximal phalanges, four medial phalanges and five distal phalanges. The big toe has two phalanges (distal and proximal) while the other toes have three.

1.2.2. Musculature and Connective Tissue

There are many muscles and connective tissues in the foot, most of which are beyond the scope of required knowledge to understand this work. Typically the muscles of the dorsal foot function to extend the toes while the plantar musculature functions to flex the toes [35]. The primary connective tissue on the plantar aspect of the foot is the plantar fascia, sometimes called the plantar aponeurosis (Figure 3). This tissue is very strong and functions to support the longitudinal arches of the foot and absorb forces experienced in activities such as walking, running and jumping [20]. The plantar fascia



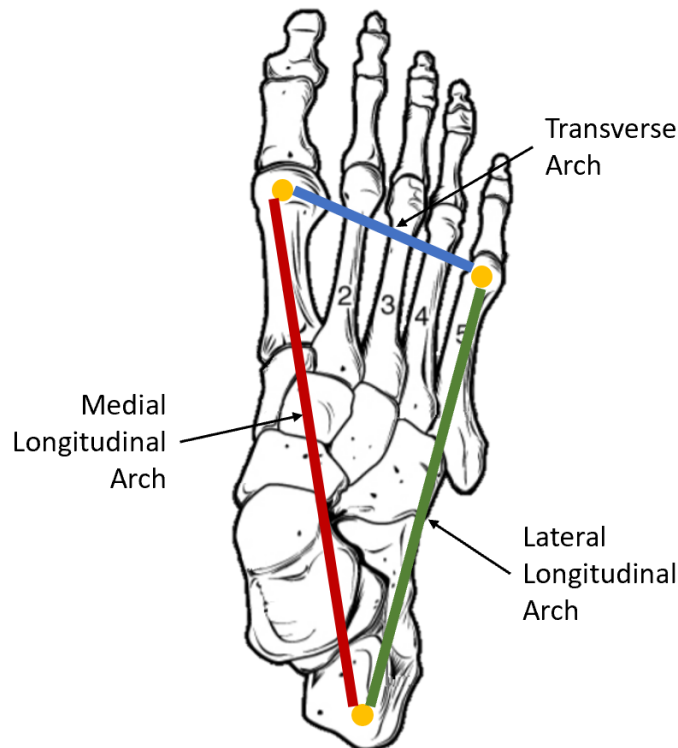
Adapted from OpenStax, *Anatomy and Physiology*. Houston, TX: OpenStax CNX, Retrieved from: <http://cnx.org/content/col11496/latest>, 2013.

Figure 3 - Location and approximate shape of the plantar fascia. Green dots represent attachment points.

originates on the plantar surface of the calcaneus and extends anteriorly splitting into five processes, one attaching to each of the toes. The central tissue is thickest with the medial and lateral tissues becoming thinner as they near the outer edges of the foot [35]. PF typically occurs at the proximal end of the plantar fascia where it connects to the calcaneus.

1.2.3. Arches

There are three arches of the foot, the transverse arch, the medial-longitudinal arch and the lateral-longitudinal arch (Figure 4). The arches are important for absorbing and distributing forces in the foot and maintaining balance. The shape of the arches is formed by strong ligaments including the plantar fascia [34].



Adapted from OpenStax, *Anatomy and Physiology*. Houston, TX: OpenStax CNX, Retrieved from: <http://cnx.org/content/col11496/latest>, 2013.

Figure 4 - Arches of the foot including the medial longitudinal arch (red), lateral longitudinal arch (green) and transverse arch (blue).

The medial longitudinal arch is formed by the calcaneus, talus, navicular, three cuneiform bones and the first three metatarsal bones. This arch is the highest of the longitudinal arches and thus has the most elasticity when loaded [35]. The lateral

longitudinal arch is formed by the calcaneus, cuboid and fourth and fifth metatarsal bones. This arch is shorter than the medial longitudinal arch and is more rigid [35]. The transverse arch is comprised of the posterior metatarsal bones.

1.3. Biomechanics of Foot Loading

1.3.1. Foot Loading and the Gait Cycle

The gait cycle describes the motions that occur in human bipedal walking. It has been shown that the kinematics and kinetics of the gait cycle of adults is very consistent [36]. The widely used terminology of the human gait cycle as developed by Perry et al. begins by dividing gait into two phases, stance and swing [37]. Stance is the first 60% of the gait cycle where the foot is in contact with the ground and swing is the remaining 40% when the foot is moving forward to begin the next step. Each of these phases is further broken down into five and three positions respectively (Figure 5).

Stance Phase of Gait

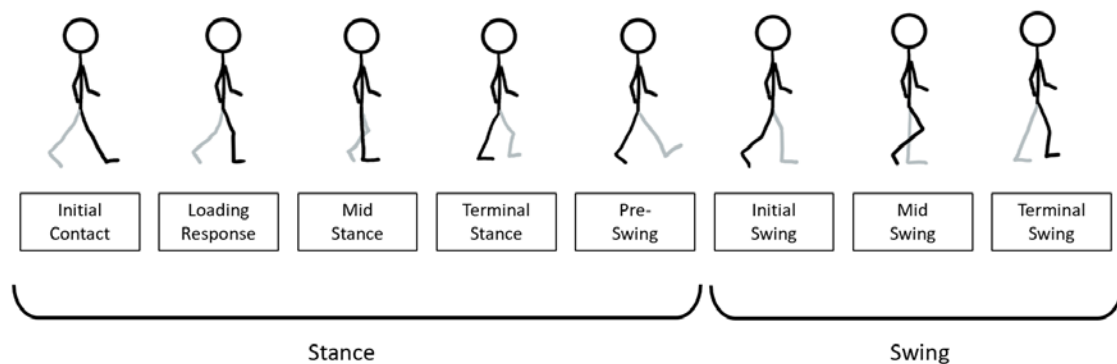


Figure 5 - Terminology of the phases of the human gait cycle. The cycle is broken into two phases, the stance phase with five positions and the swing phase with three positions. The right leg is the reference leg and is shown in black.

- **Initial contact** is when the foot first contacts the ground. In normal gait, the heel is the first contact point, hence the frequently used term 'heel strike'. The Plantar fascia begins to elongate as soon as the heel touches the ground increasing the tensile load in the tissue. Most of the body weight in this stance is transferred through the calcaneus.

- **Loading response** is the period when the weight of the body is transferred to the foot from the opposite foot. Tensile loading in the plantar fascia increases in this position.
- **Mid stance** is marked by the opposite leg moving forward to align with the now loaded leg in the sagittal plane. Tensile loading in the plantar fascia is maintained at a high level in this position and helps the longitudinal arch distribute the weight of the body across the foot (Figure 7-b).
- **Terminal stance** is the period when weight is shifted anteriorly in the foot as the opposite leg moves further forward. As the heel begins to lift off the ground and the toes begin to bend, the plantar fascia is stretched further, causing it to stiffen and increase the height of the medial longitudinal arch (Figure 7-c). Weight is primarily transferred to the ground through the metatarsal heads and the toes in this stance.
- **Pre-swing** is characterized by a marked lifting of the forefoot and toes in preparation for initial contact of the opposite foot. During this phase, the plantar fascia is fully stretched creating a nearly rigid arch capable of efficiently transferring energy from the leg muscles.

Swing Phase of Gait

- **Initial swing** begins once the foot is no longer in contact with the ground and is characterized by the swinging leg being posterior to the opposite leg. The plantar fascia is now unloaded.
- **Mid swing** is the period when the swinging leg is approximately equal to the opposite leg when viewed in the sagittal plane.
- **Terminal swing** is the period when the swinging leg is anterior to the opposite leg before the foot contacts with the ground.

1.3.2. Measuring Gait and Ambulation

When studying gait, steps or other attributes associated with human ambulation it is important to understand the sampling rate required to obtain all necessary information

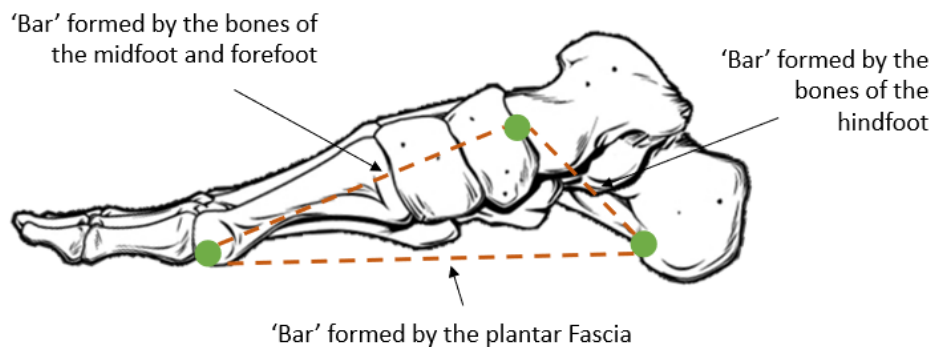
without collecting too much data. Virtually all energy associated with running and walking can be represented by frequencies below 20 Hz [38], [39]. The Nyquist Theorem suggests that when sampling a signal, the sampling rate should be at minimum twice that of the highest frequency component of interest. Therefore, when sampling walking and running, a minimum sampling frequency of 40 Hz is suggested by the Nyquist Theorem. Research devices designed to interpret gait, number of steps or time spent walking and running have a wide range of sampling frequencies including 25Hz [40], 30Hz [33], 50Hz [41], 100Hz [42] and 118Hz [43]. Some research grade devices can have sampling frequencies in excess of 200Hz [44]. This is likely because sampling rate can always be digitally reduced after collection by removing intermediate samples, but cannot be increased, so collecting too much data is preferable to collecting too little data.

1.3.3. Shock Absorption and Load Distribution

There are significant differences in the way people load their feet. Factors such as age, gender, body weight, foot anatomical differences, and shoe type have an impact on the pattern of plantar pressure loading [45]–[48]. As a result, loads are not always distributed across the foot in the same way for each person when standing, walking, running, and during other activities. The following description represents typical behavior.

The arches of the feet play an important role in absorbing the forces associated with activities such as standing, walking and running. While running, the foot can experience forces up to 2.5 times that of standing [34]. Under such loads the tendons, ligaments and muscles in the foot stretch causing the arches to collapse slightly, absorbing energy that would otherwise be transferred to the rest of the body [49]. In the process of unloading the foot, it is beneficial for the arches to return this energy creating a spring like response and reducing energy expenditure [50]. The plantar fascia is one of the connective tissues that absorbs and returns this energy. While acting in this way reduces the likelihood of injury in other locations such as the knees and hips, overloading can have negative effects on the plantar fascia [51].

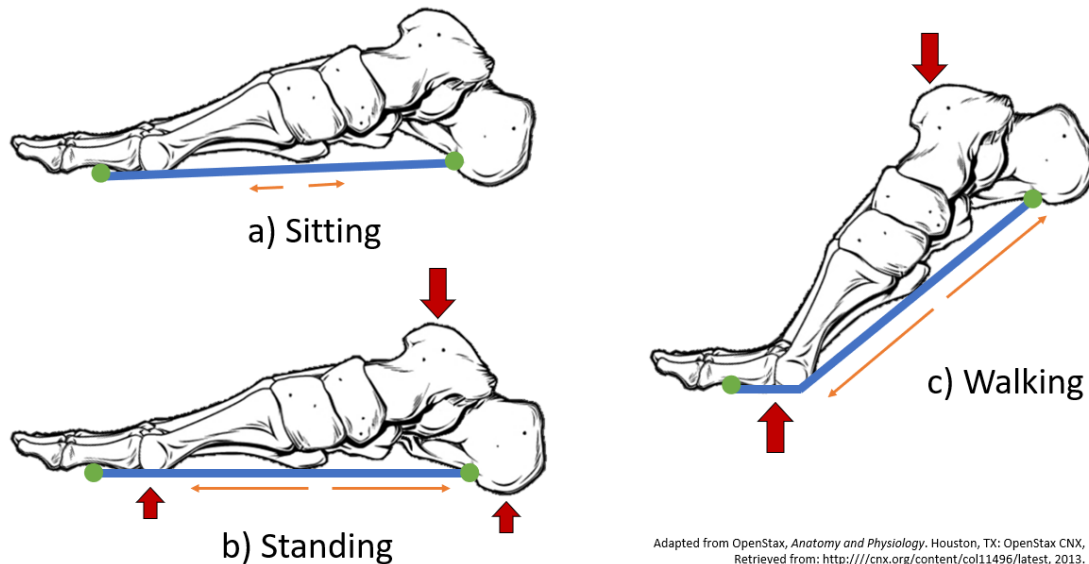
The medial longitudinal arch can be thought of as a three-bar triangular truss with the bony pathway from the calcaneus through to the connection of the plantar fascia at the metatarsal heads / proximal phalanges as the upper two bars and the plantar fascia as the lower 'bar' that prevents the top two bars, from collapsing (Figure 6). The upper two bars of the truss maintain a relatively constant stiffness since they are made up of bony pathways. The properties of the plantar fascia thus control the movement of the three-bar truss under loading.



Adapted from OpenStax, *Anatomy and Physiology*. Houston, TX: OpenStax CNX, Retrieved from: <http://cnx.org/content/col11496/latest>, 2013.

Figure 6 - The medial longitudinal arch as a three-bar truss. The top two 'bars' are comprised of the bones of the forefoot, midfoot and hindfoot, the lower 'bar' is the plantar fascia.

To act both in an elastic manner as a shock absorber, and rigidly to efficiently transfer energy, the foot uses a technique called the windlass mechanism (Figure 7). This mechanism allows the plantar fascia to vary its effective length based on the position of the phalanges [52]. When the phalanges are in a neutral position such as when standing or sitting (Figure 7-a/b) the plantar fascia is relatively elastic allowing the truss of the medial longitudinal arch to act as a spring-damper system cushioning the forces associated with shifting weight and other unexpected motions. When taking a step or otherwise pushing off the toes, the phalanges dorsiflex causing the plantar fascia to stretch over the metatarsal heads known as the windlass mechanism (Figure 7-c). This stretching of the plantar fascia pulls the calcaneus towards the forefoot, heightening and strengthening the truss of the medial longitudinal arch, a function necessary for efficient locomotion [53], [54].



Adapted from OpenStax, *Anatomy and Physiology*. Houston, TX: OpenStax CNX, Retrieved from: <http://cnx.org/content/col11496/latest>, 2013.

Figure 7 - The plantar fascia in sitting standing and walking. While sitting (a), the plantar fascia is unstretched and therefore under low tensile load (represented by orange arrows). When force (represented by red arrows) is applied to the foot while standing (b) the plantar fascia experiences a high tensile load to hold the shape of the arch. During the terminal and pre-swing positions of walking (c) the windlass mechanism stretches the plantar fascia over the metatarsal head by dorsiflexing the phalanges. This motion draws the calcaneus towards the forefoot and strengthens the medial longitudinal arch.

1.3.4. Plantar Tissue Loading

The most likely cause of PF and plantar foot pain is mechanical stress applied to the plantar fascia [51], [55]. The plantar fascia is dynamically loaded when taking a step due to the nature of loading the foot in the stance phase and the release of stress during the swing phase of gait. The plantar fascia is statically loaded to maintain the shape of the arch when standing [12]. This loading is primarily exhibited as axial stress in the plantar tissue.

Cyclical tensile loading of tendons has been shown to help maintain their structural integrity and health [56]. However, too much or too little cyclical loading can have detrimental effects. This could explain why prolonged standing (low cyclical loading) or long periods of time running or walking (high cyclical loading) have been identified as key contributing factors leading to the microtears exhibited in PF [3], [4], [20]. These microtears are often found near the calcaneal attachment of the plantar fascia. Once present, the stress on the remaining tissue is increased, sometimes leading to a cascading effect culminating in the painful heel or plantar aspect of the foot known as plantar fasciitis.

1.4. Monitoring Workplace Activities

1.4.1. Self-Report Data

Research into risk factors of PF typically requires participants to self-report the time spent on their feet throughout the day. However, self-reporting is not an accurate measure of time spent in different activity states, as shown in a recent study where participants incorrectly reported over 3 hours of activity time over a 24 hour period [6]. Importantly, self-reporting also lacks the temporal resolution to track short duration changes in posture which may affect overall plantar tissue loading exposure.

The Occupational Sitting and Physical Activity Questionnaire (OSPAQ) is a survey commonly used to determine a participant's activities throughout a work week [57]. It asks participants to report the time they spent at work and the percent of time spent sitting, standing, walking and doing heavy labour. While it has an excellent test - re-test validity, the comparison to accelerometer measures of actual workplace activities showed deviations of up to 12 hours per week for sedentary activities and 4-5 hours for standing and walking [58]. The OSPAQ is easy to use as it takes only a few minutes to complete and participants only have to fill it out once per week. This has led to widespread adoption in workplace activity reporting. While it is low-cost and easy to use, the OSPAQ does not show the differences in activities between workdays within the week. Additionally, it does not provide the temporal resolution necessary to investigate changes in activity throughout the course of the day.

Self-reported workplace activity has been used in much of the current research investigating correlations between workplace exposure and PF [3]–[5]. These studies have all found moderate correlations between the time spent weight bearing and the presence of PF, however the results have not been widely accepted due to the methodological limitations of self-reported workplace activity data [7]. Werner et al. have shown that a 10% increase in the time spent weight bearing at work is correlated with a 52% increase in the risk of PF. To measure impacts of a 10% change in workday activities a method of classifying such activities with a minimum accuracy of 90% is required.

1.4.2. Accelerometer Based Activity Trackers

Accelerometers have been widely used for activity classification beginning with basic step counters and evolving into sophisticated devices capable of tracking many of the activities of daily living [28]. Accelerometers are extremely low cost and require less power than gyroscopes or magnetometers [59] and thus present an excellent opportunity for wearable devices. There are a number of factors that influence the performance of an accelerometer based activity tracker including sampling rate, the window size used to calculate features, what features are extracted from the data, the location of the sensor on the body, and what algorithm is used to process the data. There are many combinations of these factors that can yield similar results [59], often with accuracies over 95% [60]–[64].

There are a number of commercially available accelerometers including the ActivPAL (PAL Technologies Ltd., Glasgow, Scotland), ActiGraph (ActiGraph LLC., Pensacola, FL, USA), and the MTw Awinda (Xsens, Netherlands). These technologies typically use high accuracy accelerometers that wirelessly connect to a smartphone or computer. Some of these devices come with proprietary algorithms to classify activities and others simply provide the raw signal data that must be interpreted. Since these devices often cost over \$5000, they are typically used in research environments rather than consumer applications. However, there is an abundance of low-cost accelerometer chips with varying sensitivities and accuracies readily available to easily integrate into a wearable device. This has spurred the widespread inclusion of accelerometers in consumer devices such as phones, computers, watches and shoes and the need for activity classification algorithms to make sense of this data.

While accelerometer based devices are typically quite good at counting steps or differentiating sedentary and non-sedentary activities [25], [60] they often fall short when differentiating between sedentary activities such as standing and sitting [59]. This is because sitting and standing produce nearly identical acceleration outputs in most configurations. For example, an accelerometer located on a user's wrist, chest or ankle experiences very little difference between sitting and standing. Though research has shown some success at activity classification using an accelerometer mounted on the chest, a sophisticated multi layer neural network was required [64]. The exception to this is when an accelerometer is placed on the thigh. In this configuration standing and sitting

have different outputs since the thigh is oriented vertically when standing and horizontally when sitting. As a result, the accuracy of thigh mounted accelerometers when classifying sitting, standing and walking is over 95% [27]. This, however, is not a desirable location for long term use as it typically requires the uncomfortable need to glue or strap an accelerometer to one's thigh.

Ultimately, while accelerometers are low-cost, readily available, widely used, low power, and easy to integrate into wearable devices they are not optimal for differentiation of passive postures (sitting/standing), a critical ability when investigating foot pain conditions.

1.4.3. Insole Based Activity Trackers

The patterns of force application to one's feet is drastically different for sitting, standing and walking. When sitting, there is little force applied to the feet. When standing there is an increase in force, and it is applied steadily. When walking, there are high forces applied to the feet but in a repetitive loaded / unloaded pattern. These distinct differences provide an excellent opportunity to place force sensors in a shoe insole to differentiate activities. This approach has the ability to provide a comfortable, non-intrusive, easy to use solution to the challenges present with other types of activity trackers. For such a device to be used in population-based foot pain research, it must have the following attributes:

- 1. Low-cost:** The device must be able to be used in large scale studies involving upwards of 100 participants. Thus, the device must be reasonably priced (<\$200) so that many devices can be purchased.
- 2. Deployable:** The device must be able to function outside of the lab environment and without expert supervision.
- 3. Non-invasive:** The device will be worn for long periods of time so must not inhibit the daily activities of the user in any way. Large, or uncomfortable devices would not be acceptable.
- 4. Easy to use:** With such a large-scale study, the device must be easy for the user or researcher to set up and maintain. This means it should not require

calibration or frequent upkeep and the battery should last for at least 12 hours to avoid needing to charge the battery throughout the workday.

- 5. Accurately track activities:** Whatever design is used, it must be able to accurately track sitting, standing and walking in a natural environment in a range of shoe styles.

Several studies have shown the feasibility of placing sensors in shoe insoles for use in a wide variety of applications including gait analysis, pressure distribution mapping and ground contact kinetics [43], [65]–[69]. In addition, there are insoles that have been developed to classify activities (see Table 1). While these insoles have shown promising results with accuracies up to 99%, all were tested on less than ten participants in a lab setting only.

Table 1 - Comparison of shoe insoles developed for activity classification

	Hegde et al. [30] 'SmartStep'	Chen et al. [70]	Kawsar et al. [71]
Sensors used	Two circular FSRs, one rectangular FSR and one 3-axis accelerometer	Four round FSRs	Eight pressure sensors, accelerometer and gyroscope used from smartphone
Sampling frequency	25-75 Hz	100 Hz	37 Hz
Calibration required?	Unknown	Yes	Unknown
Data processing method	Multinomial logistic regression	Decision tree and linear discriminant analysis	Decision trees with majority vote
Activities classified	Lie down, sit, stand, walk, cycle	sitting, standing, level walking, obstacle clearance, stair ascent, and stair descent	Sitting, standing, walking
Accuracy	98.3%	98.4%	99%
Validation method	Three healthy adult participants. In-lab validation only.	Five able bodied subjects and one amputee subject. In-lab validation only.	One subject in a lab setting.

Sensor location is a critical aspect when designing smart insoles. While Sazonov et al. did optimize the number and location of sensors used for activity classification, they began with only 5 sensors placed in anatomically significant locations [29]. The locations chosen were the heel, the first, third and fifth metatarsal heads, and under the big toe. This eliminated many locations that may be significant for activity classification such as the medial and lateral arch. Merry et al. began with a much larger set of potential locations systematically covering the entire insole to identify a list of most relevant locations for activity classification [72]. The research presented in this thesis builds on the findings from the work done by Merry et al.

There are commercially available insoles with the ability to measure plantar pressure. A summary of some of the more common insoles is found in Table 2. These devices have varying degrees of accuracy, resolution, and price. There is no one device that is widely accepted in research. Additionally, devices intended for consumer applications are being developed but have not yet been widely adopted and are primarily focused on sports analytics, not activity classification.

Table 2 – Comparison of commercially available pressure sensing insoles

Company	Tekscan	Novel	Moticon	Noraxon
Model	F-Scan	Pedar	Science	Medilogic
Number of sensors	954	256	16 Pressure sensors + accelerometer	240 Pressure sensors
Type of sensor	Resistive	Capacitive	Capacitive	Resistive
Approx. Price (CAD)	\$23,000 (w/ software)	\$40,000 (w/ software)	\$3,000 (w/ software)	\$17,500 (w/ software)
Sampling frequency	Up to 100 Hz	Up to 235 Hz	Up to 100 Hz	Up to 300 Hz
Data Processing	Wireless or wired communication to a computer. Limited onboard storage	Wireless or wired communication to a computer. Limited onboard storage	Wireless communication to a computer. Up to 16h onboard storage of basic data	Wireless or wired communication to a computer. Limited onboard storage

In summary, commercially available insoles are primarily intended for in-lab research applications as evidenced by their high price, large form factor, and need for pairing to a computer. The Moticon Science insole could be used for such research, but the data recorded from it would have to be further processed to classify sitting, standing and walking and the cost is still prohibitively expensive for a large-scale study. The insoles developed by Hegde, Chen and Kawsar are very close to what is required for this research; however, the locations of sensors have not been optimized for activity classification, appear to require calibration, and most importantly none have been tested in real-world scenarios. Additionally, none are commercially available so any research using such devices would require either partnership or developing a similar device.

1.5. Problem and Need:

The overarching problem driving this research is that while correlations have been shown between load bearing and foot pain, causation has not been established. This is because not all people who are on their feet for long periods of time throughout the day get foot pain. The causes of foot pain need to be more clearly defined. I hypothesize that the relationship between workplace activities and foot pain can be more clearly defined with a better understanding of the variations in foot loading between individuals in the same work environment and across work environments. To answer this question, we need a method of objectively determining the duration and variation of postures people are doing at any time throughout the workday (walking, sitting standing etc.).

The problem encountered when attempting to identify people's activities throughout the day is that existing technologies and methods used to do so are either inaccurate (self-reporting), invasive (video recording), uncomfortable (thigh worn accelerometer), or prohibitively expensive (lab-grade instrumented insoles). There is a need for a non-invasive, comfortable, low-cost method of accurately identifying people's activities throughout the day. This will lead to a much clearer understanding of what people are doing throughout the day, ultimately helping to clarify the factors that cause foot pain.

1.6. Hypothesis

The overarching hypothesis investigated in this work is that a device that improves accuracy and resolution of measuring workplace activities will enhance the ability to identify specific workplace activities that are causes of PF.

The following specific hypotheses are tested throughout the chapters of this thesis. All relate to the problem and need discussed in Section 1.5.

1. A low-cost unobtrusive device can be made that collects data from a participant in their natural work environment for use in activity classification.
2. An algorithm can be developed to classify a participant's activities as sitting, standing or walking to greater than 95% accuracy using the data collected from the novel device.
3. The PDI can be used to unobtrusively and accurately gather activity data about participants in their natural workplace environments and improve on self-reported activity durations.
4. Specific aspects of workplace activities will be correlated to the presence or absence of plantar foot pain. Particularly the amount of time spent weight bearing throughout the workday and how long workers stand still before unloading their feet.

1.7. Objectives

To address the overarching and specific hypotheses, several objectives were defined for this thesis:

1. Design a prototype device for activity monitoring in the workplace and investigate the feasibility of using this prototype device for an extended duration in a workplace setting.
2. Develop an optimized machine learning algorithm and sensor combination that produces a high degree of activity classification accuracy while identifying redundant sensors.
3. Conduct an out-of-lab study using the prototype device to show its feasibility of use in a workplace setting and collect activity data from participants in a variety of workplaces to compare their self-reported activity data with data collected by the device.

4. Investigate correlations between foot pain and specific workplace activities when the activities are measured objectively using the PDI to lay the groundwork for larger population studies including symptomatic and control groups.

1.8. Scope of the Thesis

Chapter 1 presents background information relevant to this research.

A novel technology to record data from participants in their natural work environment is detailed in **Chapter 2** by completing the following steps: **1.** Reviewing existing research to determine the feasibility and practicality of using existing devices. **2.** Using recommendations from this research to determine the type and specific locations of sensors on the body of the participant. **3.** Designing a device utilizing these sensors and locations. **4.** Testing the device five participants in the lab and one participant wearing the device for up to a week in their natural work environment. The device developed in this chapter is designed to test feasibility for use in a population study and therefore the design has not been optimized and it is not fully deployable, but rather operated and repaired by a researcher.

Activity classification accuracy of the novel device is described in **Chapter 3** by completing the following steps: **1.** Gathering data from participants wearing the device while completing a sequence of specified activities for approximately 20 minutes while simultaneously recording video footage to determine the participants actual activity state. **2.** Designing a machine learning algorithm to output activity state (sitting, standing, walking) based on input from seven FSRs on the insole of a participant's shoe and an accelerometer. **3.** Using 70% of the data to train and cross validate the parameters of the machine learning algorithm. **4.** Using the remaining 30% of the data to compare the output classifications from the trained algorithm with the video analysis to determine the classification accuracy of the device and algorithm. The limited number of participants means this algorithm may not be entirely able to generalize to an entire population and while activity classification was defined to be robust to different shoes, floor materials and seat heights, these variables were not specifically controlled.

An out-of-lab trial using the novel device is described in **Chapter 4** by completing the following: **1.** Collecting activity data from participants over the course of a typical work week using the novel device. **2.** At the end of each day asking participants to self-

report the amount of time spent sitting, standing and walking throughout the day. **3.** Using the data collected by the novel device to gain insights about workers natural activities in a variety of workplaces and occupations. **4.** Comparing the activity durations recorded by each method to determine the accuracy of self-report data. The novel device was hand assembled and therefore has limitations with regard to durability. This resulted in some connections breaking and some data being unusable. In addition, the classification algorithm may have limitations in a natural environment that cannot be verified since each workday was not video recorded or otherwise verified.

Finally, in **Chapter 5** the relationship between specific workplace activities and the presence of foot pain was investigated by completing the following: **1.** Collecting activity data from 34 participants over the course of a typical workweek using the novel device. **2.** At the end of each day asking participants to self-report their foot pain using the foot and ankle disability index. **3.** Comparing reported foot pain to participant's activities to investigate the correlation between the occurrence of foot pain and factors including: **a.** The amount of time workers spend weight bearing throughout their workday. **b.** How many times workers switch activities throughout their workday. **c.** How long workers stand still before unloading their feet. This study is limited by only using data from a limited cohort of participants who only experienced mild pain.

Chapter 6 provides conclusions and highlights contributions of this research. Future research directions are proposed.

Chapter 2.

Posture Differentiating Insole (PDI) Prototype Development

2.1. Introduction

There are many fitness tracking devices currently available that count the number of steps taken in a day. Such devices are often low-cost (under \$200) and have step count accuracies ranging from 79.8% to 99.1% [73]. However, because these devices are usually accelerometer-based they typically cannot accurately differentiate passive activities (e.g. lying down, sitting, or standing). These different passive activities can have a very different impact on one's feet.

Devices that measure plantar pressure such as the F-scan System (Tekscan Inc., South Boston, MA, USA) can be used to differentiate activities, however they are bulky to wear and prohibitively expensive to use in a large-scale study or to deploy outside of the lab. However, such devices have been used to demonstrate that it is possible to accurately differentiate sitting, standing and walking with a limited number of sensors [72]. Additionally, insoles have been made using low-cost sensors, but have only been validated in controlled lab environments on one, three, nine or nineteen participants for a maximum of 4 hours [29], [30], [40], [74], [75]. None of these systems have been validated in a workplace environment for an extended period of time and only one of these studies allowed participants to use their own shoes [30].

Accelerometer based devices such as the activPAL use thigh-mounted accelerometers to track sitting, standing and walking [76]. While these devices are accurate, they are uncomfortable to wear and must be applied to the correct location on the body every day. This is inconvenient for the user and can result in misplacement of the device.

While there are commercially available devices capable of human activity recognition, they either lack the ability to differentiate sitting from standing, are too expensive to deploy on a large scale, or are uncomfortable or inconvenient to use [77], [26]. Without improvements in technology, it is extremely difficult to link PF to work-

related activities. A systematic review commissioned by WorkSafeBC to investigate the causes of PF found that there was insufficient evidence to link workplace weight bearing activities with PF [7], [10]. This study cited a lack of accurate objective measurement of workplace activity and foot loading exposure as the primary factor leading to their decision. The Posture Differentiating Insole (PDI) is an instrumented shoe insole that has been designed to address this need for continuous objective activity measurement in the workplace.

The objectives of this work were 1) to design a prototype device for activity monitoring in the workplace and 2) investigate the feasibility of using this prototype device for an extended duration in a workplace setting, particularly with regard to durability and user experience.

2.2. Posture Differentiating Insole Design

The design process used for this chapter followed the subsequent steps. 1) define the design criteria that must be met, 2) identify components that meet the criteria, 3) fabricate a prototype device, 4) test the prototype's performance in the lab to ensure it is ready for out-of-lab experimentation. The intention of this work was not to precisely optimize a final design, it was to deliver a functional prototype within the project timeline and budget capable of collecting the data required for analysis in the subsequent chapters.

2.2.1. Design Criteria

The general design requirements for the PDI are that it must be an easily fabricated, low-cost device that can be used in large population studies, is unobtrusive and easy to use, effective in a workplace setting, and objectively and accurately measures activities over an extended time period. The specific criteria are elaborated on below. The device developed in this chapter is not required to be an optimized product that meets these requirements in the best way possible. It is simply required to be a highly functioning prototype that at a minimum fulfills all the requirements listed below. This device will be used to determine the feasibility and future direction of a potential product but does not attempt to optimize the design.

1. **Easily fabricated:** The device must be able to be produced in the NeuroSpine Lab at SFU with only available resources (soldering iron, basic hand tools, 3D printer and laser cutter) in under two days by a graduate student.
2. **Low-cost:** The device must not cost more than \$150 per insole, and where possible re-use expensive components.
3. **Able to be used in large-scale studies:** The fabrication process must be repeatable and enable production of many units in a short timeframe.
4. **Unobtrusive:** The device must not interfere with the normal workday activities of participants or be uncomfortable to wear / use.
5. **Effective in a workplace setting:** Participants must be able to wear the device in their workplace without it falling off, breaking, or invading their privacy or workplace regulations.
6. **Objectively and accurately measure activity:** The device must be able to measure the time a participant spends sitting, standing and walking to at least 95% accuracy using objective measures.
7. **Measure activities for an extended period of time:** The device must be able to function for at least 12 hours without requiring any interaction since many work shifts, especially in the healthcare industry are at least this long and data will be captured and reported at the end of a shift.

2.2.2. Component Selection

Sensor selection

To meet the design criteria of objectively and accurately measuring common workplace activities, sensors were used to record information about the movements of participants. Sensors were selected based primarily on previously successful work involving instrumented insoles and accelerometer-based activity trackers [6], [29], [30], [70], [78], [79].

In-shoe Sensors

With the understanding that activities can be accurately differentiated using features derived from plantar pressure measurements, a sensor capable of measuring either force or pressure was sought out. The options found in existing research included capacitive [80], piezoelectric [66], resistive [29], [30], [41], [43], [65], [70], [74], [75], and optical force sensors [81] in addition to pneumatic pressure sensing elements [68]. Custom sensor arrays designed for specific purposes were also found in existing research [42], [67], [69], [71].

An off-the-shelf sensor was desirable for this research based on the time available to develop the technology and the ease of manufacturing. Because of these reasons, creating custom sensors was ruled out. Other sensors including optical and piezoelectric force sensors were ruled out due to their high cost (over \$20 per sensor) or difficulty of procurement. Using such a sensor would be detrimental to the cost and fabrication time of the insoles. The pneumatic sensors found were over 5mm thick and would therefore detract from the comfort and wearability of an insole designed to incorporate them. After eliminating these sensors, capacitive and resistive force sensors were left as the top choices. The Interlink 402-Short FSR was selected for use in the PDI primarily based on its low cost (\$5.81 CAD / sensor), availability in large quantities, and confidence in its performance based on use in many previous studies involving an instrumented shoe insole [33], [41], [43], [66], [75].

The Interlink 402-Short FSR (Interlink Electronics, CA) has a 1 cm² actuation area with a stand-off resistance of >10 M Ω , a minimum actuation force of 0.2N, a force sensitivity range of 0.2 - 20N, a saturation pressure of 103 N/cm², a thickness of 0.55mm and a part-to-part force repeatability of \pm 6%.

The actuation area of an FSR sensor impacts the precision of the location at which it measures force. In addition, a smaller actuation area allows more sensors to fit onto an insole. The 402-short FSR with an actuation area of 1 cm² was chosen as it was the size used successfully in prior work [41], [43], [66], [75]. The short version of the Interlink 402 FSR was chosen to minimize the overall form factor of the FSR making fabrication easier. A high standoff resistance helps reduce unwanted noise in the signal when no load is applied to the FSR.

Maximum pressure observed in young and old adults varies between different regions of the foot from a maximum of 4.6 %BW/cm² in the heel to a minimum of 0.9 %BW/cm² in the lateral midfoot [48]. Assuming a maximum participant's body weight is 100kg, the maximum pressure applied in the heel of the foot would be approximately 45 N/cm². Therefore, with a force sensitivity range of 0.2 – 20N across a 1 cm² sensor, a participant weighing 100kg will likely produce a maximum force that exceeds the sensitivity range; however, it will still be less than half of the saturation force meaning the sensor will not reach its maximum. A participant would have to weigh 228 kg to exceed the saturation pressure of 103 N/cm². Research comparing five commercially available FSRs showed that the Interlink 402 had the best repeatability in dynamic response scenarios [82], a factor that is critically important when classifying activities.

An FSR's resistance changes with the applied force. To ensure V_{out} was proportional to the resistance of the FSR, each FSR was wired with a 1 k Ω resistor as a voltage divider with V_{in} as 3.3V, and V_{out} representing the output signal from the FSR (Figure 8-a).

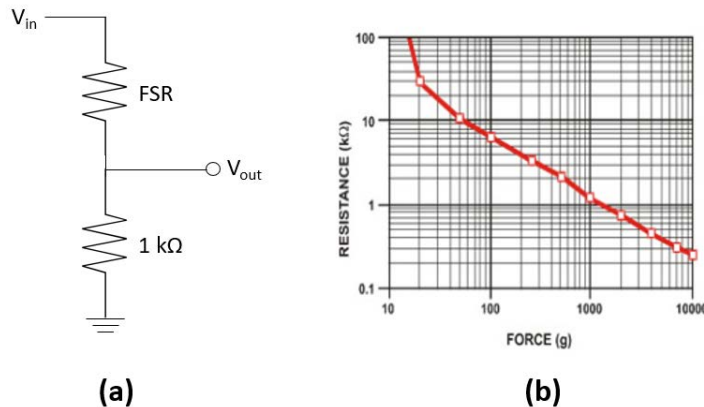


Figure 8 - (a) Typical FSR wiring layout, V_{in} is 3.3V and V_{out} is connected to an analog pin on the microcontroller. (b) Sample force response curve for the Interlink 402-Short FSR.

The force response curve of the Interlink 402 follows approximately an inverse power-law relationship with resistance decreasing as force increases (Figure 8-b). The exact relationship between force and resistance was not determined because it was not required for the method used to classify activities. The normalized relative change in loading has been shown to be sufficient for classifying activities (Chapter 3).

Inertial Measurement Sensor

There have been multiple studies using IMU based devices to successfully classify common activities[6], [78], [79], [83]. Based on this success a 3-axis accelerometer was added into the PDI design. It was anticipated that the FSRs would be capable of accurately determining workplace activities without additional sensors; however, adding an accelerometer into the design allowed for evaluation to prove this hypothesis.

All accelerations experienced at the ankles while ambulating at a pace of 1 m/s or slower is contained within $\pm 6g$, and 96% of the acceleration of the ankles is contained within $\pm 6g$ when ambulating at a rate of 4 m/s [84]. Because of this, a readily available, low-cost accelerometer with a measurement range of $\pm 8g$ (MMA8451 3-axis accelerometer (Adafruit, NY)) was selected to encompass the expected range of accelerations experienced in normal walking at approximately 1.5 m/s. This accelerometer was purchased pre-connected to a breakout board to enable easy assembly to the microcontroller.

Microcontroller

A microcontroller was required to collect data from the FSRs and accelerometer at a consistent sampling rate and write the collected data to a microSD card for later analysis. The requirements of this microcontroller are that it has a small form factor, low cost, and ideally a build in microSD card port. Because of prior familiarity with the Arduino environment, an Arduino Uno was initially used to prototype this device. However, the Arduino Uno has a form factor that is much larger than is desired for this application (5.3cm x 6.8cm) and therefore alternate microcontrollers were investigated. The Teensy 3.6 was chosen based on its small form factor (1.8cm x 6.1cm), presence of a microSD card port, and low cost (\$29.25 USD). In addition, the Teensy is compatible with the Arduino environment and has many pre-developed libraries and resources enabling rapid prototype development. It also contains a built-in real-time-clock chip enabling the current date and time to be stored at all times on the device. To capture and record data each day without requiring Bluetooth or other wireless communication, data was stored on a 16GB microSD card. A typical day of data from one insole was approximately 80 MB so multiple days of data could be recorded without the need to clear the microSD card.

Battery

The PDI is required to last for at least 12 hours of continuous data recording. Once the selected components were assembled and the code was developed to run the device the battery life was calculated by testing the current draw of the device under normal operating conditions. The PDI used 76.1 mA at 3.7V, resulting in a power consumption of 282 mW. The battery capacity required to last for 12 hours under normal operating conditions is $76.1 \text{ mA} \times 12\text{h} = 913 \text{ mAh}$. Therefore, a readily available standardized battery capacity of 1200 mAh (LP503562 3.7V 1200 mAh li-ion battery (Shenzhen PKCell Battery, China)) was selected enabling the PDI to operate for over 15 hours. A coin cell battery (CR1220) was added to the device to continually power the real-time-clock chip built into the Teensy 3.6. This allowed the device to keep track of time when the main battery died or was disconnected for charging. This was important as the current time was used to generate a unique filename each time the device was turned on.

2.2.3. Sensor Locations

The locations of the FSRs can affect the accuracy of the activity classification and the number of sensors needed for accurate classification. Locations were largely guided by findings from Merry et al. exploring variations in plantar biomechanics for different postures [72], [85]. Using the F-Scan, locations where loading patterns were most distinct between sitting, standing and walking were identified [72].

In this research, a modified version of the PRC mask (Novel GmbH, Munich, Germany) was used to subdivide the foot into ten anatomical regions: hallux (HA), second toe (T2), third to fifth toes (T35), medial forefoot (MFF), central forefoot (CFF), lateral forefoot (LFF), medial midfoot (MM), lateral midfoot (LM), medial heel (MH), and lateral heel (LH) (Figure 9-a). This method of subdividing the foot has been used in previous plantar pressure research and provides equal or better detail than other masking methods [86]–[88]. Potential sensor locations were determined and placed on the sensor mask (Figure 9-c). Merry concluded that the top ten sensor locations in rank order were sensor 15, 18, 8, 9, 12, 17, 20, 10, 11, and 16. However Merry showed that classification accuracy for sitting, standing and walking only falls below 95% for all algorithms tested when 3 or fewer sensors were used. Based on these findings and the

requirement of a minimum of 95% accuracy, 4 sensors placed at locations 15, 18, 8 and 9 (Figure 9-c) would meet the minimum requirement. However, since the sensors used by Merry were simulated by taking 5 elements from an F-Scan dataset, it was unknown if actual FSRs would provide identical outputs at each location. Since it was possible to digitally remove sensors after the data was collected, it was decided that having more sensors in this initial prototype was preferred. This gave a margin of error to ensure that sufficient classification accuracy was attained.

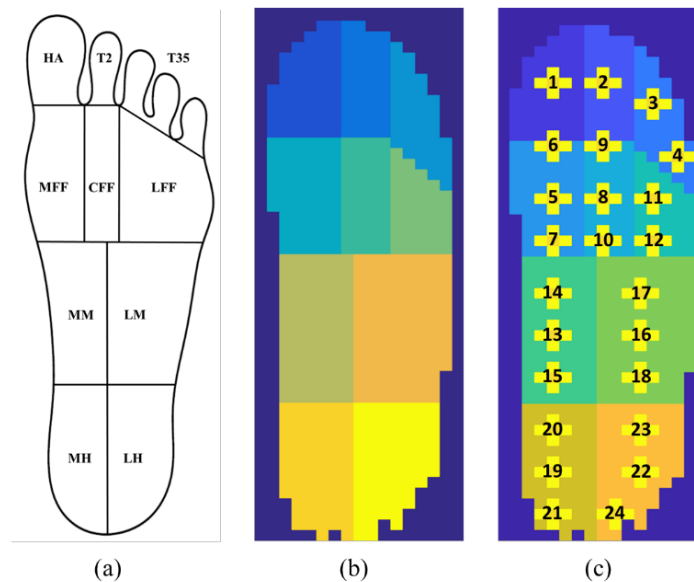


Figure 9 – Breakdown of the foot into ten anatomical regions per the PRC mask. Region locations depicted on a foot (a), on F-Scan data (b), and with sensor locations overlaid onto the masks (c) (from Merry, 2017)

The top 5 sensors (15, 18, 8, 9, 12 in Figure 9-c) were used in the PDI design. In addition to the top 5 locations, a sensor placed between locations 19 and 20 was added to gather data from the MH region that other research studies have utilized in the past [29], [32], [66], and a sensor at location 11 was added to better represent the LFF region.

The PRC mask is designed to reference foot anatomical features. The masking method used in this work was therefore is a version of the PRC mask modified to reference insole geometry since only the participant's shoe size was known ahead of time, not their specific foot shape. A table of insole dimensions for shoe sizes ranging from women's size 4-12 and men's size 6-14 was developed by measuring insoles from

four different sizes of Nike running shoes (sizes W6, W8, M9, and M12) and interpolating or extrapolating each dimension to subsequent shoe sizes. This resulted in a consistent design across all shoe sizes. The PRC mask references foot geometry beginning with a line drawn from the center of the heel to the center of the second toe. Since the end of the second toe cannot be located using insole geometry alone, the following method was developed to determine a consistent centerline across insole geometries. The width of the insole was measured at 10% of insole length and 66% of insole length measured from the heel. The centerline was then drawn from the middle of the 10% of insole length line through a point on the 66% of insole length line that is 40% of the width away from the medial side of the insole (Figure 10-a).

Next, lines were drawn in the medial / lateral (M/L) direction at 27% (green), 55% (red) and 80% (blue) of insole length to divide the heel, midfoot, forefoot and toes (Figure 10-b). These dimensions correspond exactly to lines used in the PRC mask method, only referenced from the heel end of the insole instead of the toe of the foot [87]. A diagonal line (purple) from 68% of insole length connects to the 80% line (blue) forming the boundary between the LFF and toes 3-5. This line was not described in any known description of the PRC mask method and therefore was determined by averaging its location in three of the masks used in Merry's work [72]. The exact placement of this line is not critical as it was not referenced for sensor placement. The MFF and LFF were divided in the M/L direction at 30% (orange) and 45% (yellow) of insole width respectively as determined by the PRC mask method. The medial and lateral midfoot and heel were divided in the M/L direction by the centerline. Since no sensors were placed in the toe area, the hallux and toes 2-5 were not divided into regions. The final result has eight regions: the toes (T15), medial forefoot (MFF), central forefoot (CFF), lateral forefoot (LFF), medial midfoot (MM), lateral midfoot (LM), medial heel (MH), and lateral heel (LH) (Figure 11-a).

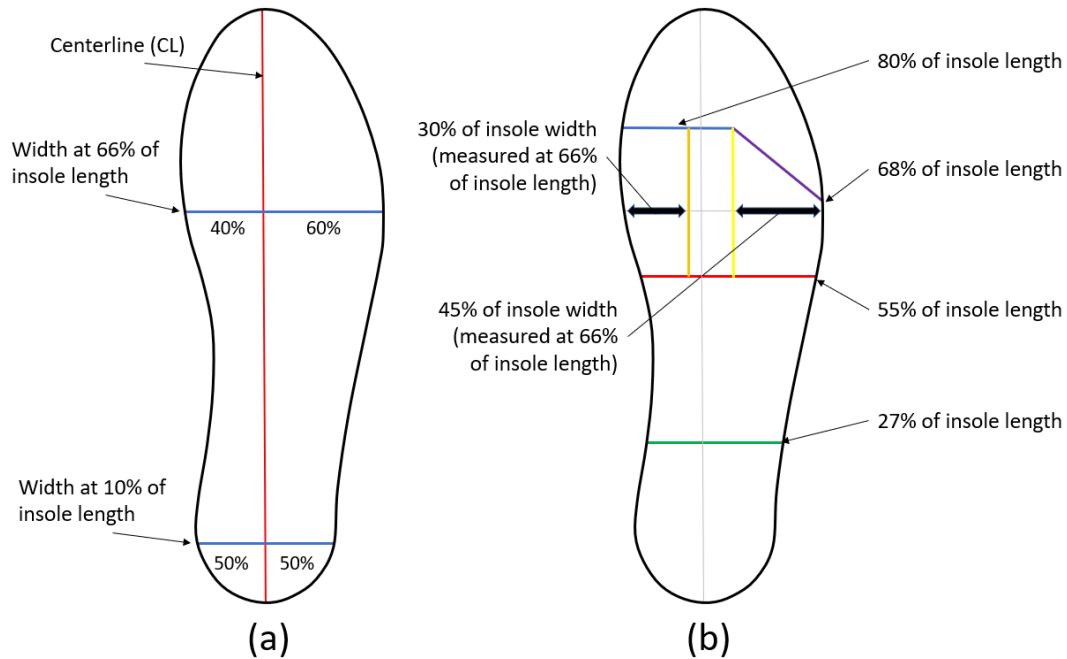


Figure 10 - Developing segmented insole regions roughly corresponding to the PRC mask method. A centerline is drawn based on insole widths at 10% and 66% of insole length measured from the heel (a). Regions are segmented based on percentages of insole length measured from the heel and width(b)

The placement of the FSR sensors was determined based on the geometry of the segmented regions and the placement of the sensors used by Merry (Figure 11-b). The seven FSRs are identified as FSR-1, FSR-2 etc. in the following text. FSR-2 was placed at the center of the CFF region. FSR-1 was aligned in the M/L direction with the center of the CFF region but was offset by 10% of the insole length in the anterior direction. FSR-3 was aligned with the center of the CFF region in the anterior / posterior (A/P) direction and the center of the LFF region in the M/L direction. FSR-4 was aligned with FSR-3 in the M/L direction and offset by 10% of the insole length in the posterior direction. FSR-5 was aligned along the A/P midline of the MM region and offset by 10% of the insole length in the posterior direction from the midpoint of the MM region. FSR-6 was aligned along the A/P midline of the LM region and offset by 10% of the insole length in the posterior direction from the midpoint of the LM region. FSR-7 was aligned along the A/P midline of the MH region and offset by 5% of the insole length in the anterior direction.

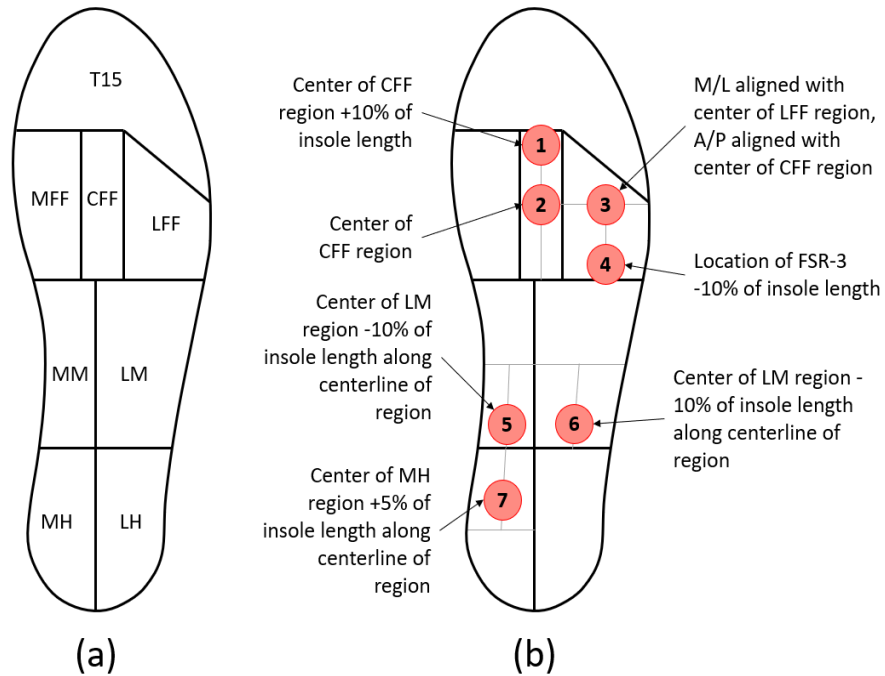


Figure 11 - Segmented insole regions (a), and FSR sensor locations (b)

2.2.4. Final Design - Hardware

The final design of the PDI consists of two components shown, the electronics case and the instrumented insole (Figure 12). These components are attached together by a connection cable consisting of 8 wires. The design of each component is detailed below.

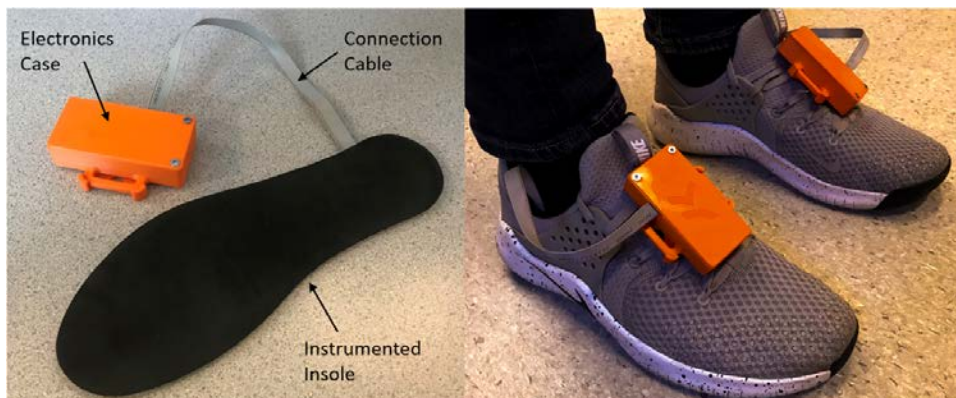


Figure 12 - Photo of a complete PDI insole showing the electronics case, the instrumented insole and the connection cable. The electronics case attaches to the shoelaces and the insole goes inside the participant's shoe.

Instrumented Insole

Sensor Hardware

The instrumented insole contains seven Interlink 402-Short FSRs (Interlink Electronics, CA), arranged in specific locations. The sensors are connected to the microcontroller in the electronics case using a connection cable (Figure 12).

Insole Materials

The insole is made from two layers of foam, a white EVA foam with a thickness of 3mm, and a black puff foam with a thickness of 1.5mm. A laser cutter was used to cut the shape of each foam piece and to etch channels into the white EVA foam. Once the FSRs and wiring was attached to the white foam base, the black puff foam was glued to the EVA foam.

Sensor Locations

The seven FSRs are placed in the locations shown in Figure 11-b. One side of each FSR is connected to a digital output pin on the microcontroller using 26-gauge wire soldered to the connection pin on the FSR. The other connection of each FSR is attached to a common analog input pin on the microcontroller. Each FSR is glued in place to ensure it does not shift while in use. When assembling the insole, the placement



Figure 13 - A pair of insoles with FSRs and connection wires installed. Wires are all inlaid into the white foam to provide a flat top surface. The black puff foam cover has not yet been added.

of each FSR is determined by reference geometries laser cut into the white EVA foam, removing errors associated with hand-measuring the locations.

A full description of the fabrication process used to make the instrumented insoles can be found in Appendix B. A pair of insoles with all FSRs connected before the puff foam was added is shown in Figure 13.

Electronics Case

For this pilot study, it was desirable to have the electronics be modular, replaceable, and easily accessible for the investigator, but with a small footprint to minimize the impact on subjects' biomechanics (Figure 14).

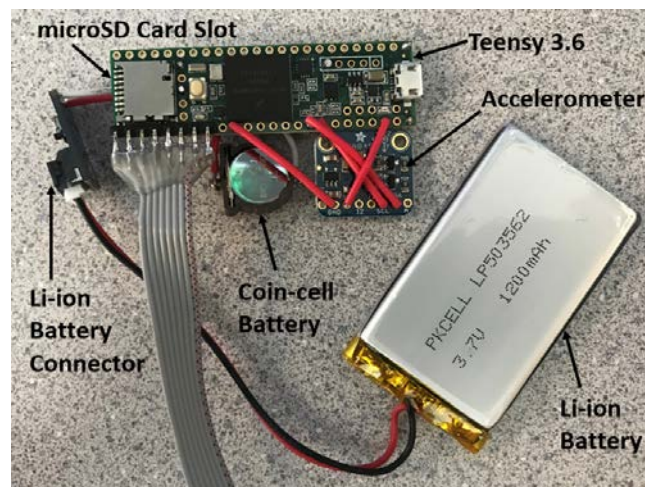


Figure 14 - Completed assembly of the components inside the electronics case

The microcontroller, accelerometer and battery were therefore housed inside a 3D printed case that attaches to the shoelaces of a participant's shoes. The 3D printed case is made of 3 components, the body, the lid, and the shoelace clip (Figure 15). The lid is fastened to the body using two screws. This enables relatively easy access to the electronics for the investigator, but prevents the participant from accidentally opening the case throughout the day. The shoelace clip is designed to slide underneath the shoelaces and then clip onto the body, quickly and easily fixing the entire case on the shoelaces. In a long term application where the device may not need to be removed each day, the shoelaces can be threaded through the holes on the sides of the body to attach the case to the shoes.

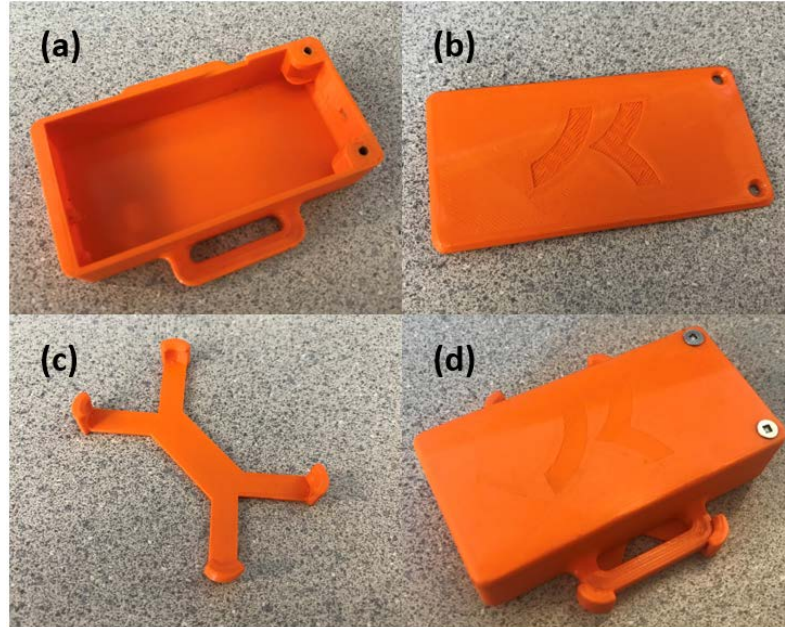


Figure 15 - 3D printed electronics case that attaches to the shoelaces of the user's shoes. Consists of the body (a), the lid (b), and the shoelace clip (c). The lid is fastened to the body with screws and the shoelace clip attaches to the bottom of the body (d).

2.2.5. Final Design - Software

The Teensy 3.6 was programmed using the Arduino IDE. The code for the PDI was designed to record the sensor output values to an onboard microSD card at a specific sampling frequency. The following pseudocode outlines the process used to accomplish this. When the PDI is turned on, it is initialized to save a new filename to the microSD card based on the current time and subject ID number and checks for any connection issues. The code described in Loop is run continuously.

Loop - Main loop that runs infinitely while PDI is turned on

- 1: **if** there are no buffers that are full
 - 2: Execute **Yield** to get more data
 - 3: **else** if there is at least one buffer that is full of new data
 - 4: Turn on LED
 - 5: Write data from full buffer to microSD card
 - 6: Move buffer to the empty stack to prepare it for more data
 - 7: Turn off LED
 - 8: **Repeat**
-

Yield is called whenever the Teensy is not doing anything else. This includes instances when the data on the microSD card is being rearranged as part of the process of saving new data. Calling yield in this way ensures that the sampling rate is kept

consistent. In a 4-hour test, no samples were more than 2µs off the specified sampling interval when sampled at 45Hz.

Yield - Called whenever the Teensy is not doing anything. Samples data at 45Hz

- 1: **if** data is already being collected
- 2: **Return**
- 3: **If** there is no buffer available to store data in
- 4: **Get** an empty buffer from the empty stack and **Set** it as the current buffer
- 5: **if** it is time to collect a sample (collected at 45 Hz sampling frequency)
- 6: **acquireData** to add new data to the current buffer
- 7: **Set** next sample time to current time + sampling interval
- 8: **if** next sample time is greater than the overflow value for the microsecond clock
- 9: **Reset** next sample time to next sample time - maximum microsecond value
- 10: **if** the current buffer is full
- 11: **Move** the full buffer to the full stack
- 12: **Return**

Each sample is recorded using the acquireData function. In this function, data is sampled from the timer, each of the 7 FSRs and each of the 3 axes of the accelerometer and then stored in a buffer to be saved to the microSD card once full.

acquireData - Reads data from the sensors

- 1: **Get** time in microseconds (4 bytes)
- 2: **Save** it in position 0 of data block
- 3: **Get** FSR1 value (4 bytes)
- 4: **Save** it in position 1 of data block
- 5: **Get** FSR2 value (4 bytes)
- 6: **Save** it in position 2 of data block
- 7: **Get** FSR3 value (4 bytes)
- 8: **Save** it in position 3 of data block
- 9: **Get** FSR4 value (4 bytes)
- 10: **Save** it in position 4 of data block
- 11: **Get** FSR5 value (4 bytes)
- 12: **Save** it in position 5 of data block
- 13: **Get** FSR6 value (4 bytes)
- 14: **Save** it in position 6 of data block
- 15: **Get** FSR7 value (4 bytes)
- 16: **Save** it in position 7 of data block
- 17: **Get** X acceleration value (4 bytes)
- 18: **Save** it in position 8 of data block
- 19: **Get** Y acceleration value (4 bytes)
- 20: **Save** it in position 9 of data block

- 21: **Get** Z acceleration value (4 bytes)
 - 22: **Save** it in position 10 of data block
 - 23: **Add** data block to the current buffer
 - 24: **Return**
-

The complete code can be found in Appendix C.

2.2.6. Synchronization of Data

Since two PDIs were used for each participant (one in each shoe), the data from each of the devices needed to be synchronized after being collected. This was done in two different ways. The first method used a light that blinked when the PDI turned on and began recording data. By video recording the devices being turned on, it was possible to determine the time elapsed between the start of each recording. This time was then used to synchronize the data. The process of video recording the devices being turned on is not practical for large scale studies where the device must be turned on every day, so another method was developed to synchronize the data based on step patterns. First, a visual synchronization was completed to line up the data to approximately ± 2 seconds. This was done by finding a time where the participant stood up or sat down and lining up the corresponding increases or decreases in output from the FSRs. Next, walking data was used to precisely synchronize the data. Since gait in healthy humans is symmetrical in the anterior posterior direction [89], when a participant is walking at a constant rate the heel strikes of one foot should occur exactly halfway between heel strikes of the other foot. Using this assumption, the signal from FSR-7 located in the heel was processed to determine each instance when the signal increased to above a specified threshold. The time between these crossings was then calculated. If more than 5 of these crossings fell within $\pm 5\%$ of each other, the participant was considered to be walking consistently. The fifth step from each foot was then used to synchronize the data by placing the heel strike from one foot exactly in between the times of heel strikes of the opposite foot (Figure 16). The heel strikes on the right foot are exactly halfway between the heel strikes of the left foot.

This method was validated by comparing the synchronization attained from the video recordings with the synchronization attained from heel strike measurements on the same data. The average absolute difference between the methods was 0.073 ± 0.024 seconds (mean \pm standard deviation) for $n=22$ participants. This shows that the heel strike method of synchronization is a valid method for this sample population. Further discussion around the impact of incorrect synchronization can be found in Section 3.4.5.

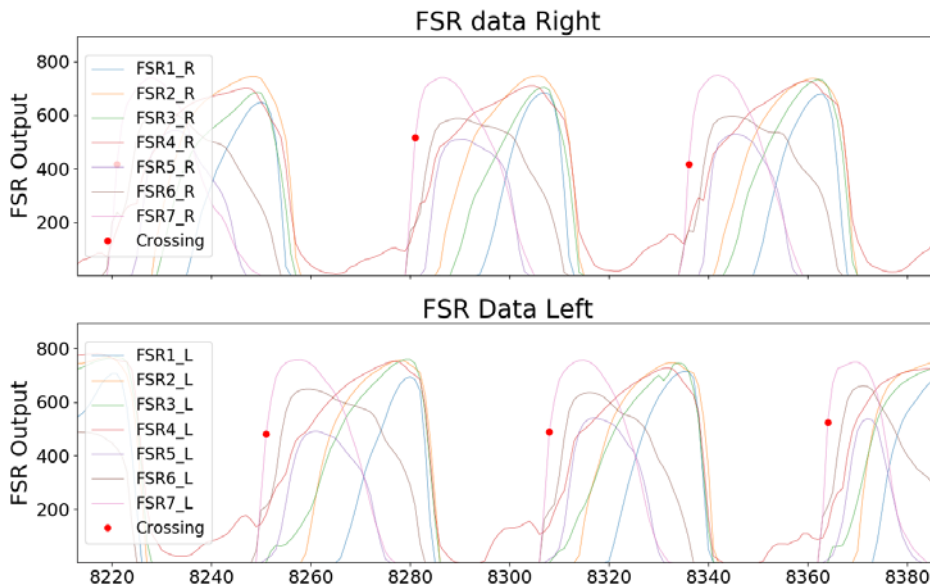


Figure 16 - Synchronization method using heel strikes. Red dots represent heel strikes. Data is shifted such that heel strikes on the right foot fall exactly between heel strikes of the left foot.

2.2.7. In-lab Performance Evaluation

Once the PDI was fabricated and the software was uploaded to the Teensy, it was tested to ensure it functioned properly before being put into a participant's shoes. This testing involved turning the device on, firmly pressing each of the FSRs, shaking the electronics case, and finally leaving the device on for approximately one hour. After the hour, the temperature of the PDI was tested by feeling the microcontroller and battery which should be cool or slightly warm to the touch. The microSD card was removed from the PDI and the data from it was uploaded to a computer. The FSR data were all plotted to ensure that each FSR was correctly measuring forces from the correct location (wires were not crossed). Accelerometer values were plotted to ensure that each axis was collecting data. Finally, the time data was analyzed to ensure that samples were being collected at the correct sampling frequency. If an insole met all of

these requirements it was then installed into a participant's shoe and worn while walking, sitting, and standing.

Data from five preliminary participants (4 males, 1 female) with weights ranging from 58 kg to 90 kg was collected to verify the functionality of the PDI and identify any potential issues prior to out-of-lab deployment. Each participant was asked to wear one PDI in each shoe for approximately 20 minutes while being recorded on video. For the first ten minutes, each participant followed a pre-designed pattern of sitting, standing and walking in one-minute blocks. For the second ten minutes the participant was asked to do everyday activities that may confuse a classification algorithm such as standing on one foot, crouching, leaning on a counter, running, jumping, and sitting in abnormal positions. This data was collected to verify the durability of the device, check that the FSRs selected can measure forces over a wide range of weights without saturating and help inform the design of a classification algorithm.

One researcher wore the PDI in their shoes consistently for five days. This researcher put the insoles into their shoes when leaving the house in the morning and wore the devices for the entirety of the day. Each day, the PDI was left on so that it would record data until the battery ran out to test the real-world battery life. Since each datapoint was timestamped it was possible to determine how long the battery lasts.

2.3. Results

2.3.1. Design verification

The PDI outlined in this chapter meets all of the design criteria specified in Section 2.2.1 (Table 3). The PDI was made from off the shelf components that were soldered together and placed in a 3D printed case. The entire manufacturing process for a pair of PDIs took approximately 12 hours and was primarily completed in the NeuroSpine Lab at SFU using a soldering iron, hot glue gun, 3D printer, and basic hand tools. The laser cutting was done in the neighbouring SIAT shop space.

The components for a complete PDI cost \$139 CAD, \$11 less than the targeted \$150. While a new insole component (including FSRs) was made for each participant, the electronics case could be easily re-used from one participant to the next. This saved significant money since the components in the electronics case cost \$96 CAD.

A total of 70 PDIs (35 pairs) were made by hand by one person over the course of 4 months, with 42 of those being made within 2 months. This shows that the PDI can be used in large scale studies where many devices need to be made in a short timeframe. The quantities made in this research study could be scaled up significantly by having more people making the devices and optimized manufacturing techniques.

The results of training a preliminary algorithm showed promising classification results leading to the belief that 95% classification accuracy can be attained with a larger dataset including more participants. A complete analysis including classification accuracy results can be found in Chapter 3.

The PDI was worn by this researcher for up to 15 hours at a time in a workplace environment without any issues requiring the researcher to remove the device. There were no instances where the battery ran out during the day. This shows that the PDI is capable of capturing data for an extended period of time in a workplace setting.

Table 3 - Results of PDI design verification

Criteria	Met? (Y/N)	Details
Easily fabricated: The device must be able to be made in the NeuroSpine Lab at SFU with only available resources (soldering iron, basic hand tools, 3D printer and laser cutter) in under two days by a graduate student.	Y	<ul style="list-style-type: none"> - Fabricated using soldering iron, hot glue gun, wire cutters, 3D printer and laser cutter - Entire fabrication process for a pair of PDIs took approximately 12 hours
Low-cost: The device must not cost more than \$150 per insole, and where possible re-use expensive components.	Y	<ul style="list-style-type: none"> - Components for one PDI cost \$139 CAD - Electronics case (total cost of \$96 CAD) can be re-used
Able to be used in large-scale studies: The fabrication process must be repeatable and possible to make many of in a short timeframe.	Y	<ul style="list-style-type: none"> - Laser cutting of foam including FSR alignment geometries ensures that insole shape and FSR locations are highly repeatable. - Prefabricated components ensure inter-part consistency and reduces assembly difficulty - 70 PDIs (35 pairs) were made by hand by one person in 4 months.

Criteria	Met? (Y/N)	Details
Unobtrusive: The device must not interfere with the normal workday activities of participants or be uncomfortable to wear / use.	Y	<ul style="list-style-type: none"> - The insole component of the PDI is 4.5mm thick enabling it to comfortably replace the standard shoe insole. - Electronics case is small and lightweight and attaches to the shoelaces.
Effective in a workplace setting: Participants must be able to wear the device in their workplace without it falling off, breaking, or invading their privacy or workplace regulations.	Y	<ul style="list-style-type: none"> - The PDI only records foot pressure and movement, not location, audio or video. - The PDI never unattached from the shoe in preliminary testing - The device malfunctions experienced in preliminary testing were minor and largely due to hand assembly mistakes - Device recorded pressure and acceleration data correctly across a range of body weights, shoe sizes, and activities
Objectively and accurately measure activity: The device must be able to measure the time a participant spends sitting, standing and walking to at least 95% accuracy using objective measures	Y	<ul style="list-style-type: none"> - Preliminary testing showed promising results indicating that 95% accuracy can likely be achieved with data from more participants - See Chapter 3 for a complete analysis of this design criteria
Measure activities for an extended period of time: The device must be able to function for at least 12 hours without requiring any interaction since many work shifts, especially in the healthcare industry are at least this long and data will be captured and reported at the end of a shift	Y	<ul style="list-style-type: none"> - In preliminary testing, the battery life of the PDI was approximately 17 hours

2.3.2. Participant Feedback on Design

Participants that used the PDI were asked if they had any complaints about wearing the device in/on their shoes. Most participants stated that the PDI felt different in their shoes but was comfortable. They stated that they did not notice the electronics case attached to the outside of the shoes and that it did not impeded their activities. A

few participants reported that their shoes felt slightly tighter than usual due to the PDI but also said that it didn't bother them too much. The researcher that wore the device for five days found that the PDI did not interfere with their normal workday activities and the neither the electronics case nor the connection cable caught on any objects, even when riding a bike.

The PDI designed in this chapter was used in 35 participant out-of-lab study, the results of which are presented in the following chapters. Specific performance results related to the design of the PDI can be found in Section 4.3.3

2.4. Discussion

After preliminary testing, it was determined that the prototype design was ready for out-of-lab testing as it clearly met all of the design requirements. The design of the PDI was similar to other devices in that it used the same Interlink FSRs, and had similar electronic components [41], [43], [66], [75]. The PDI differed from other designs particularly in the sensor placement. Existing designs have used bony anatomical features as placement points such as the center of the heel, metatarsal heads and pad of the big toe or have placed as many sensors as possible on the surface of an insole [29], [30], [41]. These studies did not begin with sensor locations most capable of differentiating common activities as this study has done. Many existing devices do not list the overall device costs. The studies known that list the cost of their insoles report device costs of under \$500 per shoe [66] and under \$800 for a pair of shoes [68]. The longest testing reported in the known literature was a 4 hour in-shoe test completed in a lab [40] and a 36 hour cyclical linear load test [74]. While the linear load test showed repeatability of sensor measurements, it did not accurately test the device durability as it did not include any bending of the device.

2.4.1. Hardware Durability

Within the project constraints, this prototype device showed excellent durability, however there are some aspects that arose in initial testing that could be improved in future designs.

Due to the cost limitations and the relatively small number of devices that were made it was decided that multicore layup wires would be used within the insole to connect the FSRs. These wires allowed the insole to flex but came at the cost of a relatively low tensile strength. In some instances, this caused a wire to break, particularly at connections that had been soldered and in high bending areas such as the balls of the feet. Conductive thread made of stainless steel was investigated, however the fabrication process was slow, and the inability to solder the stainless steel wire at connections caused connectivity issues decreasing the signal integrity, particularly when moving around. A likely solution to this problem would be to create a custom printed flexible electronic component with the FSR sensors and connections built into it. This option was explored, and a company called Tangio Printed Electronics in North Vancouver was willing to make such a design, however the cost was too high for such a small number of devices.

The holder used for the coin cell battery was selected based on an extremely affordable price (\$0.76 CAD each) and ability to purchase in large quantities. The integrity of this holder was found to be quite poor when soldered directly to wires instead of being fixed to a flat surface. This issue caused the device to reset, losing the current date and time and requiring connection to a computer to re-program. This shortfall was remedied by wrapping the holder in electrical tape, however in future designs a perpetual solution to this problem should be investigated.

The Interlink FSRs used in the PDI were chosen for their low cost (\$5.81 CAD each) and successful use in many previous studies. While these sensors initially responded as expected, in some specific instances the sensors began to degrade in sensitivity. This meant the same applied force resulted in a lower output signal (higher FSR resistance). In preliminary testing, this only occurred when a researcher wore the PDI while running for an hour and did not occur when wearing the device while sitting, standing or walking for long periods of time. Since the forces experienced while running are higher than when walking or standing it was assumed that the maximum force of the FSRs was reached and caused damage. Therefore; it was assumed that if worn only in a workplace setting where running is uncommon, the Interlink FSRs would not exhibit this degradation. Had cost and development time not been a constraint I would have liked to investigate the potential of capacitive force sensors and/or other FSRs that may be more durable.

2.4.2. Sensor Calibration

The FSR sensors were not calibrated in this research meaning that outputs from one sensor to the next can experience variability. Calibrating each sensor is a time-consuming process that should be avoided where possible particularly for a device being deployed in a large population study. FSR sensors are shown to drift over the course of a few hours due to movement of particles in their materials [82]. If these sensors were designed in this device to require calibration the device would need to be re-calibrated once every day at a very minimum. This would put a significant resource strain on such a study, potentially making it unfeasible to conduct.

Distinct differences in uncalibrated sensor outputs were observed in preliminary testing between sitting (consistent output of approximately 0-200), standing (consistent output of approximately 200-600) and walking (rapidly changing output between 0-800). The effect of force application from changing activities on sensor output was therefore much greater than the approximately 10% drift observed in static weighting for one hour [82].

Because of the clear distinction of sensor outputs experienced in different activities across the pilot study group and prior use of uncalibrated FSRs in existing research [29], [30], [41], [90] it was decided that calibrating the FSR sensors was unnecessary.

2.5. Future Work

The PDI developed in this chapter is a highly functioning prototype that has successfully show that it is possible to make an easily fabricated, low-cost device that can be used in large population studies, is unobtrusive and easy to use, is effective in a workplace setting, and objectively and accurately measures activities over an extended time period. However, this device is not perfect and still has plenty of room for improvement.

Some participants said that the PDI, while comfortable, they did not like how it looked and that would deter them from wearing the device. I recommend for future designs to integrate the components of the electronics case into the insole so that the user does not need to wear a case on their shoelaces. This would involve miniaturizing

the electronic components used and reducing the power consumption to minimize the size of the battery. With this integrated design, it should still be possible for the expensive components to be removed and re-used in a different insole since this was a valuable aspect of the current design, particularly when only using the insole for a short period of time.

The next recommended improvement would be to use a flexible printed component in the insoles. This should include the FSRs along with the connecting wires minimizing fabrication time, increasing reliability, and reducing potential breakage points. This component should be very durable to both direct force and bending. This may involve selecting FSRs that are capable of handling a higher bending force than the ones used in this device or switching to a different type of force sensor.

In future revisions of the PDI design it is recommended that the FSR sensors either be placed in locations with low forces such as 5 and 6 where they are less likely to degrade in sensitivity over time, or to use a different sensor that is more resilient to the extremes of possible forces experienced by an insole. It is interesting to note that none of the studies that used these specific sensors in a shoe insole reported similar issues [41], [43], [66], [75]. This issue didn't arise until the very end of a long period of high forces, so it is likely that the experiments run in previous studies were not tested over the same duration or in situations where the user was applying such high forces to the sensors. These situations may be of importance, particularly for studying plantar fasciitis and other overuse injuries in the workplace, so these findings should be considered for future revisions of the PDI design.

The heel strike synchronization method used in this study assumes gait symmetry which may not be a perfect assumption for all healthy participants and likely will not be true for symptomatic participants [91]. Future revisions of the PDI could incorporate a wireless connection between devices allowing them to synchronize automatically. Once synchronized automatically, the PDI could potentially be used to measure gait asymmetry.

Chapter 3.

Classification of Activities from PDI Data

3.1. Introduction

Sensors are increasingly relied upon for healthcare and activity monitoring applications including fall detection, step counting, cardiac monitoring and sleep tracking [92]. These sensors are typically built into devices that can be worn for extended periods of time, also known as wearables. An area of particular interest is the proliferation of gyroscopes and accelerometers in smartphones and wearables allowing for continuous classification of the user's activity. With wearables becoming commonplace devices, researchers have begun to investigate more challenging questions. However, due to insufficient classification algorithms or sub-optimal sensor locations, many devices lack the accuracy required for these challenging applications [73].

Researchers have tried to improve the accuracy of activity classification algorithms used to interpret accelerometer and gyroscope data collected from user's cell phones [93], [94]. Classification accuracy has been improved for some activities; however, these algorithms typically still fall short when differentiating between passive activities such as sitting and standing [28]. This is due to the similarity of the signals produced by an accelerometer during these activities, unless multiple accelerometers are placed at specific locations on the user's body [25]. This shortfall has inspired other researchers to use pressure sensors in a shoe insole to differentiate activities [29], [32], [65], [69], [95]. Basic classification algorithms have been used to produce a classification accuracy of approximately 95% in a lab setting [40] but to the best of my knowledge, none of the insoles have been used to classify activities in a workplace setting. The design of these insoles has typically included an IMU or accelerometer [29], [32], [95], leading to an increased cost and more complex design. These insole designs have placed sensors in anatomically significant locations such as the heel or ball of the foot but have not assessed the possibility of using other potential locations on the foot that may result in higher classification accuracy [29], [69], [96]. Recent research has shown locations of the foot where loading is most different between sitting, standing and walking [85]. By using sensors in an optimized set of these locations, it is hypothesized that classification

accuracy can be improved while reducing computational cost and simplifying the algorithm.

The focus of this chapter is to design an optimized machine learning algorithm and sensor combination that produces a high degree of classification accuracy while identifying redundant sensors and reducing computational cost. This is necessary to lower the cost of the PDI, improve battery life, and reduce manufacturing time enabling its use in larger studies with more participants. The data used to train and test this algorithm was collected using the PDI developed in Chapter 2. This chapter outlines the design and optimization of a machine learning algorithm capable of classifying workplace activities as sitting, standing or walking. The algorithms chosen were a Support Vector Machine (SVM) and Multinomial Logistic Regression (MLR). An SVM was chosen based on its ease of use and robustness at classification problems. MLR was chosen as a comparison based on success in other insole based projects, particularly with respect to computational cost [40]. The number and specific location of sensors was investigated to determine the impact on classification accuracy.

3.2. Methods

3.2.1. Participants

One group of participants was used for all studies involved in this thesis. Participants were selected based on the inclusion and exclusion criteria listed below and the amount of time they spend on their feet throughout the day. For this preliminary exploration of the insole technology and its application, the target was a dataset that reflected the possible variation in workplace exposure. This included people that ranged from very little time spent weight bearing to most of the day spent weight bearing.

Participant inclusion criteria:

1. Between the ages of 19 – 60
2. Body Mass Index (BMI) less than 30
3. Employed with at least 6 hours of work per shift
4. The ability to walk without the use of an ambulation aid (e.g., walker or cane) or external orthosis

5. Ability and agreement to wear footwear with shoelaces and a removable insole for the duration of the study

Participant exclusion criteria:

1. Any musculoskeletal injury or condition that inhibits your ability to sit, stand or walk.
2. Currently performing modified work tasks due to an existing workers compensation claim of any variety
3. Any lower extremity amputations
4. Any history of lower extremity surgery
5. Any systemic diseases that could affect lower extremity or foot posture
6. Any history of acute trauma to either foot, lower extremity, or lumbosacral region within the past 6 months prior to the start of the investigation
7. Any chronic condition that significantly compromises lower extremity function

A total of 34 participants were recruited for this study (10 males, 24 females, age: 33.1 ± 9.4 (mean, \pm standard deviation) years old, mass: 64.9 ± 11.6 kg, height: 1.7 ± 0.1 m). Each participant consented to participation in this study approved by the Simon Fraser University Office of Research Ethics. Each participant was asked to participate for their typical work week, usually meaning 4 or 5 days depending on the length of the work shift. Some participants were not able to complete the entire week due to schedule restrictions, in these instances data from the available days was used. In addition to recording data while at work each participant was asked to participate in a 30-minute calibration activity. Participants wore self-selected lace-up shoes and worked in a variety of workplace settings. The data collected from these participants was used for each of the following chapters.

The data from the calibration activity from 21 of these participants (4 males, 17 females, age 32 ± 9.7 years) was used for the analysis in this chapter. Calibration data from 13 participants was not used in this chapter for a variety of reasons. Three calibration datasets were lost due to theft, so were not available for analysis. Four calibration datasets had data recorded only from one insole due to an issue with a component hitting the reset button when the case was closed that was later resolved.

The remaining six datasets excluded were recorded in the participant's last two days of wearing the PDI and had at least one sensor that was not performing as anticipated. Such data had a high likelihood of influencing the classification algorithm in an unpredictable way and therefore was excluded from this analysis. The resulting dataset contains 1,200,259 datapoints (~440 minutes) from 20 sensors.

3.2.2. Raw Data

The data collected from one PDI insole consists of one voltage output from each of the seven FSRs (Interlink 402-Short FSR, Interlink Electronics, CA) and X, Y and Z acceleration measurements from the accelerometer (MMA8451 3-axis accelerometer, Adafruit, NY). The output voltage from each FSR was read by the microcontroller as an analog measurement with an integer value between 0 and 1023 where 0 corresponds to 0V (extremely high FSR resistance) and 1023 corresponds to a voltage equal to that of the voltage supplied to the FSR (an FSR resistance of zero). Preliminary results did not show a need for a calibration factor for the FSR output values, so FSR signals were not further processed to simplify the analysis. The FSRs used have a force response that approximately follows an inverse power-law characteristic with the exception of very low forces (Figure 8-b). This means that FSR measurements are more sensitive to changes in force applied to the feet when the feet are not heavily weighted (such as when sitting) and less sensitive when the feet are heavily weighted (standing and walking). This has the benefit of tending to naturally normalize data to body weight. At low forces the FSR will exhibit a switch response, turning on with approximately 0.196N of force. Each FSR has a slightly different force-resistance response due to a part-to-part force repeatability of $\pm 6\%$. Because of this, the analog output was not converted to a calibrated force value. Data was collected from each of the two insoles resulting in a total of 20 signals. Data was sampled at 45 Hz.

3.2.3. Data Synchronization

Since there were two insoles recording data simultaneously, it was necessary to synchronize the data from each insole so it could be collectively evaluated. Data used for the analysis in this chapter was synchronized using a light on each PDI that turned on when the data began recording. The light on each PDI was captured on one continuous video at 30fps while the devices were being turned on. The time difference

between the start of each recording was extracted from the video and the recorded data was shifted and cropped accordingly to synchronize it.

3.2.4. Calibration Data

To train a classification algorithm, training data with solutions is required. To collect this training data, participants were asked to complete a calibration sequence which took approximately 20 minutes. During this calibration sequence, participants wore a PDI in each of their shoes and were simultaneously recorded on video (GoPro Hero 4, 720p, 30fps). The PDI data and the video recordings were synchronized using the light that flashed on the PDI when it began recording data. This light was visible in the video recording. The video data was used to classify the participant's activity as either sitting, standing or walking at each instant throughout the calibration sequence. A transition between standing and sitting was defined as the instant when a participant's legs / buttocks contacts the chair. The opposite was used for the transition between sitting and standing. The walking to sitting transition was also defined by the legs / buttocks contact with the chair. The transition between standing and walking was defined as the instant the participant's foot loses contact with the ground when taking the first step. The walking to standing transition was defined as the moment when the participant's foot contacts the ground after their last step. If the transition was ever

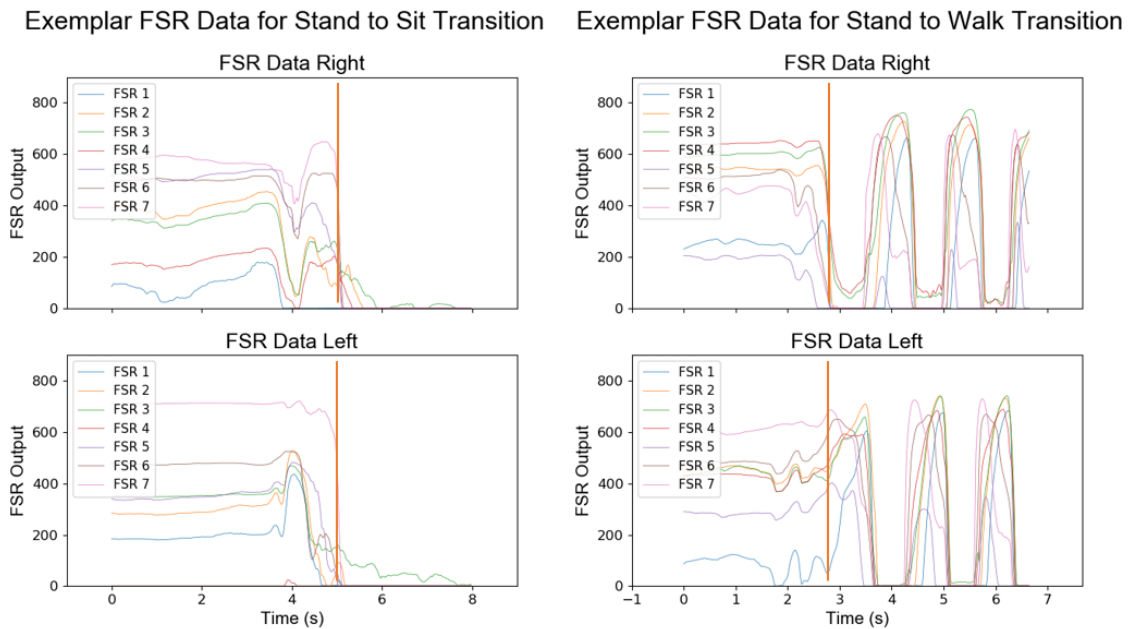


Figure 17 - Exemplar activity transitions. Time of transition is defined by the red vertical line.

unclear in the video recording the FSR data was used to determine the time when the transition occurred (Figure 17). Examples from clearly recorded transitions were referenced to ensure similarity between classification methods.

During the calibration sequence, participants were asked to sit, stand and walk in the sequence described below. A researcher timed each activity with a stopwatch and instructed the participant when it was time to change positions.

1. Sit - approximately one minute
2. Stand - approximately one minute
3. Walk - approximately one minute (walk back and forth in a straight line with a 180° turn at either end in area at least 10m long)
4. Stand - approximately one minute
5. Sit - approximately one minute
6. Walk - approximately one minute
7. Sit - approximately one minute
8. Stand with most of their weight on one foot – approximately 30 seconds
9. Stand with most of their weight on the other foot – approximately 30 seconds
10. Walk to a counter or table
11. Fill out the participant information form at a table or counter while standing (distracted standing) – approximately 8-12 minutes
12. Walk back to chair
13. Sit with feet outstretched - approximately one minute
14. Sit with feet tucked under chair - approximately one minute
15. Sit while fidgeting feet, tapping toes etc. - approximately 30 seconds
16. Sit in their favourite position - approximately 30 seconds

This was either completed in the lab at SFU or at the participant's workplace, so there are variations in chair height, table height, floor type and walkway length between participants. Participants self selected their walking speed and the shoes they were

wearing. Allowing these variations in environmental factors was intentional to test the ecological validity of the insole classification algorithms in a range of workplace settings.

Data from both insoles along with the activity classification solutions were combined to form a training dataset. To be included in the training set, at least 6 out of 7 FSRs in each insole were required to be fully functioning. Functioning was determined by visual inspection of the PDI data. If an FSR recorded only zero as an output, it was likely that the connection had come unattached. If it showed sharp drops it was likely due to a loose connection (Figure 18). An FSR was considered not functioning if it exhibited either of these characteristics. No FSR throughout the entire dataset was ever saturated (output value of 1023).

Example of Data with a Malfunctioning Connection

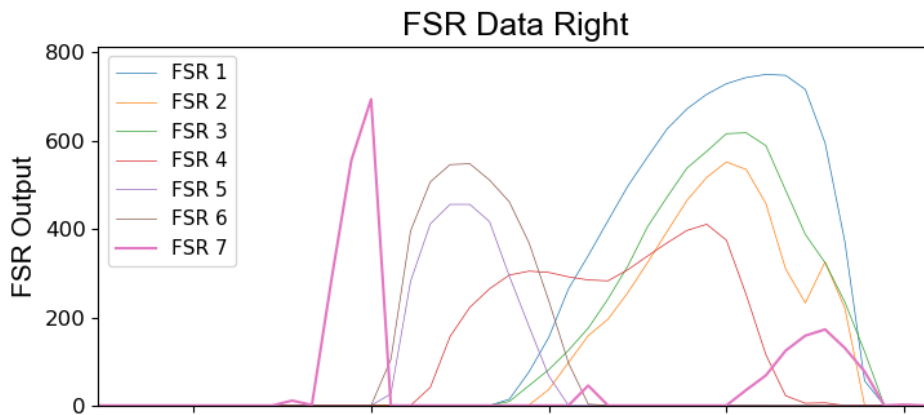


Figure 18 - Data collected with a sensor that has a malfunctioning connection. The line for FSR 7 (pink) should have a smooth curve similar to the other lines, but it instead drops off sharply. This is likely due to a broken wire that intermittently connects when the PDI is loaded or bent in a specific way.

3.2.5. Feature Generation

After the data was synchronized it was processed before being input into a machine learning classification algorithm using the following steps:

1. FSR data was normalized based on the maximum value in the training data from all 7 FSRs. This is required for input to a machine learning algorithm with inputs that have different scales. In this case the FSR data and accelerometer data have different ranges of values so they both need to be scaled to have the same range.

2. Accelerometer data was filtered with a second order low pass Butterworth filter with a cut-off frequency of 10Hz. The cut-off frequency was chosen because 98% of the power in walking is represented by frequencies below 10Hz [39].
3. The filtered accelerometer data was then combined to find the resultant acceleration by taking the square route of the sum of squares of the x, y and z components:

$$acc = \sqrt{a_x^2 + a_y^2 + a_z^2}$$

a_x , a_y and a_z are the accelerations measured on the x, y and z axis respectively.

4. Once combined, acc was normalized in the same way as the FSR data based on the maximum value of acc in the training data. After normalizing, all values from the FSRs and acc were between 0 and 1 enabling evaluation using a combined algorithm.
5. The normalized training data was then broken into buffers so that features could be extracted from the data. The optimal length of the buffer was determined by systematic exploration. A short buffer length was preferred as it would yield a higher temporal resolution, however too short of a buffer could reduce classification accuracy because the features cannot accurately represent the activity. An overlapping buffer window was investigated but ruled out to simplify the number of independent variables.
6. Once buffered, two features were extracted from the data from each sensor: Mean and standard deviation. This produced a total of 32 possible inputs for the machine learning algorithm (2 features from 16 sensors).

3.2.6. Algorithms

Two algorithms were optimized and tested. Both algorithms were implemented in Python using the Scikit Learn library. The first was an SVM, an algorithm widely used for classification problems due to its robustness; however SVMs can be computationally

expensive [29]. This is not currently a problem since the data is processed offline but may become a problem in future iterations of this design in which processing is completed in the PDI or on a smartphone. Three attributes of the SVM were manipulated to maximize performance. These were the kernel type (polynomial, radial basis function (RBF), linear or sigmoid), penalty parameter (C), and the kernel coefficient (gamma). These parameters were optimized using a grid search. The second algorithm was an MLR. It was chosen based on success in a similar application, particularly at reducing the computational cost by over two orders of magnitude [40]. The parameters modified in the MLR algorithm were the solver type (newton-cg or lbfgs), the tolerance for stopping (tol), and the inverse of regularization strength (C). These parameters were again optimized using a grid search.

3.2.7. Classification Accuracy

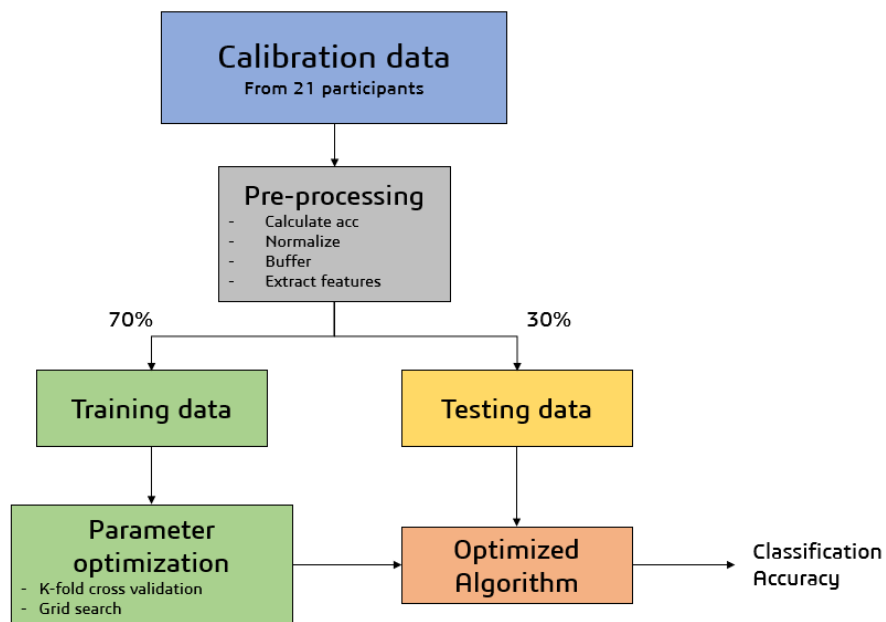


Figure 19 – Flow chart showing the process used to train and test the machine learning algorithm.

Figure 19 outlines the process used to determine classification accuracy. The calibration data was pre-processed using the method described in section 3.2.5 and then randomly split into training and testing data with a split proportion of 70% / 30% respectively. This data was randomly split once at the beginning of the analysis. The training data was used to perform the grid search and K-fold cross validation to determine the algorithm attributes that provide the highest classification accuracy for the

training data. Five folds were used for K-fold cross validation. An optimized algorithm using the best features was then trained with the training dataset and tested on the unseen testing data to determine the classification accuracy.

3.2.8. Sensor Reduction

In designing the PDI it was unknown exactly how many sensors were required to provide adequate activity classification accuracy. Previous work had determined a reduced set of potential locations and began to investigate the number of sensors required [72]. For this reason, seven FSRs and an accelerometer were built into the PDI, more than were thought to be necessary based on the previous work. A wrapper-based approach using backward elimination and forward selection was used in which sensors were digitally removed from the data one at a time until only one sensor remained. The sensors were then added back one at a time until all sensors were included. This approach is similar to that suggested by Maldonado and Weber [97] but was modified slightly. The approach used for this analysis added a 5-fold cross-validation using the training data to calculate the accuracy of each sensor elimination step. The cross-validation accuracy was used to select the sensor to be added or removed. Trained model accuracy was then calculated using the unseen testing data. The backward

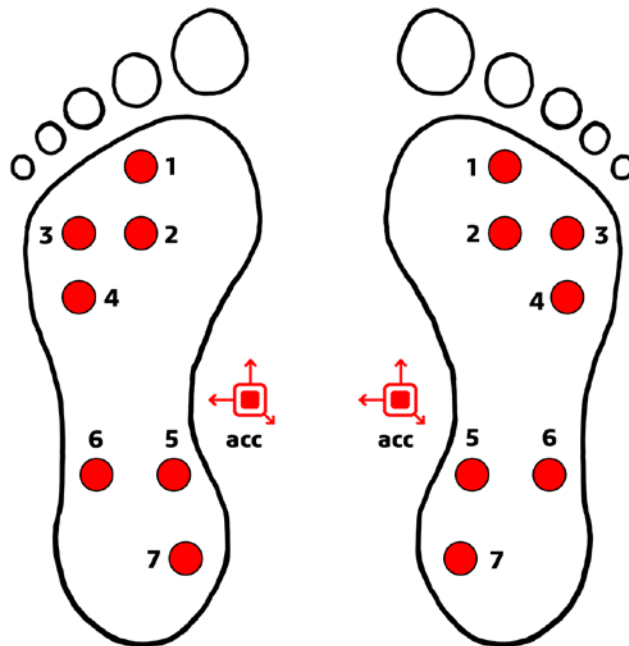


Figure 20 - Approximate location of FSRs in the PDI insole. Red circles are FSRs and the shape labeled acc is the accelerometer that is located on top of the foot in the electronics case.

elimination process was completed as follows: First, the classification accuracy of the training data was calculated using all seven FSRs and the accelerometer from each insole, 16 sensors in total (Figure 20). Each red dot is an FSR and the accelerometer is shown beside the foot.

Next, each pair of sensors was removed one at a time from the data (the same sensor from each shoe) and the resulting classification accuracy was determined using 5-fold cross-validation. The pair of sensors that had the lowest impact on classification accuracy when removed was taken out of the data. The model was then trained and tested with the reduced feature set. The same process was completed until only one pair of sensors remained. The opposite process was then completed for forward selection in which sensors were added starting from one pair and working up to all 16 sensors. Pairs of sensors were added in based on the highest increase in classification accuracy. The same method was performed for each algorithm.

3.3. Results

3.3.1. Raw data

The raw data collected from the PDI consisted of 14 outputs from FSRs (seven from each foot) and six outputs from accelerometers (X, Y and Z acceleration from each

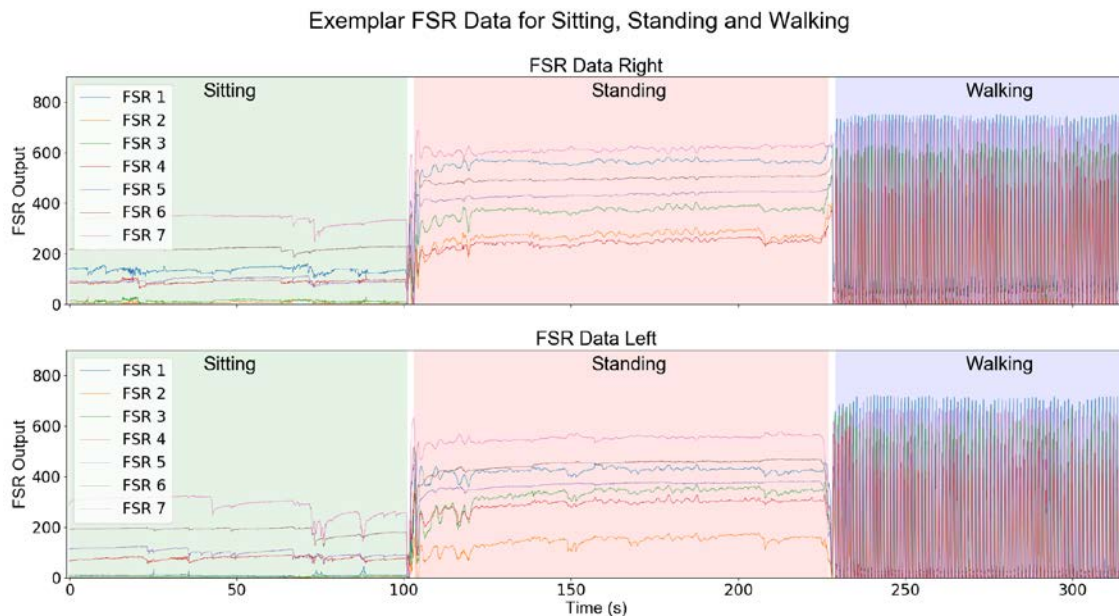


Figure 21 - Exemplar data from the seven force sensitive resistors in both the left and right shoes of a participant showing sitting, standing and walking

foot). With participant body weights ranging from 44 kg to 88 kg none of the FSRs reached saturation. Examples of this raw data can be seen in Figure 21 and Figure 22.

In Figure 21 the differentiation between sitting, standing and walking can be easily seen. When the participant is sitting, the output from each of the FSRs is relatively low and remains mostly constant. When the participant is standing, the outputs increase but are still relatively constant. When the participant is walking, the outputs fluctuate from 0, to a level higher than that of standing during the impacts of heel strike and toe off. When a participant is sitting and fidgeting or standing on one leg these clear distinctions become less obvious. The maximum values of all FSR outputs from all participants was 815 (Table 4). This was observed in the data from SID06 at FSR 1.

Table 4 - Maximum FSR value for each location recorded in each participant's calibration data. Maximum values are in bold.

Participant	FSR 1	FSR 2	FSR 3	FSR 4	FSR 5	FSR 6	FSR 7	Maximum
SID05	758	748	788	765	497	726	765	788
SID06	815	788	795	752	563	727	780	815
SID07	781	776	748	673	671	719	775	781
SID08	728	783	755	768	506	620	757	783
SID09	809	794	809	784	677	726	787	809
SID10	773	769	791	790	632	683	762	791
SID12	775	758	778	740	475	691	772	778
SID13	798	787	785	785	540	742	795	798
SID14	787	661	748	625	597	686	724	787
SID15	735	701	753	652	541	638	752	753
SID16	680	714	767	688	620	747	783	783
SID17	725	544	746	725	689	681	755	755
SID19	592	551	685	612	672	632	633	685
SID20	755	517	688	597	648	634	743	755
SID24	794	752	751	671	661	678	791	794
SID25	774	782	783	701	575	596	694	783
SID26	687	472	767	753	645	679	694	767
SID30	800	647	744	665	716	706	723	800
SID32	777	809	797	736	529	665	801	809
SID34	793	759	770	703	591	695	772	793
SID36	748	752	772	650	652	675	728	772

A participant's maximum FSR output occurred at FSR 1 eight times, FSR 2 two times, FSR 3 nine times, and FSR 7 twice.

Figure 22 highlights the difficulty of using only accelerometer data to differentiate between sitting and standing. The two activities look identical since the foot is typically in similar orientations and lacks distinct motion when sitting and standing. When a participant is walking there are noticeable acceleration spikes that coincide with foot contact and foot swing.

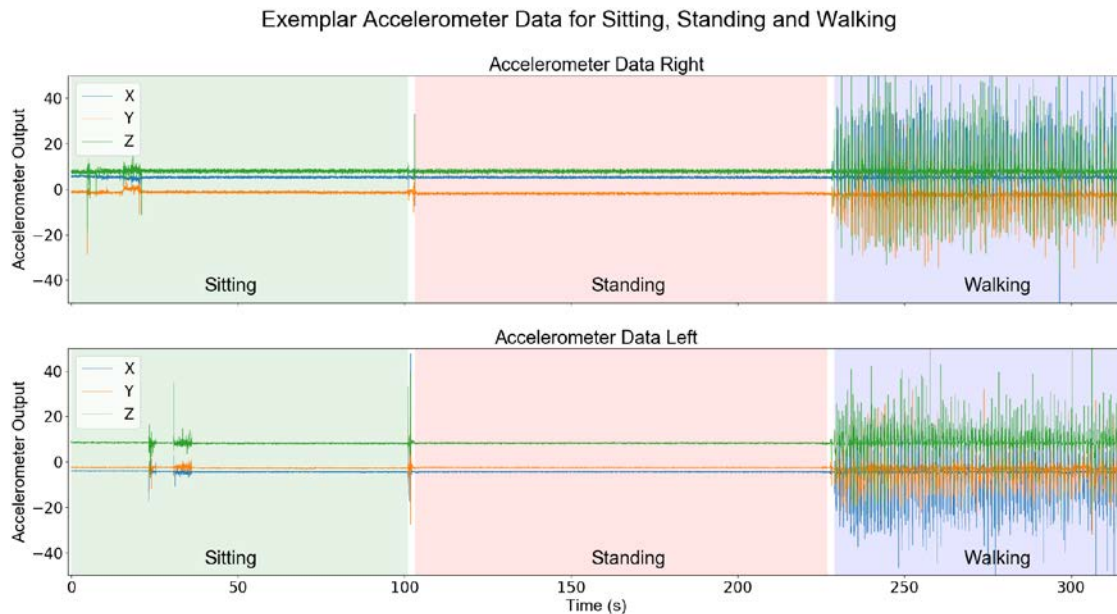


Figure 22 - Exemplar data collected from the accelerometer on a participant's right and left shoe while sitting, standing and walking.

3.3.2. Activity Classification Accuracy

The results of the grid search method for optimizing both algorithms were as follows. For the SVM algorithm, accuracy was as low as 83% and was maximized using the polynomial kernel with $C = 105$ and $\gamma = 0.05$. This produced the highest classification accuracy on the training set at 99.31% using all 16 sensors. The MLR algorithm produced accuracies as low as 92% and was optimized using the newton-cg solver with $C = 5000$ and $\text{tol} = 0.01$. This produced a maximum classification accuracy on the training set of 99.10%. Both algorithms showed the highest classification accuracy when using a buffer length of 40 samples, ~ 0.88 seconds. When considering only classification accuracy with a full set of sensors, the SVM algorithm outperformed the MLR algorithm by 0.21%. Table 5 below shows a confusion matrix for the results of the optimized SVM and MLR algorithms when tested on the test dataset. The SVM

algorithm yielded a test accuracy of 99.31% and the MLR algorithm yielded a test accuracy of 99.11%

Table 5 - Confusion matrices showing results of both the SVM and MLR algorithms when tested on the test dataset using all sensors

		SVM Algorithm		
		Predicted Value		
		Sit	Stand	Walk
True Value	Sit	3198	2	4
	Stand	7	4577	15
	Walk	6	28	1165

Accuracy: 99.31%

		MLR Algorithm		
		Predicted Value		
		Sit	Stand	Walk
True Value	Sit	3190	10	4
	Stand	14	4571	14
	Walk	9	29	1161

Accuracy: 99.11%

3.3.3. Sensor Reduction

When sensors were digitally removed one at a time the classification accuracy decreased. The decrease in accuracy when removing three sensors was 0.08% for the SVM algorithm and 0.11% for the MLR algorithm. With only one sensor, the SVM and MLR algorithms had classification accuracies of 93.33% and 96.81% respectively. This shows that the full set of eight sensors is not required to maintain a classification accuracy of over 99%.

Results from the backward elimination procedure for the SVM algorithm can be seen in Figure 23 below. Classification accuracy was 99.31% with all the sensor pairs being used. This reduced to 93.33% using only one sensor. Classification accuracy was not reduced by more than 1% until seven pairs of sensors were removed. The sensors that had the most impact on the classification accuracy of the SVM algorithm were the heel sensor (FSR 7), and the sensor on the lateral longitudinal arch (FSR 6). The accelerometer was removed immediately showing that it had limited impact on the classification accuracy of the SVM algorithm.

When applying the forward selection procedure, very similar results were obtained (Figure 24). The same two sensors, numbers 6 and 7, were the most important sensors and the accelerometer was the least important. The only difference was between the order of sensors 1, 2 and 5. The agreement between the backward elimination and forward selection suggests that the order of feature importance is not coincidental.

Results of the sensor reduction procedure using the MLR algorithm can be seen in Figure 25 below. The accuracy ranges from 99.11% with all sensor pairs being used to 96.81% when only one sensor pair is used. Classification accuracy is not reduced by more than 1% until 6 pairs of sensors are removed. Similar to the SVM algorithm, sensor number 6 on the lateral longitudinal arch has a large impact on classification. Sensor number 3 also has a large impact on classification for the MLR algorithm, similar to the results of the SVM algorithm where it was third most important. The accelerometer was the 4th least important sensor for the MLR algorithm. Sensor number 2 was the least important sensor. While the MLR algorithm has a slightly lower classification accuracy

when using all sensors, it has a 3.48% higher classification accuracy when using just one sensor.

The results from the sensor addition procedure using the MLR algorithm were quite different from the results from the sensor reduction procedure (Figure 26). This is likely due to the reduced capability of the MLR algorithm at handling colinear data compared to the SVM algorithm [98], [99]. However, the single most optimal sensor selected in both procedures was the same: sensors number 6.

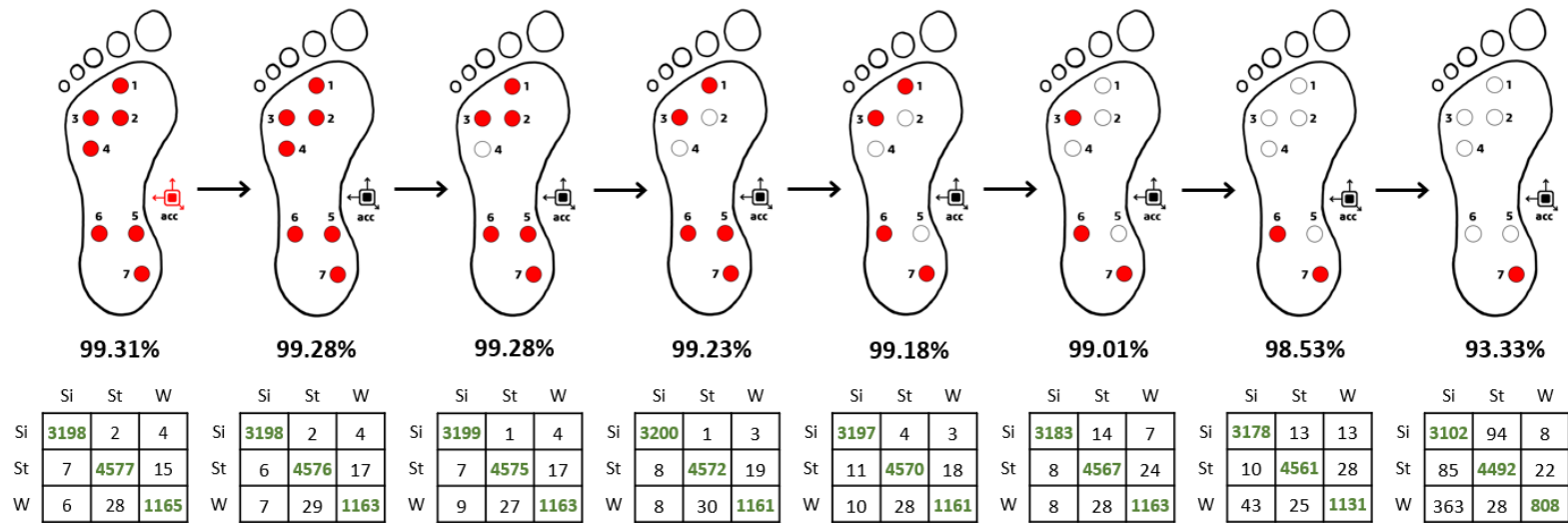


Figure 23 - Results of the backward elimination procedure for the SVM algorithm. A sensor shown in red means that it was included, white or black sensors were digitally removed from the data. The number below the image is the classification accuracy of the SVM algorithm when tested on the test dataset using the sensor configuration depicted above. The confusion matrix below the accuracy displays predicted values on the horizontal axis and true values on the vertical axis.

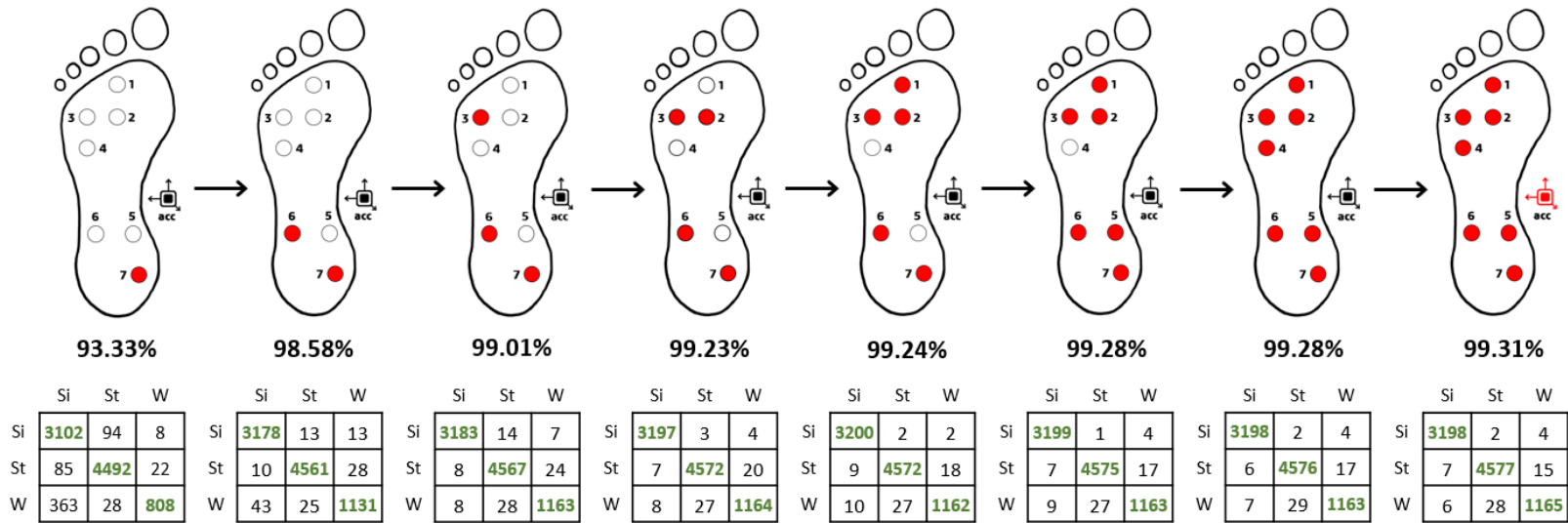


Figure 24 - Results of the forward selection procedure for the SVM algorithm. A sensor shown in red indicates that it was included, white or black sensors were digitally removed from the data. The number below the image is the classification accuracy of the SVM algorithm when tested on the test dataset using the sensor configuration depicted above. The confusion matrix below the accuracy displays predicted values on the horizontal axis and true values on the vertical axis.

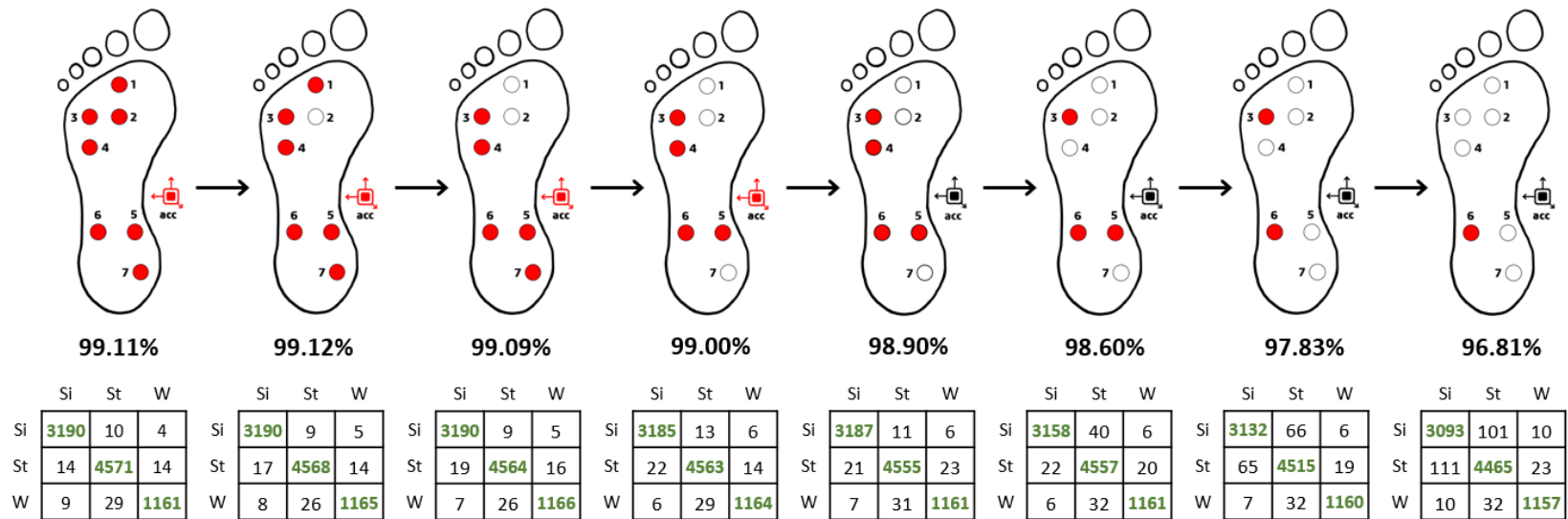


Figure 25 - Results of the backward elimination procedure for the MLR algorithm. A sensor shown in red indicates that it was included, white or black sensors were digitally removed from the data. The number below the image is the classification accuracy of the MLR algorithm when tested on the test dataset using the sensor configuration depicted above. The confusion matrix below the accuracy displays predicted values on the horizontal axis and true values on the vertical axis.

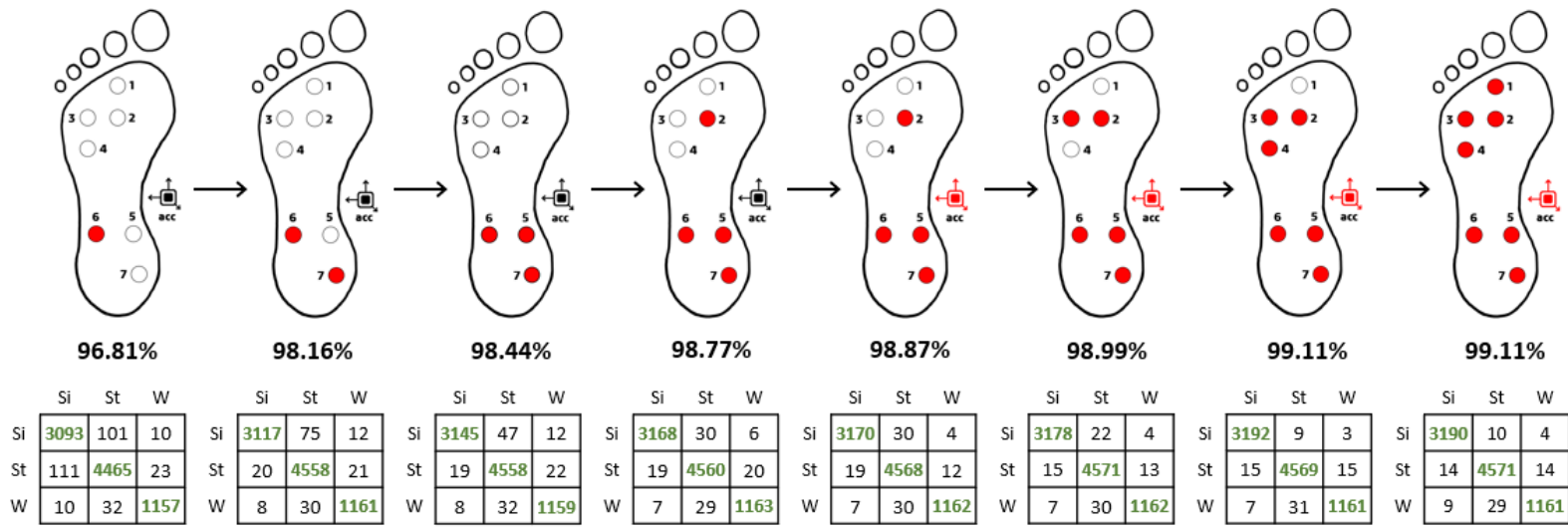


Figure 26 - Results of the forward selection procedure for the MLR algorithm. A sensor shown in red indicates that it was included, white or black sensors were digitally removed from the data. The number below the image is the classification accuracy of the MLR algorithm when tested on the test dataset using the sensor configuration depicted above. The confusion matrix below the accuracy displays predicted values on the horizontal axis and true values on the vertical axis.

3.3.4. Activity Specific Sensitivity and Specificity

Sensitivity and specificity of each activity were calculated to demonstrate the performance of both the SVM and MLR algorithm at individual activity classification. Sensitivity, or true positive rate, was excellent for both the SVM and MLR algorithms for sitting and standing, remaining greater than 99% even with only 4 sensors in use. Sensitivity for walking however was lower, indicating that walking was more difficult to classify than sitting or standing for both algorithms. The sensitivity for walking using the MLR algorithm remained relatively constant as sensors were removed while the sensitivity for walking using the SVM algorithm dropped off significantly when only one sensor was used. This was due to significant misclassification of walking as sitting. Specificity, or true negative rate, was excellent for all activities, remaining greater than 99% even with only 4 sensors in use. Table 6 and Table 7 below show the complete results of this analysis.

Table 6 – Sensitivity and specificity (%) for the SVM algorithm broken down by activity type. Sensors used are per Figure 23.

#	SVM Algorithm					
	Sitting		Standing		Walking	
	Sens.	Spec.	Sens.	Spec.	Sens.	Spec.
8	99.81	99.78	99.52	99.32	97.16	99.76
7	99.81	99.78	99.50	99.30	97.00	99.73
6	99.84	99.72	99.48	99.36	97.00	99.73
5	99.88	99.72	99.41	99.30	96.83	99.72
4	99.78	99.64	99.37	99.27	96.83	99.73
3	99.34	99.72	99.30	99.05	97.00	99.60
2	99.19	99.09	99.17	99.14	94.33	99.47
1	96.82	92.27	97.67	97.23	67.39	99.62

Table 7 - Sensitivity and specificity (%) for the MLR algorithm broken down by activity type. Sensors used are per Figure 25

#	MLR Algorithm					
	Sitting		Standing		Walking	
	Sens.	Spec.	Sens.	Spec.	Sens.	Spec.
8	99.56	99.60	99.39	99.11	96.83	99.77
7	99.56	99.57	99.33	99.21	97.16	99.76
6	99.56	99.55	99.24	99.21	97.25	99.73
5	99.41	99.52	99.22	99.05	97.08	99.74
4	99.47	99.52	99.04	99.05	96.83	99.63
3	98.56	99.52	99.09	98.36	96.83	99.67
2	97.75	98.76	98.17	97.77	96.75	99.68
1	96.54	97.91	97.09	96.98	96.50	99.58

3.3.5. Leave-One-Out Cross-Validation

Leave-one-out cross-validation (LOOCV) was performed on the optimized SVM and MLR algorithms with all sensors included to determine the impact of excluding a participant's data from the training data. This is particularly important for future applications of the PDI device in which a new user will not be asked to complete the calibration sequence, but instead will be given the already trained device to use. LOOCV was performed using the data from all participants except one as training data, and the data from the excluded participant as testing data. This process was repeated for each participant resulting in 21 folds of unequal length.

The results of LOOCV show that both the SVM and the MLR algorithms are capable of classifying activities of subjects even when data collected from them is not included in the training set (Table 8). The SVM algorithm using all sensors had an overall accuracy of 98.30% with a standard deviation of 3.62% while the MLR algorithm using all sensors had an overall accuracy of 97.81% with a standard deviation of 4.00%. While the SVM outperformed the MLR algorithm in 17 of 21 cases, both performed exceptionally well. These results show that it is feasible to design an algorithm using a small sample of participants that can then be utilized in a much larger population without the need to calibrate the device to each user.

Table 8 - Results of leave-one-out cross-validation (LOOCV). The classification algorithm was trained on all participants except one. Classification accuracy is calculated based on subject's data that was excluded.

Excluded Participant ID	SVM Classification Accuracy (%)	MLR Classification Accuracy (%)
SID05	99.35%	96.68%
SID06	96.95%	97.99%
SID07	99.44%	99.30%
SID08	99.25%	98.87%
SID09	82.70%	80.81%
SID10	99.10%	98.91%
SID12	99.27%	97.55%
SID13	99.13%	97.57%
SID14	99.68%	99.56%
SID15	98.65%	96.62%
SID16	98.77%	98.28%
SID17	99.00%	98.81%
SID19	98.89%	99.34%
SID20	99.30%	99.43%
SID24	98.66%	98.93%
SID25	99.65%	99.65%
SID26	99.46%	99.38%
SID30	99.53%	99.41%
SID32	99.20%	98.96%
SID34	99.21%	99.00%
SID36	99.06%	98.98%
Mean (+/- STD)	98.30% (+/- 3.62%)	97.81% (+/-4.00%)

3.3.6. Activity Misclassification

While most participants LOOCV results showed a classification accuracy over 98%, there were two instances where the SVM algorithm fell short, namely SID06 and SID09. These are interesting cases to look at to better understand how the classification

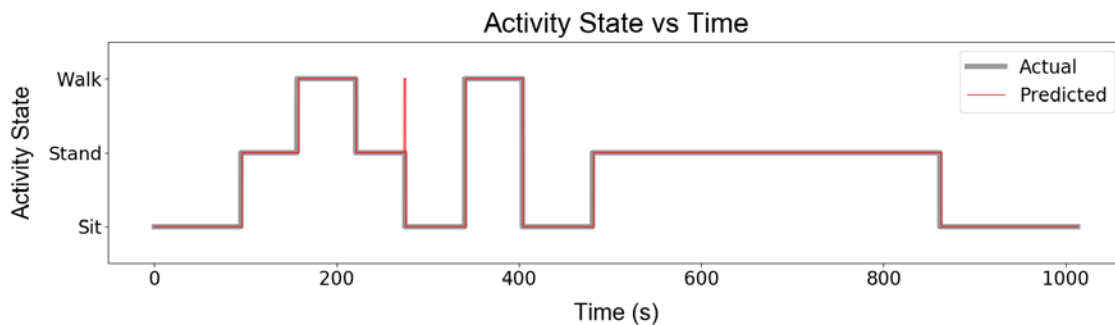


Figure 27 - Activity classification results using the MLR algorithm for SID25.

algorithm can be improved in the future. Figure 27 shows exemplar data from SID25 where all but one instance was classified correctly. The grey line represents the correct activity classification obtained from the video analysis. The red line is the activity state predicted by the classification algorithm. The one instance that was misclassified was during the first stand to sit transition. The algorithm determined that the participant was briefly walking before sitting down. In reviewing the data, it was apparent that the participant briefly shifted their weight from one foot to the other to position themselves to sit down. The algorithm interpreted this shifting of weight as walking.

Activity classification results for SID06 can be seen in Figure 28 and Figure 29. These results show that much of the misclassification came from the phase of the

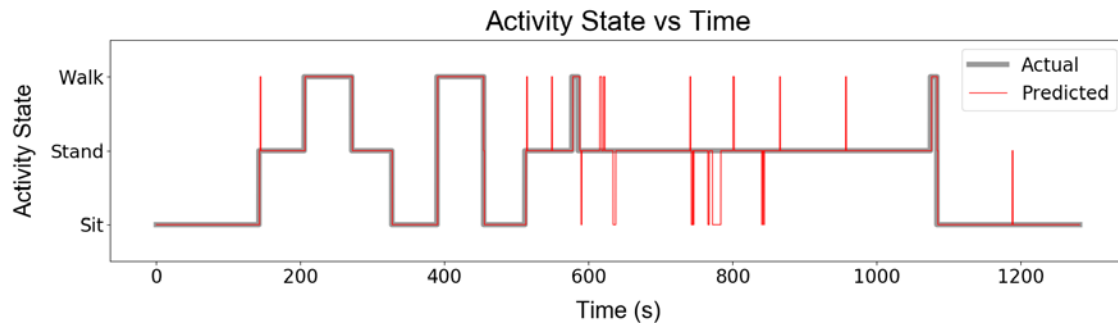


Figure 29 - Activity classification results using the SVM algorithm for SID06

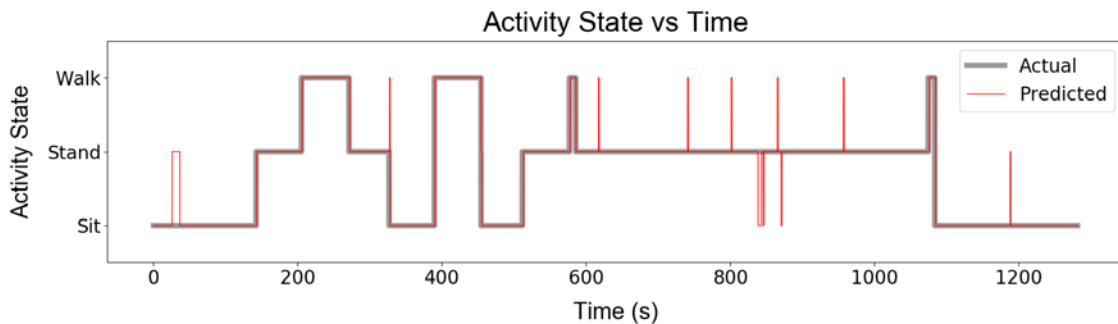


Figure 28 - Activity classification results using the MLR algorithm for SID06

calibration sequence when the participant was standing at the counter filling out a form. In reviewing the video recording of this segment, it became clear that the participant often shifted their weight quickly between their feet and was leaning heavily on the counter. The combination of these two factors could have led to the algorithm misclassifying activity as walking (when shifting feet) or sitting (when too much weight is transferred through the participants arms to the counter).

Figure 30 and Figure 31 show the classification results for SID09, another participant with a low LOOCV classification accuracy. In this case, much of the classification error came from misclassifying sitting as standing. Analysis of the video recording showed the participant sitting on the edge of the chair the entire time when sitting except at the end when they were sitting with feet under the chair etc. This method of sitting likely increased the weight transferred through the participant's feet and made the activity appear to be closer to standing than sitting, explaining the misclassification.

The activity directly on either side of a sit to stand or stand to sit transition was where most of the misclassification occurred for many of the LOOCV cases. This is

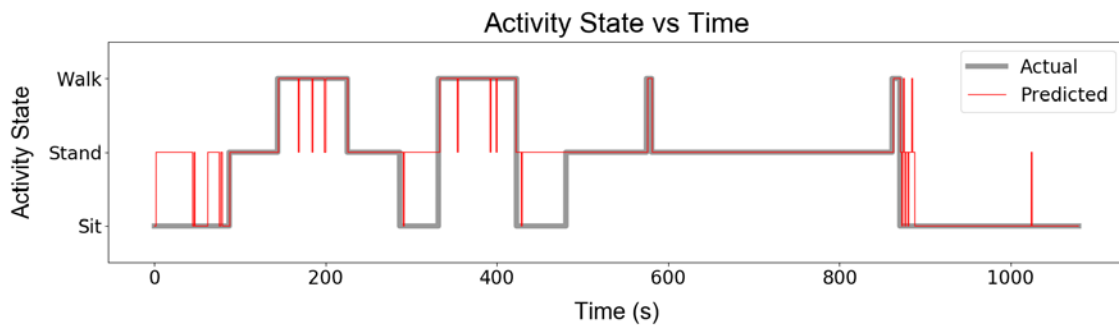


Figure 31 - Activity classification results using the SVM algorithm for SID09

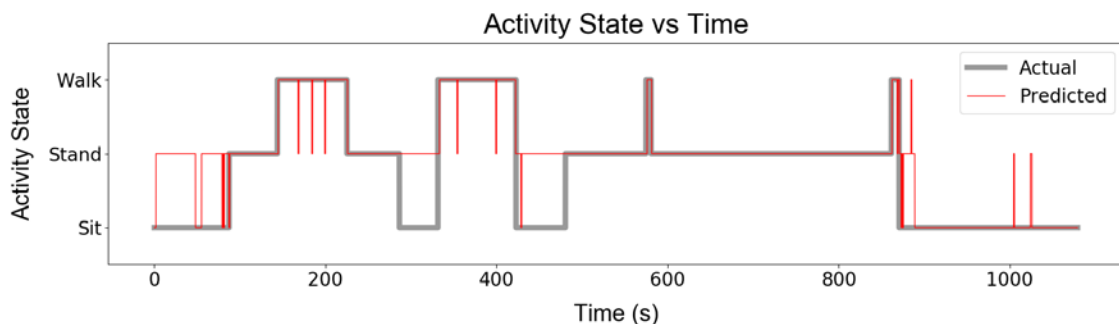


Figure 30 - Activity classification results using the MLR algorithm for SID09

because it was quite common for participants to take a few steps to reposition themselves before sitting or move away from the chair when standing up. These instances could be classified as either standing or walking. The decision was made to label these instances as standing since it was typically only a minor shift of weight. Had these transitions been labeled as walking when the participant shifted their feet the classification accuracies would have likely been slightly higher. The standing to walking transition did not exhibit many issues.

3.3.7. Algorithm Resource Intensity

Resource intensity was measured as the amount of time that each algorithm took to classify the test dataset. Each algorithm was tested on the same computer (Intel Core i7-4800MQ CPU) using the exact same method, simply the type of algorithm was different. The SVM classification took 0.254 seconds to complete and the MLR classification took 0.002 seconds. Based on these results, the MLR algorithm required significantly less computational power.

3.3.8. Impact of Incorrect Synchronization

Analysis was performed to better understand the impact of incorrect synchronization of the data from the left and right PDI devices. The calibration data that was synchronized using the video footage was used for this analysis. LOOCV using all subjects and the SVM algorithm described above was used to test the classification accuracy. To simulate incorrect synchronization, the data left out in each validation (test data) was manipulated such that data from one insole was offset from the data from the other insole by a known time difference. Average classification accuracy and average decrease in classification accuracy were calculated (Table 9). These results show that deviations less than 0.3s have very little impact on classification accuracy (<0.1% decrease in classification accuracy). Even with an offset of 1.98s (90 samples), the average decrease in classification accuracy was only 0.94% \pm 0.42%.

Table 9 - Results of incorrect synchronization analysis. R offset means data from the right foot was offset by the specified duration. L offset means data from the left foot was offset by the specified duration.

	Average Classification Accuracy (\pm STD)			Average Decrease in Classification Accuracy (\pm STD)		
1.98s L offset	97.43%	\pm	3.88%	0.86%	\pm	0.65%
0.99s L offset	97.85%	\pm	3.86%	0.45%	\pm	0.37%
0.66s L offset	97.74%	\pm	3.82%	0.56%	\pm	0.53%
0.33s L offset	98.15%	\pm	3.74%	0.14%	\pm	0.25%
0.22s L offset	98.24%	\pm	3.73%	0.06%	\pm	0.20%
0.11s L offset	98.26%	\pm	3.67%	0.03%	\pm	0.11%
Synchronized	98.30%	\pm	3.62%			
0.11s R offset	98.24%	\pm	3.62%	0.06%	\pm	0.12%
0.22s R offset	98.21%	\pm	3.66%	0.09%	\pm	0.20%
0.33s R offset	98.16%	\pm	3.72%	0.14%	\pm	0.33%
0.66s R offset	97.78%	\pm	3.72%	0.52%	\pm	0.46%

	Average Classification Accuracy (\pm STD)		Average Decrease in Classification Accuracy (\pm STD)	
0.99s R offset	97.80%	\pm 3.68%	0.50%	\pm 0.32%
1.98s R offset	97.36%	\pm 3.80%	0.94%	\pm 0.42%

3.3.9. One Insole vs. Two Insoles

Using only one insole to classify activities would cut the cost of instrumenting one participant in half and reduce the data processing requirements. However, doing so reduces the classification accuracy of the PDI. This was shown by performing the same LOOCV for both the SVM and MLR algorithm as was completed in Section 3.3.4 except using only data from the right insole. The classification accuracy of the SVM algorithm was reduced to 90.78% \pm 6.56% (mean \pm STD) and the classification accuracy of the MLR algorithm was reduced to 88.55% \pm 8.25%. This is a reduction in accuracy of 7.5% and 9.3% respectively (or 36 min and 45 min respectively per eight-hour day).

3.3.10. Impact of Sampling Frequency

Sampling frequency is an important factor to consider when designing a device such as the PDI. There is an inherent trade-off between the accuracy attainable with a higher sampling frequency and the power consumption reduction that comes with using a lower sampling frequency. The PDI was designed with a sampling frequency of

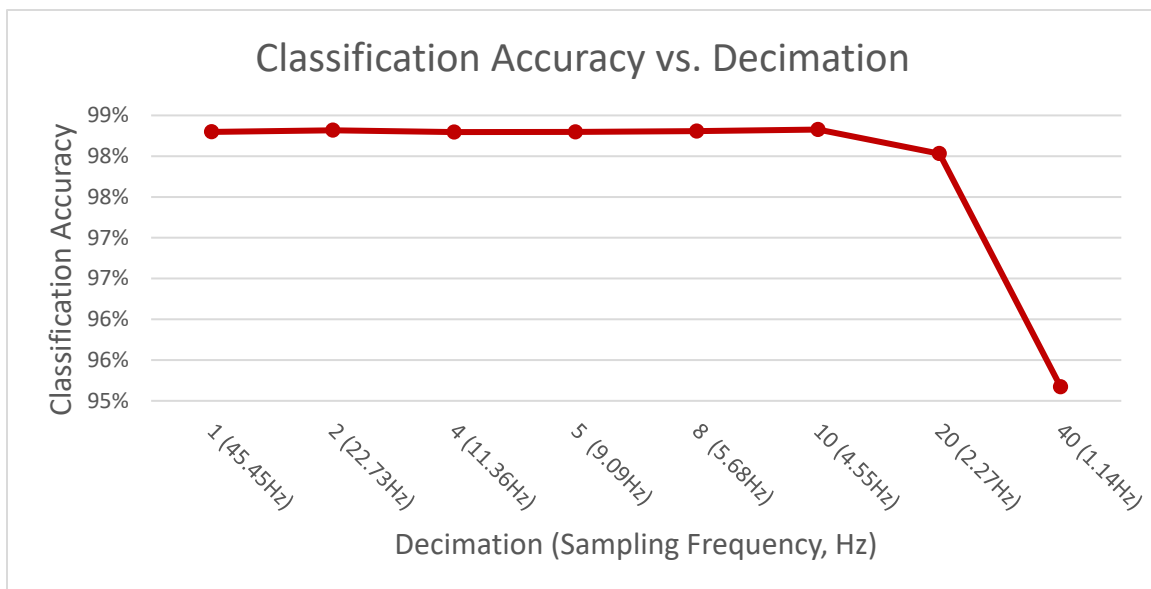


Figure 32 - Classification accuracy as a function of decimation. Equivalent sampling frequency shown in parentheses

45.45Hz with the intention of investigating what impact down sampling this data would have on the classification accuracy. The same LOOCV approach was used for this analysis as in Section 3.3.4 using the SVM algorithm. The data was down sampled at various decimation factors (1,2,4,5,8,10,20, and 40) (Figure 32). These results show that there is no significant decrease in classification accuracy until the decimation reaches 20 (equivalent to a 2.27Hz sampling frequency). The average classification accuracy with a decimation of 10 (4.55Hz sampling frequency) was $98.33\% \pm 3.59\%$ (mean \pm STD), nearly identical to the classification accuracy with a decimation of 1 (original data) at $98.30\% \pm 3.62\%$.

3.4. Discussion

This chapter focused on designing an activity classification algorithm capable of accurately classifying sitting, standing and walking using FSR sensors and an accelerometer. Both the SVM and the MLR algorithms performed exceptionally well at classifying sitting, standing and walking from the FSR and accelerometer data. These algorithms had classification accuracies of 99.31% and 99.11% respectively when trained on data from 21 participants. This result was validated using LOOCV resulting in classification accuracies of 98.31% and 97.81% respectively showing the ability of these algorithms to generalize to an unknown participant. The SVM algorithm performed marginally better on the LOOCV, likely due to its slightly better ability to generalize to new data. This is due to the formation of the algorithm, in which a decision boundary is placed to maximize the distance between only the closest separating points. The MLR algorithm optimizes its decision boundary based on all of the datapoints, and as such is more susceptible to outliers in the data. The same reason is likely why the MLR was better at classifying activities using only one FSR. It was able to better comprehend the decision boundary from just one sensor where the SVM benefits from more sensors. This finding is similar to results found for other classification problems using SVM and MLR algorithms [100]. With a reduced set of just three FSR sensors and no accelerometer, the SVM and MLR algorithms used in this research could still classify sitting, standing and walking with an accuracy of 99.01% and 98.60% respectively. The accuracy obtained using this algorithm is comparable to existing work classifying activities using an instrumented insole at an accuracy of 98.3% in a lab environment with only three participants [30].

Additionally, it has been found that SVM algorithms perform better than MLR algorithms on datasets with data that is highly correlated [98]. The features in this dataset were highly correlated as many of the sensors were placed in close proximity. This could also explain why the MLR performed better than the SVM with one sensor (not highly correlated data) and worse when more sensors were included.

The results of this research show that the PDI and the two algorithms developed for activity classification are suitable for use in classifying sitting, standing and walking in a workplace environment. Algorithm development and testing combined many of the standard machine learning procedures used in existing work including feature selection, sensor reduction, algorithm parameter tuning and sampling rate reduction [29], [32], [70], [101]. In addition, this work added to what had been previously reported by recording data in loosely controlled environments (e.g. self-selected shoes and walking rate, a variety of chair heights and walking distances, different workplace environments, and different floor types). Rather than detracting from the validity of the results, this highlights the ability of these algorithms to classify data that is not structured in the exact same way every time. This is an important feature for a device that will be used in a natural work environment. The recommendations outlined in a recent article highlighting best practices in machine learning for human movement biomechanics [102] were followed including the following:

1. The number of features was significantly less than the number of observations.
2. Two simple models were explored for classification due to the relatively small amount of data available.
3. All data was re-scaled before input to the algorithm to ensure that each feature had the ability to contribute equally to the outcome and no bias was present.
4. Algorithm parameters were tuned using only the training data, leaving the testing data as an unbiased measurement of the classification performance of the algorithm. The parameters were explored in a systematic grid search.

5. LOOCV was used to test the algorithms ability to generalize to new data. This method removed all data from a particular subject from the training data and then asked the algorithm to classify data from a subject whose data had not previously been seen by the algorithm.
6. Multiple evaluation metrics were reported including a confusion matrix, not simply the overall accuracy. This enables critical evaluation and future verification of results.

3.4.1. Impact of Classification Accuracy

Maximizing classification accuracy is important especially when dealing with large quantities of data as is the case in this study. 95% accuracy over the course of a 12-hour workday would result in ~35 minutes of a day being misclassified, whereas 99.3% accuracy would result in just 5 minutes of misclassification. What may be even more important however is the temporal resolution of activity classification. The temporal resolution of the PDI is ~0.9 seconds. This allows the PDI to capture activity data at approximately 2x the resolution of previous research [29]. This increased temporal resolution allows for a closer look into exactly what activities a participant is doing throughout the day and enables the PDI to capture things like a brief pause while walking, or taking a few steps instead of standing still, factors that could be important to foot health.

3.4.2. Are Accelerometers Necessary?

While accelerometers are widely used in current technology and have seen widespread success at counting steps, their ability to differentiate between sitting and standing is limited. The reason for this can be seen in Figure 22, where the output from the accelerometer is nearly identical between sitting and standing. The accelerometer does have properties that can help to identify walking, but if the FSRs alone can be used for accurate classification removing the accelerometer would help to simplify the device, reducing cost and lowering power consumption. To test the importance, the accelerometer was removed from the full set of sensors and the accuracy was recorded. Removing the acceleration from the SVM classifier reduced the classification accuracy from 99.31% to 99.28%. Removing the acceleration from the MLR classifier reduced the

classification accuracy from 99.21% to 99.04%. These results show that accelerometers are not a critical component of the PDI design and removing them does not have a detrimental effect on the classification accuracy. While the accelerometer does not represent a large proportion of the entire system cost (\$10.50 CAD), removing it simplifies the design and reduces power consumption.

3.4.3. Additional Considerations

Reducing computational time was not a major consideration for this study since the data was being processed on a computer after being collected. However, a reduction in computational complexity could be useful for future applications of this technology where real-time classification may be run on a phone connected to the PDI or on the PDI itself. A trade-off does exist between the 0.20% lower classification accuracy and over 120x faster classification time.

Using the synchronization method based on heel strikes outlined in Section 2.2.6, it would not be possible for the data to be offset by more than a full step. It is therefore unlikely that synchronization would be anywhere close to the 1.98s offset considering the average step ranges from approximately 0.3-1 second during walking [103]. As a result, the synchronization method used in this analysis would have introduced at very worst a classification error of 0.5% validating the use of this method for future analysis on healthy subjects.

Much of the misclassification observed when using only one insole resulted from standing on one foot. In this posture one foot is loaded and the other is not. The PDI on the loaded foot would classify this data as standing but the device on the unloaded foot would classify it as sitting. Since it is quite common for people to stand with uneven weight distribution when they are in a natural environment this is an unacceptable misclassification and one that would result in incomplete data. This would be particularly true in a natural environment where activities are not as clear cut as they were in this study.

The sampling frequency of 45Hz used in this research had the benefit of collecting a very rich dataset. However, analysis showed that using a sampling frequency of ~5Hz in future designs would still produce excellent activity classification

accuracy. This reduced sampling frequency would reduce the size of the data files by 9x, improve computational efficiency and reduce power requirements. These are all aspects that would enable a more compact, efficient PDI design.

One weakness of this study is the relatively small number of participants that were involved ($n = 21$). While this is more subjects than any previously known work using novel instrumented shoe insoles to classify activities, it is still likely not sufficient to presume generalizability to any population. This is evident in the increased misclassification of activities in select participants (Table 7).

3.5. Future Work

While the classification algorithm developed in this research is quite good, there is still room for improvement. One particular way that this algorithm can be improved is by developing a more rigorous calibration sequence including a wider range of typical daily postures. These could include activities such as standing on toes, sitting on a stool, running, ascending or descending stairs, and crouching. Including these in the calibration sequence and labeling them as either sitting, standing or walking will enable the algorithm to classify natural environment data in a more predictable way.

In analyzing the inconsistencies in activity classification, the observation arose that simply classifying activities as sitting, standing or walking, while easy to verify on video may not be the most appropriate measure when investigating foot health. A more appropriate measure may be the overall level of force applied to one's foot or the strain put on the plantar fascia in each position. For example, if a participant is sitting on the edge of their chair for a large portion of the day with a significant amount of weight being transferred through their feet, the tissues in their feet are likely under more strain than someone who is sitting back in a chair. While not possible to classify with the data collected in this study, this could be a useful direction for future research.

Additionally, the algorithm could be trained to classify more activities than sitting, standing and walking, particularly if they have significantly different patterns of strain on the tissues of the foot. This could include activities such as running, biking, climbing and descending stairs, lifting weight, or climbing a ladder. This would potentially enable an even better understanding of a worker's activities.

Since the PDI has a sampling rate of 45 Hz, it is likely possible to use it to investigate different gait characteristics. In visually inspecting the data during walking it is possible to notice differences in the way that different subjects load their feet. Some are quite heavy on their heels causing high spikes in sensors number 5, 6 and 7 when their foot first hits the ground while others tend to walk mainly on their forefoot and toes causing a much lower spike in sensors 5, 6 and 7 and an earlier spike in sensors 1, 2, 3 and 4. These are purely observations at this point, however this may be an interesting area for future research. This also shows that the activity classification algorithms developed in this chapter are adaptable to various gait and foot loading characteristics.

Chapter 4.

Workplace Postures

4.1. Introduction

It is estimated that 10% of the global population experiences plantar foot pain at some point in their lives [14]. Studies have shown that this number rises substantially in individuals when subjected to prolonged periods of weight bearing (standing or walking) [3]. This can be seen in retail workers where 50% have reported foot pain during work [16]. Approximately 2.77 million people per year in the United States report having PF [1]. This has an estimated economic burden of \$284 million per year [2]. While the exact etiology of PF is unknown, it is thought that prolonged standing is a key contributing factor leading to microtears in the plantar fascia causing pain and inflammation [4], [51]. The US Bureau of Labour Statistics reported that 47% of workers in the US spend over 60% of their workday on their feet, which could put them at risk of developing PF [104]. However, due to a lack of objective evidence regarding workplace postures [7] the causal contribution of prolonged workplace standing on foot pain or PF has not yet been explained.

Research into risk factors for PF typically requires participants to self-report the time spent on their feet throughout the day. However, self-reporting is not an accurate measure of time spent in different activity states, as shown in a recent study where participants incorrectly reported over 3 hours of activity time over a 24 hour period [6]. Importantly, self-reporting also lacks the temporal resolution to track short duration changes in posture and total number of activity changes in a day which may affect overall plantar tissue loading exposure. While there are commercially available devices capable of human activity recognition, they either lack the ability to differentiate sitting from standing, are too expensive to deploy on a large scale, or are uncomfortable or inconvenient to use [77], [26]. Without improvements in technology, it is extremely difficult to link PF to work-related activities and differentiate individual behaviours in the same workplace. This challenge is evident in worker compensation claims where an average of 13 claims relating to PF were accepted and 39 denied per year by

WorkSafeBC between 2009 and 2013 [10]. This challenge is further exaggerated by the number of people that do not submit claims, anticipating that they will be rejected [8], [9].

Accelerometer based devices such as the activPAL use thigh-mounted accelerometers to track sitting, standing and walking [76]. While these devices are accurate, they are uncomfortable to wear and must be applied to the correct location on the body every day. Insole based devices that measure plantar pressure such as the F-scan System (Tekscan Inc., South Boston, MA, USA) can be used to differentiate activities, however they are bulky to wear and prohibitively expensive to use in a large-scale study. Research has shown that pressure sensors integrated into a shoe insole can be used to track activities, but these devices have not been validated in a workplace environment [74]. The PDI described in Chapter 2 uses low-cost pressure sensors in combination with a machine learning algorithm to provide the activity differentiation accuracy of an expensive device at a low cost.

With the PDI capable of tracking common workplace activities to over 99% accuracy in a relatively controlled environment, it is hypothesized that workplace activities can be investigated unobtrusively and objectively leading to a much more accurate picture of activities in the workplace than is possible with self-report data.

To demonstrate this, an out-of-lab study conducted using the PDI was conducted to show the feasibility of using this device in a workplace setting for an extended duration. During this study, data was collected about the activities of a group of workers in a variety of workplaces with workdays ranging from primarily sitting to primarily standing. This data was used to demonstrate the efficacy of the PDI in a wide range of workplaces. This data was then used to compare participant's self-reported activity times to the actual times recorded by the PDI to demonstrate the improvements to self-report data made possible by using such a device.

4.2. Methods

4.2.1. Participants

A total of 34 participants were recruited for this study however only data from 29 participants was used for this analysis due to incomplete or corrupt data caused by issues inherent with a hand-made prototype device. Each participant was asked to

participate for a typical workweek of 3-5 days with days ranging between 5-13 hours depending on the length of their work shift. Participant's were primarily nurses (n = 20) but also included students (n = 6), an engineer (n = 1), an administrative assistant (n = 1) and a manual labourer (n = 1).

4.2.2. Data Collection and Analysis

At the beginning of each workday, the participant's shoes were fitted with PDI insoles that recorded data throughout the day. The participant was informed that they would need to report their sitting, standing and walking times at the end of the day. At the end of each day participants were asked to report the time spent sitting, standing and walking throughout their workday. Participants were asked to report this time in hours and minutes (e.g. 4 hours and 35 minutes of sitting). The PDI insoles were removed from the participants shoes at the end of the day to collect the data and re-charge the battery. This procedure was completed each day for the duration of a participant's workweek. Activity durations were calculated from the resulting PDI data using the optimized SVM algorithm with all sensors included (99.3% accuracy) described in Chapter 3.

4.2.3. Device Validation

The PDI design criteria outlined in Section 2.2.1 were validated in an out-of-lab setting by taking the following steps:

1. Asking participants for their feedback after wearing the device each day about the PDIs comfort and obtrusiveness, and if there were any unexpected issues.
2. Testing the sensors in each PDI at the end of every day to determine if any had broken or come disconnected and checking to ensure that the battery had not run out.

4.2.4. Comparison of PDI Results to Self-report Data

Statistical analysis was completed using the Scipy Stats package for Python. A significance level of 0.05 was used for all analysis methods. The two methods (self-

report and PDI) were compared using a Bland-Altman plot to investigate the bias in measurement techniques. Additionally, a Pearson Product Correlation was used to determine if a relationship existed between the activity times reported in the self-report data and the activity times recorded by the PDI. Overall classification error was calculated as follows:

$$\text{Classification Error} = \frac{\left(\frac{\text{Sum of Overestimates} + \text{Sum of Underestimates}}{2} \right)}{\text{Measured Activity Duration}} * 100\%$$

4.3. Results

4.3.1. Participant Demographics

Data from a total of 34 participants was collected for this analysis. Device malfunctions inherent in using a hand-made prototype device occurred for five of these participants so their data was excluded leaving data from 29 participants for use in this study. The age of the participants was 32.6 ± 9.4 years (mean \pm standard deviation). There were 21 females and 8 males, with a BMI of 22.9 ± 2.9 (Table 10). These participants were primarily nurses ($n = 20$) but also included students ($n = 6$), an engineer ($n = 1$), an administrative assistant ($n = 1$) and a manual labourer ($n = 1$). The job titles were not included in the demographics table for participant privacy reasons.

Table 10 - Participant demographics

Participant	Age (years)	BMI	Height (cm)	Gender
SID01	30	23.9	171	M
SID02	27	27.0	180	M
SID03	26	21.5	178	M
SID05	22	21.7	183	M
SID06	23	26.5	168	M
SID07	31	19.0	152	F
SID08	31	19.8	160	F
SID09	25	25.8	173	F
SID10	23	21.7	183	M
SID11	27	23.7	188	M
SID12	27	18.3	165	F
SID13	27	24.3	170	M
SID14	27	20.9	171	F
SID15	30	20.7	175	F
SID16	28	24.8	163	F

Participant	Age (years)	BMI	Height (cm)	Gender
SID17	29	20.8	155	F
SID19	35	23.3	165	F
SID20	51	20.0	165	F
SID21	29	17.8	175	F
SID24	32	20.6	159	F
SID25	25	22.7	160	F
SID26	22	24.8	160	F
SID28	36	25.8	165	F
SID30	50	23.0	152	F
SID31	45	23.3	165	F
SID32	53	22.7	168	F
SID33	52	30.4	157	F
SID34	40	26.7	157	F
SID36	42	22.3	157	F

4.3.2. Workplace Activities

The total time each participant spent sitting, standing and walking was determined based on the activity classification produced by the SVM algorithm. For comparison, total time of each activity was converted to percent of workday spent doing

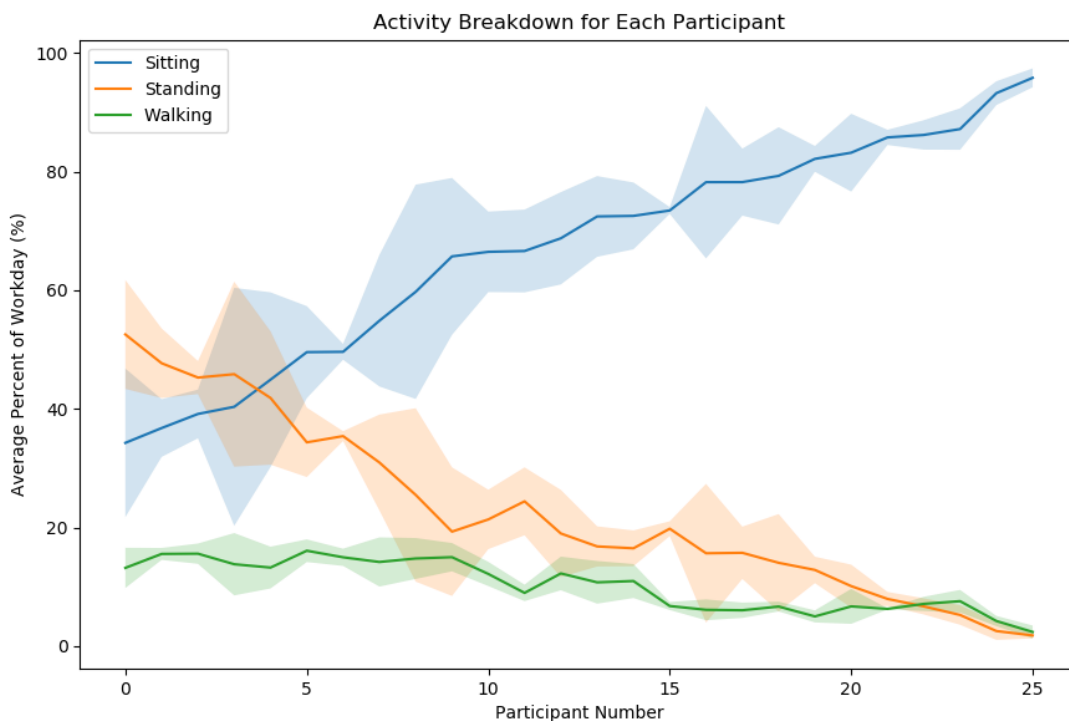


Figure 33 - Activity breakdown for each participant averaged over their workweek. Shaded regions represent +/- one standard deviation.

each activity. Mean and standard deviation were determined for each participant. The results were plotted in ascending order of percent of workday spent sitting (Figure 33).

The average time sitting throughout the workday ranged across participants from 34.26% to 95.80% with standard deviations between 0.57% and 20.05% of workday. The average time standing throughout the workday ranged from 1.81% to 52.54% with standard deviations between 0.51% and 15.59%. The average time walking throughout the workday ranged from 2.39% to 16.09% with standard deviations between 0.10% and 5.25%. Standard deviation was lower for participants who spent most of their workday sitting, and with a few exceptions increased in participants who spent more of their workday on their feet.

The average number of activity transitions throughout a participant's workday ranged from 46 to 759 (Figure 34). This indicated that some people spent most of their day doing one activity while others were almost constantly changing activities. The number of activity transitions was consistently higher for participants that spent most of their day on their feet. Standard deviation was over 100 for four participants, however,

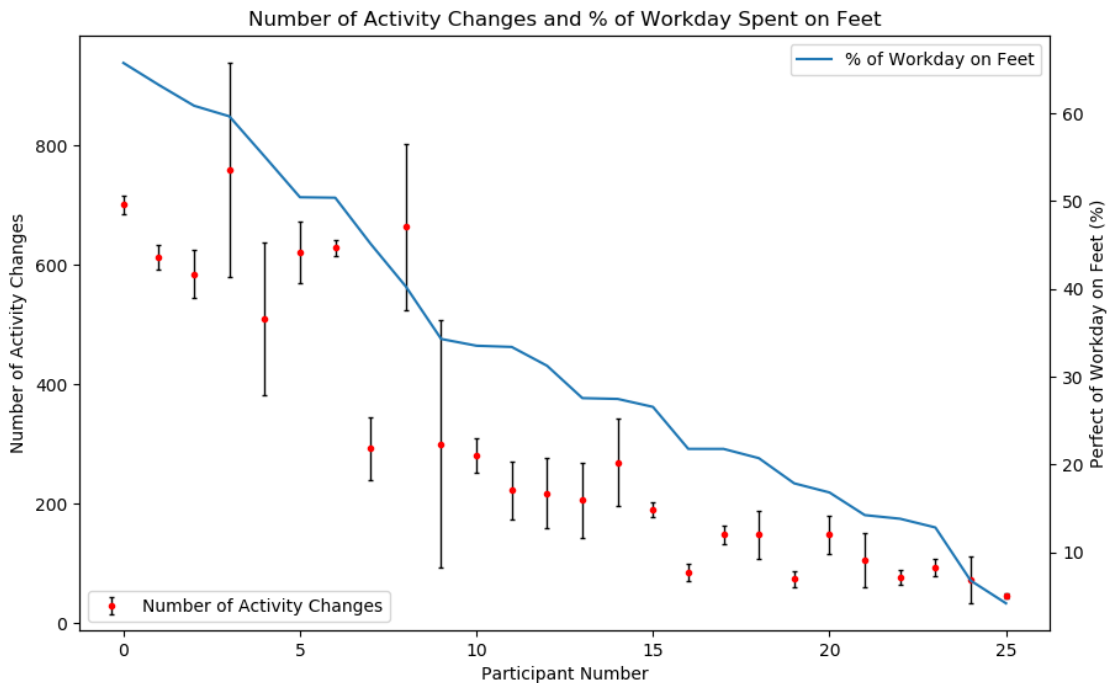


Figure 34 - Plot of the average number of activity changes made throughout the workday for each participant. Participant number is arranged in order from most time spent weight bearing to least time spent weight bearing. The error bars represent the standard deviation in activity changes throughout a participant's workdays.

was less than 75 for the rest indicating that with the exception of some participants, the number of activity changes remains relatively constant throughout a typical work week.

4.3.3. Out-of-lab PDI Design Validation

During this research, the PDI was used by 34 participants for three to five days each. There were no instances where a device fell off of a shoe, a connection cable broke, a battery ran out, an accelerometer stopped functioning, or a 3D printed case broke. This showed that the device was effective in a workplace setting. There were a number of instances where either an FSR or a wire connecting it to the connection cable broke or came unattached. See Section 2.4.1 for further discussion regarding durability.

The PDI was tested for up to 13 hours at a time in a workplace environment without any issues requiring a researcher to go to the workplace to remove the device. There were no instances where the battery ran out. This shows that the PDI is capable of capturing data for an extended period of time in a workplace setting.

The PDI was tested for a total of 133 days by 34 participants. 69% (n=92) of these days resulted in useable data where no more than one sensor per insole was malfunctioning. 30% (n=40) of these days resulted in no sensors being damaged at all. In the cases where data was not useable, 71% (n=29) were caused by the common ground wire either partially or completely disconnecting. The other 29% (n=12) of cases where data was not useable were due to an FSR sensor either becoming disconnected or degrading in sensitivity. FSR degradation was typically seen later in the week after the insole had been used for several days. It was also much more common in participants with a greater weight. This degradation resulted in much higher FSR resistances, causing lower output values.

Participants that used the PDI over the course of their workday were asked if they had any complaints about wearing the device in/on their shoes. Of 35 participants asked to wear the PDI in their natural work environment for a week, most reported not noticing the PDI at all after the first few minutes. One participant even completely forgot to return the device at the end of their workday, indicating they had forgotten the device was on their shoes. A few participants reported that their shoes felt slightly tighter than usual due to the PDI but also said that it didn't bother them too much. No participants

had to remove the insole from their shoes before the study was completed indicating that the devices were not overly uncomfortable to wear and did not interfere with the normal workday activities of the participants.

4.3.4. Classification Error

Classification error was investigated in each participant's first day of participation in the study. There is a large spread of participants both over and underestimating activity times for all activities. While some participants are nearly perfectly accurate at estimating activity times, others misclassified over 4 hours of an eight-hour day. The average difference (average of the absolute values of the differences) was used as a measure of how far off of the PDI data the self-report estimates were (either overestimate or underestimate). It was found that participants were worst at self-reporting the time spent walking with an average difference of 163% (1.7 hours). Participants typically overestimated the time they spent walking as evidenced by the number of overestimates compared to underestimates (Table 11). Participants underestimated their time standing with an average difference of 79% (1.3 hours). Participants were approximately even with regard to overestimating or underestimating the time they spent sitting with an average difference of 31% (1.5 hours). Participants were not always accurate at reporting the length of their workday, so the sum of the underestimates did not always equal the sum of the overestimates.

When classification error was calculated for all activities and averaged over the number of participants, the result was an overall classification error in the self-report data of 24%. This means on average; participants incorrectly classify 2.3 hours of their workday when asked to self-report their activities. The classification error ranged from 5% to 56% resulting in a range of 22 minutes to 5.8 hours of misclassified workplace postures when self-reported.

Table 11 – Results of comparison between self-report data and PDI data. All times are in minutes.

Participant Number	Sitting			Standing			Walking		
	Measured Time (PDI)	Difference (PDI - SR)		Measured Time (PDI)	Difference (PDI - SR)		Measured Time (PDI)	Difference (PDI - SR)	
		Minutes	%		Minutes	%		Minutes	%
SID01	274	-176	64%	21	21	100%	19	-11	54%
SID02	308	158	51%	177	-63	36%	102	12	12%
SID03	255	-105	41%	31	-29	95%	16	-44	286%
SID05	387	-53	14%	30	15	50%	34	9	27%
SID06	384	-56	15%	30	15	49%	39	14	36%
SID07	260	140	54%	118	58	49%	68	-172	255%
SID08	252	72	29%	85	-5	6%	65	-115	175%
SID09	360	-90	25%	74	74	100%	55	25	46%
SID10	409	49	12%	18	-12	69%	15	-45	302%
SID11	356	-4	1%	9	-21	236%	12	-18	158%
SID12	310	-35	11%	46	31	67%	26	-4	14%
SID13	557	17	3%	7	-8	102%	8	-37	498%
SID14	155	35	23%	431	11	3%	98	-82	84%
SID15	155	-145	93%	436	76	17%	121	61	50%
SID16	216	-54	25%	46	41	89%	38	13	34%
SID17	330	-30	9%	101	-199	197%	41	-139	336%
SID19	243	-117	48%	391	211	54%	118	-62	52%
SID20	220	100	46%	284	224	79%	111	-369	331%
SID21	307	187	61%	295	55	19%	134	-226	168%
SID24	188	-7	3%	387	87	23%	150	-90	60%
SID25	329	149	45%	305	185	61%	129	-291	227%
SID26	91	1	1%	422	302	72%	108	-282	262%
SID28	388	148	38%	262	142	54%	108	-252	234%
SID30	283	43	15%	159	39	25%	54	-66	121%
SID31	421	241	57%	32	-148	455%	19	-71	371%
SID32	401	101	25%	64	-11	18%	27	-18	65%
SID33	388	-17	4%	97	82	85%	39	9	23%
SID34	357	117	33%	106	-14	14%	39	-81	206%
SID36	347	167	48%	275	155	56%	128	-292	229%
	Average*	90	31%	Average*	80	79%	Average*	100	163%
	# of Overestimates	13		# of Overestimates	10		# of Overestimates	22	
	# of Underestimates	16		# of Underestimates	19		# of Underestimates	7	

Note: negative classification error in minutes means overestimation of time, positive value means underestimation

* Average times are calculated as the average of the absolute values of the differences in minutes

Classification error was analyzed for each activity type, standing, walking and sitting using a Bland-Altman plot. The difference data for all three activities was shown to be from a normal distribution using a D'agostino – Pearson test for normality allowing for Bland-Altman analysis. Participants underestimated their self-reported time spent standing at work (mean difference, 45.29; 95% CI, 6.05 to 84.53 minutes) (Figure 35). The 95% confidence interval of the mean difference does not overlap the zero-difference line; therefore, this is a statistically significant result. 19 participants underestimated their standing time while 10 overestimated their standing time. 13 participants were off by over an hour when estimating their standing time. There was a positive strong statistically significant correlation ($r = 0.7$; $p < 0.001$; $n = 29$) between the self-reported standing time (118 ± 114 minutes) and the standing time measured using the PDI (163 ± 145 minutes) while at work.

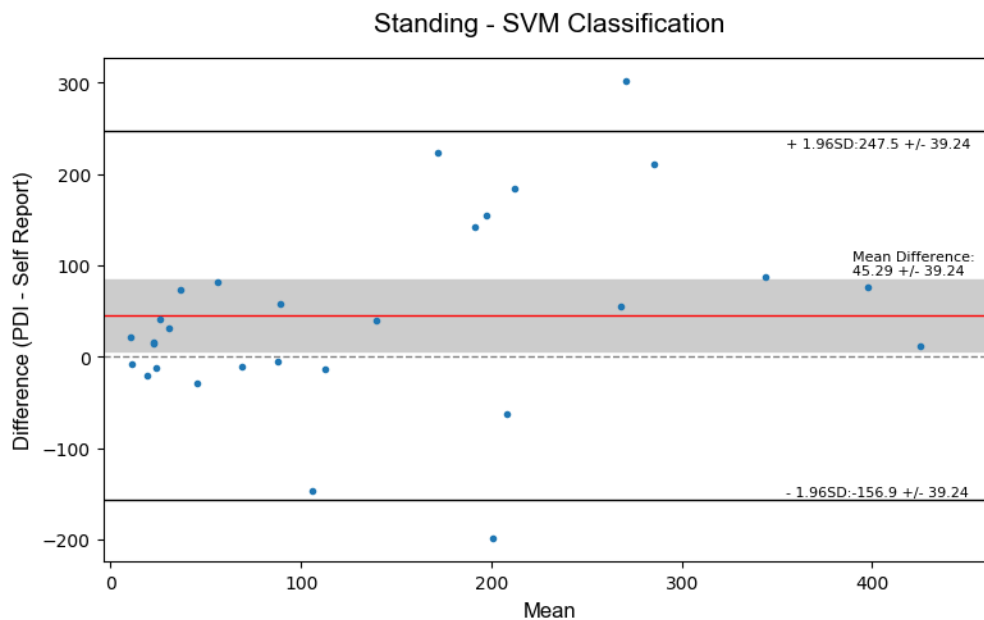


Figure 35 - Bland-Altman plot for standing classification using self-report data and PDI data. All measurements are in minutes. The grey boundary around the mean difference represents the 95% confidence interval of the mean difference value.

Participants overestimated their self-reported time spent walking at work (mean difference, -90.4; 95% CI, -47.38 to -133.42 minutes) (Figure 36). The 95% confidence interval of the mean difference does not cross the zero-difference line; therefore, this is a statistically significant result. 7 participants underestimated their walking time while 22 overestimated their walking time. 16 participants were off by over an hour when estimating their walking time. There was a positive strong statistically significant correlation ($r = 0.7$; $p < 0.001$; $n = 29$) between the self-reported walking time (157 ± 143 minutes) and the walking time measured using the PDI (66 ± 44 minutes) while at work.

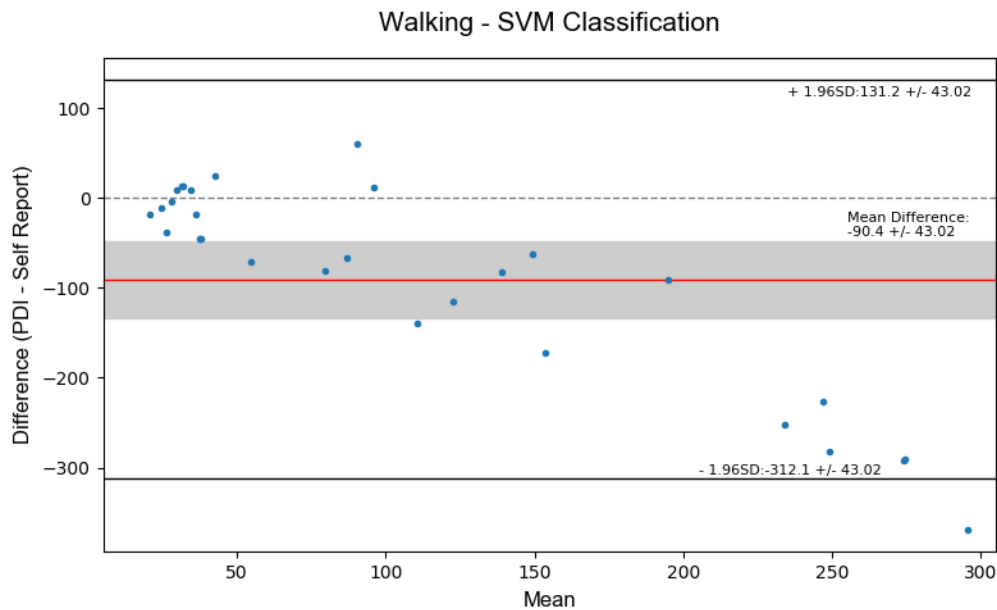


Figure 36 - Bland-Altman plot for walking classification using self-report data and PDI data. All measurements are in minutes. The grey boundary around the mean difference represents the 95% confidence interval of the mean difference value.

Figure 37 shows the Bland-Altman plot for sitting. The mean difference between the self-report data and the PDI data was 28.9 ± 40.3 minutes. This means that when self-reporting, as a whole, participants slightly underestimated the amount of time they spent sitting throughout the workday. However, since the 95% confidence interval of the mean difference slightly overlaps zero, it cannot be said that this is a statistically significant observation. 16 participants underestimated their sitting time while 13 overestimated their sitting time. 16 participants were off by over an hour when estimating their sitting time. There is a positive medium statistically significant correlation ($r = 0.5$; $p = 0.001$; $n = 29$) between the self-reported sitting time (279 ± 123 minutes) and the sitting time measured using the PDI (308 ± 96 minutes) while at work.

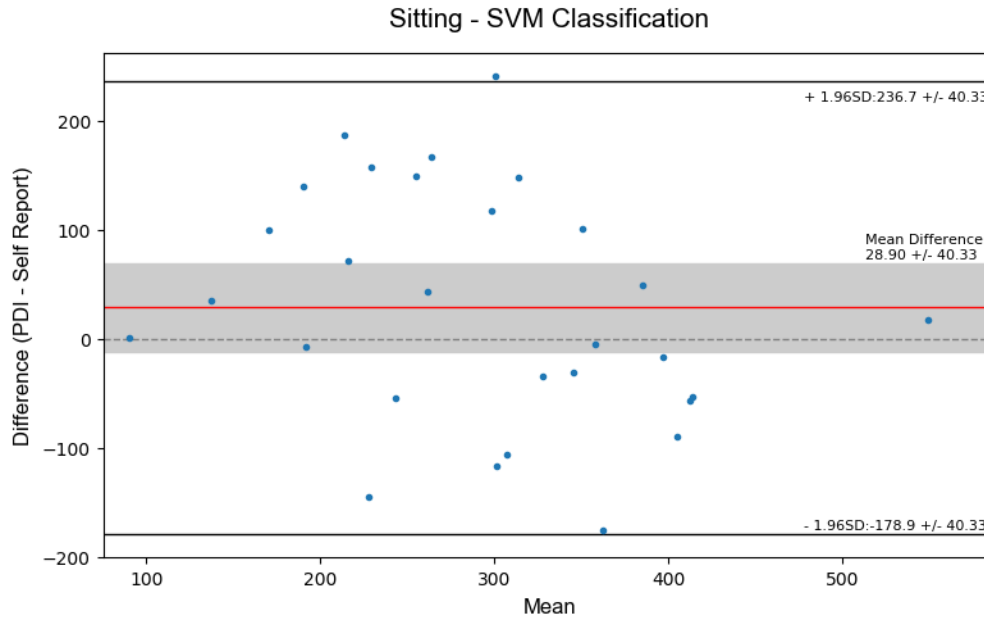


Figure 37 - Bland-Altman plot for sitting classification using self-report data and PDI data. All measurements are in minutes. The grey boundary around the mean difference represents the 95% confidence interval of the mean difference value.

4.4. Discussion

This research demonstrated the feasibility of using the PDI in a workplace setting and in doing so uncovered details about the activities of workers to a much higher degree of accuracy and temporal resolution than was possible with self-report data. While there were some malfunctions of the PDI, this is to be expected with a hand assembled prototype device when used for the first time out of the lab. While these issues had an impact on the integrity of some of the data collected, the cause was primarily due to wiring connections, something that can be easily fixed with a more robust wiring design in future versions of the device.

The other cause of data loss was the degradation of the sensitivity of the FSR. This was only apparent in the data from two participants (SID02 and SID09). This degradation was likely caused by a combination of applying too much force to the FSRs and also applying bending. It was more common for FSR-1,2,3 and 4 to malfunction in this way than FSR-5,6 or 7. This is aligned with the findings that the maximum FSR value for most participants was found in the data from FSR-1,2,3 or 4 (Table 4). FSRs in location 6 which did not break once in the 133 testing days. FSRs placed in location 7 were also quite resilient and only degraded in 9 cases.

In future revisions of the PDI design it is recommended that the FSR sensors either be placed in locations such as 6 and 7 where they are less likely to degrade in sensitivity over time, or to use a different sensor that is more resilient to the forces experienced in standing and walking. It is interesting to note that none of the studies that used these specific sensors in a shoe insole reported similar issues [41], [43], [66], [75]. This issue didn't arise until the very end of the first day of testing at the earliest, so it is likely that the experiments run in previous studies were not tested over the same duration or in situations where the user was on their feet most of the day. These situations are of critical importance, particularly for studying plantar fasciitis and other overuse injuries in the workplace, so these findings are extremely important to consider for future revisions to the PDI design.

The workplace activity times recorded from each participant showed that workers who sit for the majority of the day have less variation in their workdays than those who are on their feet for a larger portion of the workday. The variation in number of activity changes however does not follow the same trend. There were four participants with very high variation in their number of activity changes from one day to another. These four participants were all nurses who worked two day shifts followed by two night shifts. The tasks a nurse completes on a day shift are typically quite different from the tasks completed on a night shift when most patients are asleep. This is likely the cause of the variation seen in those four particular participants as the percent of workday spent on their feet also had the highest standard deviations of all participants (STD in percent of workday spent on feet: 13.2%, 14.7%, 18.1% and 20.0%).

When investigating the difference between the total time spent sitting, standing and walking, the results displayed that as the mean amount of time spent walking increases, the difference between the PDI data and self-reported data increases (Figure 36). This suggests that the more time a participant spends walking throughout the day the more they will overestimate the time they spent walking. The same relation does not appear to be true for sitting or standing. This analysis shows the variability exhibited in the difference between self-report data and the actual activity times recorded by the PDI and clearly highlights the need for an objective measurement of activity data in the workplace.

4.4.1. Implication for Research and Policy Decisions

Comparison between the self-report and PDI activity duration data showed the importance of using the PDI device in quantifying workplace exposure. Without a device to accurately measure activity times, researchers have relied on self-report data, which this study has shown to have a wide range of accuracy, with an average classification error of 24%. As a result, outcomes from research that depends on self-report data may not be completely accurate. While averaged self-reported activity values using a large number of participants may converge towards a reasonable representation of activity classifications, the higher accuracy measurement of the PDI presents the potential of reducing the number of participants required to reach statistical power in future studies.

The accuracy of self-report data identified in this study is similar to findings from previous studies investigating the use of the Occupational Sitting and Physical Activity Questionnaire (OSPAQ) for self-reporting activity durations [6],[105]. However, these previous studies used expensive or time-consuming technologies and analysis methods to accurately record workplace activities [3], [106]. The PDI provides a low-cost and easy to use tool to objectively and accurately measure workplace activities for the first time.

The results of this study show that the PDI can significantly improve on self-report data. With a device capable of providing accurate activity information with a high temporal resolution in a natural environment, researchers will be able to gain a better understanding of the precise activities of workers. This study has shown that the amount of time spent sitting, standing and walking throughout a workday cannot be accurately captured with self-report data, a finding that Waclawski et al. [7] cited as a shortcoming of existing research into the etiology of PF [3], [4], [22]. Werner et al. found that a 10% increase in the time spent weight bearing throughout the day is correlated with a 52% increase in the risk of PF [3]. The average time spent weight bearing in this cohort was 195.5 minutes, therefore; a 19.5-minute increase in the time spent weight bearing throughout the day could increase the risk of PF by 52%. To study a factor with this level of sensitivity, a classification accuracy of at least 96% is required to ensure that no more than 19.5 minutes out of an eight-hour workday is misclassified. To address increases in risk of less than 52%, even greater accuracies are required. Self-report data was shown on average to underreport standing by 45.3 minutes and overreport walking by 90.4 minutes. These misclassifications are enough to prevent research into the relationship

between time spent weight bearing and risk of plantar fasciitis, as these are over double the increase in time spent weight bearing that has been shown to affect a 52% increase in the risk of PF. Because of this shortcoming, organizations such as WorkSafeBC have been reluctant to change their policy regarding workers compensation for PF claims [10]. By conducting research using the PDI technology there is great potential to affect meaningful change to workplace safety policy and to identify the specific risk factors related to prolonged standing at work.

Future research involving tracking time for any of these activities in a workplace setting should use a device such as the PDI to quantify activity times, avoiding the inaccuracy of self-report data. Previous studies have typically been limited to measuring workplace exposure over a single day [3]–[5], [22]. These studies used a combination of self-report data, video snapshots, and in-person observation which did not capture the entirety of the day. Existing technologies to objectively measure activities are often difficult, time consuming or prohibitively expensive to use for more than a portion of a workday. Since the PDI is integrated into a worker's shoe, comes at a low cost, and is non-intrusive, it has the capability of being used for multiple days in a row giving researchers a clearer understanding of workplace activities.

4.4.2. Limitations

The PDI is a technology that is still being developed, meaning there is a chance that some of the activity data reported by the PDI may not be completely accurate. While the system was calibrated in the workplace for most participants, the collection of data over the complete workday was not directly validated. This means there is the potential for errors in the day long activity classification. This can be seen in Section 3.3.4 where cross subject validity is tested. While the PDI performs quite well on data from a new unseen participant, it does still make some errors. Additionally, the data used to calibrate the PDI was from a relatively controlled sequence of activities. Natural workplace activities may be more sporadic than this calibration data so some misclassification may result from this.

4.4.3. Natural Environment Validity

Unlike the calibration sequence, when participants were asked to use the PDI for the day while at work they were not supervised and as a result there were no solutions available for this data. The purpose of developing the classification algorithm was to acquire these solutions. To validate that the algorithm was correctly classifying the natural environment data, random samples from each participant were visually inspected. A sample of this inspection is shown with the solutions output from the trained algorithm overlaid in shades of grey (Figure 38). This classification was produced by the SVM algorithm using all seven of the FSRs but no accelerometer.

By comparing what sitting, standing and walking look like in the calibration data, it was possible to visually inspect this data and determine what portions should be sitting, standing and walking. In this case, most of the classifications appear to be correct. The first 41 seconds show low steady values from the right insole's FSRs and the values from the left insole are all zero, indicating the participant was most likely sitting cross legged with one foot completely unweighted. At 41 seconds, the subject stood as seen by a sudden spike in values from both the left and right insole. From 42-50 seconds the participant was likely standing with most of their weight on their left foot and then at 50 seconds took a few steps, paused and then walked steadily until 70 seconds. The subject then stood still until 120 seconds when they walked again, pausing briefly at 134 seconds, standing with most of their weight on their right foot. The subject then walked again until 144 seconds. The section between 144 seconds and 158 seconds was classified as sitting however may not in fact be sitting. In that time period the 4 sensors in the toe of the insole were showing high outputs and the three heel sensors were showing little or no output meaning most of the participant's weight was in their forefoot. This could either mean the participant was standing on their toes, leaning forwards, leaning against a high stool or some other posture that would have resulted in that output. While standing on toes and sitting on the edge of a high stool produced a similar loading pattern when re-created in a lab environment, there is no way to know for certain what this particular participant was doing at this moment other than knowing that there was a significant amount of force applied to the forefoot. Next, the participant walked with a brief pause at 168 seconds and then stood with relatively evenly distributed weight from 192 seconds to 211 seconds. Finally, the participant took a few steps before sitting down until the end of the snapshot. While there is one 14 second

section of data (~6%) that could be questioned, the rest of the 230 second snapshot appeared to be correctly classified. Similar results were found when visually inspecting other random samples of natural environment data from other subjects suggesting that the SVM algorithm using just FSRs was correctly classifying natural activity data.

Exemplar FSR Data for Sitting, Standing and Walking

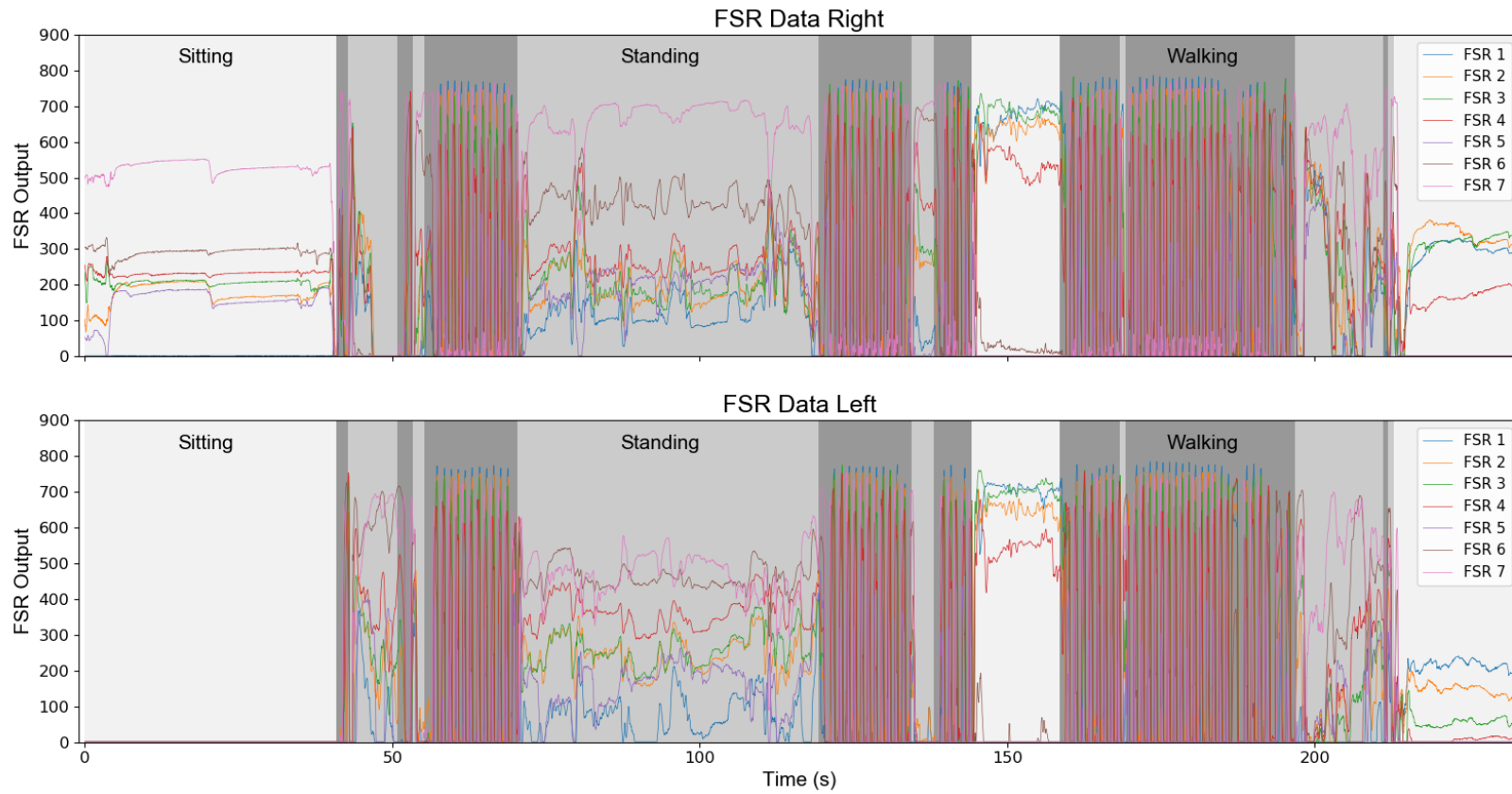


Figure 38 - Natural environment data recorded from one participant. All 7 FSRs are used in each shoe but no accelerometer is used for this classification. Solutions from the SVM classification algorithm are overlaid on top of the raw FSR signals showing the predicted activity. White is sitting, light grey is standing, and dark grey is walking.

4.5. Future Work

This research clearly shows the variability present in self-reported data. This leads to the recommendation of using a tool such as the PDI to objectively measure activities at work when studying conditions such as PF. That being said, the PDI does still have some limitations, particularly around its use in natural environments as discussed in Section 4.4.3. Future work can be done to improve on this shortcoming by obtaining training data from natural environment scenarios. This could be done by video recording participants while they are performing their normal workplace tasks. This would be a more involved process and would likely not be possible in many workplaces due to confidentiality and privacy concerns, however, would provide valuable data that has the potential to significantly improve the natural environment classification accuracy of the PDI.

Alternatively, the PDI could be trained for each specific workplace to include job relevant activities such as climbing ladders for construction workers, sitting in a car for police officers or truck drivers, or bending over and heavy lifting for warehouse staff. Training the algorithm for the activities associated with a particular workplace could help to further improve the accuracy of the PDI. If conducting research with many participants in one workplace this would be a more feasible methodology than if conducting research across multiple workplaces.

Future designs revisions of the PDI are necessary before deployment in large scale population studies. The current design has some shortcomings including the wiring design and larger than necessary form factor. Both could be addressed to create a more reliable and self-sufficient device that participants could take home with them for weeks at a time without researcher involvement.

An improved PDI could be used to characterize both total exposure and variations in exposure throughout the day for different professions. It could additionally be used to redo other exposure studies that previously used self-report data as a measure of activity classification to provide more objective results.

Chapter 5.

Effects of Workplace Standing on Plantar Foot Pain

5.1. Introduction

It is estimated that approximately 10-24% of the global population will be impacted by foot pain at some point in their lives [14], [15]. Studies have shown that this number rises substantially in individuals subjected to prolonged periods of weight bearing (standing or walking) [3]–[5]. This can be seen in retail workers where 50% have reported foot pain during work [16]. Other occupations where weight bearing is prevalent have reported similar prevalence of foot pain including assembly plant workers (69% [17]), and nurses (55 - 74% [18], [19]). While certain working populations have a higher prevalence of PF and foot pain it is not universal in such workplaces. It is therefore important to understand how workplace weight bearing interacts with other risk factors such as BMI, sex, age etc. to affect the prevalence of PF. Recent research has shown that static loading in tissues, such as that experienced in the plantar fascia when standing, can detrimental impacts on tissue structural integrity and health [56]. However the link between tissue loading and PF and generalized foot pain remains inconclusive largely due to a lack of objective evidence [7].

PF is characterized as degeneration induced by repetitive microtears in the plantar fascia [20]. PF and general plantar foot pain have been associated with multiple different factors. Older adults, particularly females have been found to have a higher prevalence of PF [107]. Increased BMI has commonly been linked to the occurrence of PF [4], [22]. Other factors that have shown some degree of correlation with PF include time spent walking [4], walking on hard surfaces [3], reduced ankle dorsiflexion [22], and calf and hamstring tightness [21]. While factors such as age, BMI and ankle dorsiflexion can be studied very accurately in relation to PF, it is much more difficult to determine the exact time that a participant spends sitting, standing or walking.

Much of the existing research attempting to link workplace activities and PF has used self-reported workplace activity durations [3], [5], [22]. Self-reported activities are known to have errors up to 24% and lack the temporal resolution to distinguish the frequency of changes in posture throughout the day. One study has been done with

multiple brief activity observations throughout the workday and showed increased changes in foot pain thresholds and higher levels of discomfort in workers who stood more throughout the day [108]. However, brief observations still ignore both the overall exposure and changes in activities throughout the day. Werner et al. used a combination of observation, video recording and pedometers to determine activity data [3]. This led to a much more complete and accurate dataset but still did not completely capture each participant's activities. It is hypothesized that objective measurement of workers activities throughout their entire day / week with a high temporal resolution, will lead to a clear link between particular workplace activities and PF and foot pain.

The lack of objective and accurate workplace activity measurements in the previous research has meant that the link between workplace activities and prevalence of PF cannot be conclusively drawn. The long-term objective of this research is to define the relationship between workplace exposure and PF. The specific objective of this chapter is to investigate correlations between foot pain and specific workplace activities when the activities are measured objectively with high temporal resolution (< 1 sec). This preliminary study will help to lay the groundwork for larger population studies including symptomatic and control groups.

5.2. Methods

34 participants were recruited to participate in this study over the course of a standard work week. Inclusion / exclusion criteria and demographics of participants is described in Section 3.2.1 as the same participant group was used throughout this thesis. The duration and location of work varied for all participants. Participants wore lace up shoes of their choice to accommodate the PDI. At the end of each workday, participants were asked to fill out the Foot and Ankle Disability Index (FADI) form (Appendix D). At the end of the first workday participants were asked to complete a demographic survey (Appendix E).

5.2.1. Activity Classification

The data from the PDI consisted of outputs from the FSRs in the insole and the accelerometer. This data was broken into samples that resulted in a temporal resolution of approximately 0.9s. Each sample showed a snapshot of the participant's activity. The

data from the calibration sequence, along with the solutions attained from the video analysis (Section 3.2.4) were used to train a machine learning algorithm to classify each of these snapshots as either sitting, standing or walking (Chapter 3). The optimized SVM algorithm using all sensors with an accuracy of 99.31% was used to classify each participant's activities throughout their workday as sitting, standing or walking.

5.2.2. Pain Measurement

The dependent variable in this study is the level of foot pain reported by the participant each day. Foot pain was measured using the FADI form. Specifically, questions 23-26 ask participants to rank their general level of pain, pain at rest, pain during normal activity, and pain first thing in the morning on a 5-point scale from '1 - no pain' to '5 - unbearable'. Participants were asked to complete a FADI form at the end of each workday.

Since the maximum value of foot pain reported in this study was two, the presence of foot pain was a binary variable with either some pain being reported, or no pain being reported. To simplify the analysis, an answer of above one on any of the questions regarding foot pain in the FADI form (questions 23-26) was deemed as having foot pain. Therefore; each day of data was classified as either having foot pain or not having foot pain.

5.2.3. Data analysis

Data from each participant's work week wearing the PDI was used in this analysis, meaning each participant contributed 2-5 days of data. Activity times for each day were analyzed in multiple ways. The first was the total amount of time that a participant spent doing each activity (sitting, standing and walking) throughout the day. This number is a good representation of overall activity exposure. Next, activities were grouped as time spent weight-bearing (standing or walking) and time spent not weight bearing. Activity data was additionally sorted into bins of time spent doing one activity before switching to a different activity. The bins selected were based on tertiles for each activity from all participants combined. Activities with a duration less than the lower cut-off of 5 seconds were removed from this analysis to remove any small incorrectly classified pieces of activity data that may cause confusing results (see section 4.4.3).

Each participant's multiple days of data was combined in two different ways to produce independent datapoints. The first method was averaging in which results for each metric were summed and divided by the number of days. This method provides an average workday exposure. This method was chosen to enable direct comparison to existing results obtained using subjective methods for workplace activity classification [3], [4]. Since averaging often removes outliers, and continuous exposure may not be the only cause of foot pain, a second analysis was conducted using data from each participant's day with the highest exposure to weight bearing activities (sum of standing and walking time).

5.2.4. Statistical Methods

Univariate analysis using t-tests (for continuous variables) or fisher exact tests (for nominal variables) was completed comparing participant demographics and job characteristics between participants with and without foot pain. Multivariable logistic regression using normalized data was used to investigate correlations between demographic factors (age, BMI, gender, dominant foot, shoe size) workplace loading and the presence of foot pain.

5.3. Results

5.3.1. Participants

Data from a total of 34 participants was collected for this analysis. Device malfunctions inherent in using a hand-made prototype device occurred for five of these participants so their data was excluded leaving data from 29 participants for use in this study. The age of the participants was 32.6 ± 9.4 years (mean \pm standard deviation). There were 21 females and 8 males, with a BMI of 22.9 ± 2.9 (Table 10). A total of 14 participants reported having foot pain (maximum FADI score of two, meaning mild average daily foot pain) and 15 reported no foot pain throughout the day.

A boxplot was used to visually analyze the data from all of the 92 available datapoints (Figure 39). This plot illustrates the relationships between sitting, standing and walking and the presence of foot pain. A trend of correlation between total time spent standing throughout the workday and foot pain is clearly seen in this plot while time spent walking has a similar but less dramatic difference. Time spent sitting appears to have no correlation with the presence of foot pain.

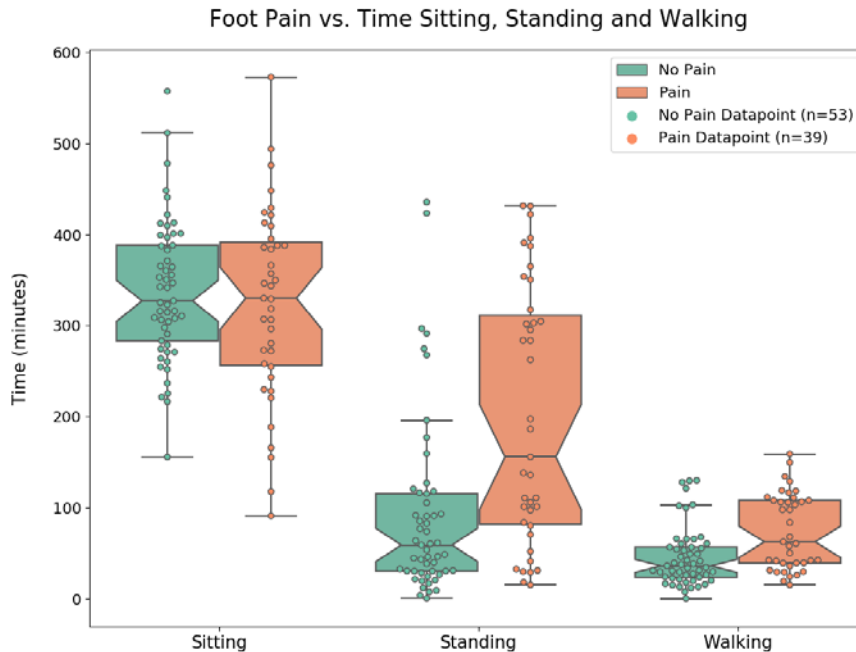


Figure 39 - Boxplot including all available data. Each activity is divided into pain and no-pain data and plotted as time spent doing each activity.

5.3.2. Averaged Days

For this portion of analysis, activity durations were averaged across all days recorded for a participant. This represents the average exposure for each participant. Results of the univariate analysis are shown in Table 11. Factors with p-values less than 0.05 were considered significantly different between the pain and no-pain groups. Time spent standing ($p = 0.01$), time spent walking ($p = 0.02$), workday duration ($p = 0.01$), and time spent weight bearing ($p = 0.01$) were significantly different between the pain and no-pain groups. This analysis does not account for relationships that may exist between factors.

Table 12 - Results of univariate analysis for an average day showing a comparison of factors between subjects with and without foot pain

Factor	Subjects with foot	Subjects without	P
	pain (n = 14)	foot pain (n = 15)	
	Mean (STD)	Mean (STD)	
Demographics			
Age (years)	33.5 (10.2)	31.7 (9.2)	0.63
BMI	23.2 (3.3)	22.6 (2.5)	0.54
Gender	12 Female / 2 Male	9 Female / 6 Male	0.21
Dominant foot	1 Left / 13 Right	0 Left / 15 Right	0.48
Shoe size (US)	7.5 (1.5)	8 (1.5)	0.48
Job Characteristics			
Time sitting (minutes)	315.4 (97.1)	337.5 (67.7)	0.48
Time standing (minutes)	216.3 (139.5)	94.4 (100.7)	0.01
Time walking (minutes)	79.9 (41.8)	46.3 (31.5)	0.02
Workday duration (minutes)	611.6 (134.6)	478.2 (124.3)	0.01
Time weight bearing (minutes)	296.2 (178.4)	140.7 (128.7)	0.01
Activity Breakdown			
Sit 5-25 sec. (count)	23.2 (29.0)	15.1 (16.3)	0.36
Sit over 146 sec. (count)	18.8 (6.7)	18.4 (7.8)	0.87
Stand 5-19 sec. (count)	59.2 (36.2)	31.8 (26.1)	0.03
Stand over 53 sec. (count)	71.2 (50.2)	31.3 (36.5)	0.02
Walk 5-12 sec. (count)	65.1 (50.6)	24.2 (28.5)	0.01
Walk over 24 sec. (count)	61.2 (42.4)	28.9 (27.8)	0.02
Activity transitions (count)	438.3 (267.8)	232.1 (192.8)	0.02

The activity breakdown data shows the average number of times that participant's activities fell into each of the bins. A participant that stood for 75 seconds and then walked for 8 seconds would add one count to the 'stand over 53 sec.' bin and one count to the 'walk 5-12 sec.' bin. This analysis is useful for looking into possible relationships between the duration of an activity, not just the sum of all activities throughout the day. This analysis showed that the duration of time sitting did not have a strong correlation with the presence of pain. While standing for both short and long periods of time had strong correlations with the presence of foot pain, standing for longer periods of time had a higher correlation with the presence of foot pain ($p = 0.02$ vs. $p = 0.03$). The opposite relationship was true for walking. Walking for short periods of time

was significantly correlated with the presence of foot pain ($p = 0.01$) and while walking for longer periods of time was still correlated with the presence of foot pain the correlation was slightly weaker ($p = 0.02$).

A multivariate logistic regression model using normalized data was built beginning with factors that had univariate p -values less than 0.25 and any additional factors that were deemed clinically relevant [109]. Time weight bearing was highly correlated with time standing and time walking (it is the sum of the two) and was therefore removed from the list of factors. BMI was included as it has widely been considered a factor related to foot pain [7]. The resulting factors used were BMI, gender, time standing, time walking, workday duration, stand 5-19s, stand over 53s, walk 5-12s, walk over 24s, and activity transitions. Factors were systematically removed based on their Wald statistic p -value indicating contribution to the model. The factor with the highest p -value was removed, the model re-fitted, and the process repeated until the p -value of the likelihood ratio test for the model was minimized. The order of removal of variables from first to last removed was activity changes, stand 5-19s, gender, walk over 24s, time walking, day duration, and BMI. The result of this analysis was a model with three factors; time standing, standing over 53s, and walking for 5-12s that was significantly correlated with the presence of foot pain ($p = 0.009$). When added into the optimized three factor model, none of the removed factors further improved the model. Each of the three factors were checked to confirm that the logit response varied linearly with the factor.

This final model displays the relative contributions of the three factors that contribute the most to the model (Table 13). None of the results are statistically significant on their own, however the model created with these three factors is statistically significant ($p = 0.009$) and it can therefore be said that total time spent standing, number of time a participant stood for more the 53 seconds, and the number of times a participant walked for 5-12 seconds are collectively correlated with the presence of foot pain.

Table 13 - Results of multivariable logistic regression for the average day with respect to the presence of foot pain.

Factor	Odds Ratio	p-value	95% Confidence Interval	
			2.5%	97.5%
Time standing	17.89	0.06	0.90	356.35
Stand over 53 sec.	0.05	0.06	0.00	1.13
Walk 5-12 sec.	1.96	0.14	0.80	4.83

Likelihood ratio test p-value = 0.009

Note: Odds ratio is based on a 10% increase in the factor value

5.3.3. Highest Exposure Day

For this portion of analysis, activity durations were taken from the day in which the participant spent the most time on their feet. This represents the participants highest exposure to foot loading throughout a typical week. Univariate analysis was only completed for the activity related factors since demographic factors did not change (Table 14). Factors with p-values less than 0.05 were considered significantly different between the pain and no-pain groups. Time spent standing ($p = 0.02$), workday duration ($p = 0.01$), and time spent weight bearing ($p = 0.03$) were significantly different between the pain and no-pain groups. This analysis does not account for relationships that may exist between factors.

Table 14 - Results of univariate analysis for highest exposure day showing a comparison of factors between subjects with and without foot pain

Factor	Subjects with foot pain (n = 14)	Subjects without foot pain (n = 15)	P
	Mean (STD)	Mean (STD)	
Job Characteristics			
Time sitting (minutes)	268.3 (90.6)	314.5 (78.5)	0.15
Time standing (minutes)	254.9 (152.5)	128.5 (116.5)	0.02
Time walking (minutes)	89.2 (45.9)	61.3 (39.6)	0.09
Workday duration (minutes)	612.46 (129.5)	504.3 (129.8)	0.01
Time weight bearing (minutes)	296.2 (178.4)	140.7 (128.7)	0.03
Activity Breakdown			
Sit 5-25 sec. (count)	22.8 (25.7)	16.2 (14.0)	0.38
Sit over 146 sec. (count)	17.0 (6.6)	18.8 (8.3)	0.52
Stand 5-19 sec. (count)	61.5 (40.9)	43.2 (30.6)	0.18

Stand over 53 sec. (count)	80.3 (57.0)	42.5 (40.1)	0.05
Walk 5-12 sec. (count)	68.9 (55.0)	36.4 (38.6)	0.07
Walk over 24 sec. (count)	64.9 (37.1)	44.9 (29.1)	0.11
Activity transitions (count)	467.5 (304.1)	305.5 (213.2)	0.10

The activity breakdown analysis showed that the duration of time was not statistically correlated with the presence of pain in any of the activities.

A multivariate logistic regression model was built using the same process as outlined above with the final number of variables being the combination that optimized overall model likelihood ratio test p-value. The order of removal of variables from first to last removed was day duration, walk over 24s, walk 5-12s, gender, time walking, BMI, stand 5-19s, and activity changes. The result of this analysis was a model that was significantly correlated with the presence of foot pain ($p = 0.01$) with two factors; time standing, and the number of times spent standing over 53s.

This final model displays the relative contributions of the two factors that contribute the most to the model (Table 15). None of the results are statistically significant on their own, however the model created with these two factors is statistically significant ($p = 0.01$) and it can therefore be said that time spent standing and times a participant stands for over 53 seconds are collectively correlated with the presence of foot pain.

Table 15 - Results of multivariable logistic regression for highest exposure day with respect to the presence of foot pain.

Factor	Odds Ratio	p-value	95% Confidence Interval	
			2.5%	97.5%
Time standing	4.60	0.05	1.00	21.27
Stand over 53 sec.	0.27	0.10	0.06	1.28

Likelihood ratio test p-value = 0.01

Note: Odds ratio is based on a 10% increase in the factor value

5.4. Discussion

The results of univariate correlation analysis show correlations between foot pain and factors including time spent standing / weight bearing throughout the workday and the duration of the workday. While these factors alone show statistically significant correlation, it is difficult to draw conclusions about causation since there is likely collinearity between many of the factors. Most notably, participants who had longer workday durations (typically nurses in this study) were also on their feet for more of the day. There were no participants to use as a control group that were sitting for the majority of the day and had a similarly long workday.

Time spent weight bearing throughout the workday and its effect on foot pain and PF has been researched multiple times finding that a 10% increase in the time standing and / or walking increases the risk of PF by 52% [3] and that spending the majority of the workday on one's feet increases the odds of presenting with PF by 3.6x [4]. Additionally Gill et al. found that a correlation exists between PF and activity level [5]. However, the methods used in these studies to determine the time a participant spent on their feet was not sufficiently accurate as previously discussed. By using the PDI, this study was able to accurately record a participant's workplace activities with a temporal resolution of less than one second and therefore obtain a clearer picture of the relationship between weight bearing and foot pain. The PDI allowed for investigation into activity intervals as small as five seconds. Based on the significance of these factors in the univariate analysis and two of these activity intervals appearing in the multivariable logistic regression this appears to be an important factor that is not possible to capture using self-reported total activity durations. The univariate analysis using an averaged day showed a strong relationship between an increased time spent weight bearing at work and the presence of foot pain ($p = 0.01$). Total time spent standing throughout the workday and time standing for over 53 seconds were both important in the multivariable logistic regression model for each analysis method, furthering the case for the suspected link between weight bearing and foot pain. This is a similar finding to previous research [3]–[5]; however, the improved methods used in this study removed much of the uncertainty identified in previous research [7]. Previous research [3]–[5] showed BMI to have an impact on the prevalence of PF, particularly in participants with BMI over 35 or weight over 200lbs. This same result was not found to be strongly correlated with the

presence of foot pain ($p = 0.54$). However, the relatively small sample size and exclusion of participants with a BMI over 30 likely had an impact on this lack of correlation.

The results from the analysis using averaged days and highest exposure day provided similar trends but different overall results. In the univariate analysis, only total time standing, workday duration and total time weight bearing were statistically significant in both models. The activity breakdown values were quite different between the two analysis methods. The lower p-values across most factors in the averaged days method indicates that it is a better method of investigation when correlating these factors to foot pain.

Total time standing throughout the workday was statistically significant when using both analysis methods for univariate analysis (averaging and highest exposure, $p = 0.01$ and 0.02 respectively) and was the most important factor with the lowest p-value using both analysis methods for multivariable logistic regression (OR = 17.89, $p = 0.06$, OR = 4.60, $p = 0.05$). This indicates that the total time spent standing throughout the workday is an important factor associated with the risk of foot pain.

The multivariable logistic regression analysis showed that total time standing, and number of times spent standing over the course of a workday had impacts on the prevalence of foot pain but did not show statistically significant results for individual factor impact. This is likely due to the relatively small number of participants ($n = 29$) and the absence of any foot pain greater than mild.

5.4.1. Limitations

This study was designed to be a pilot study laying the groundwork for future research using the PDI device. As such, there are some limitations to this study. The major limitation of this study is that data was only collected from relatively healthy participants. While some participants reported pain, it was not severe pain, and none were diagnosed with any foot pain conditions such as Plantar Fasciitis. The relatively small number of participants in this study is a limitation that has an impact on the ability to draw statistical significance from the resulting data.

No data was collected using the insole outside of work hours. Activities outside of work could impact the participant's level of pain. To begin to capture this correlation,

participants were asked to self-report their activities outside of work. Each participant only wore the device for up to five days. While this gave a good representation of their typical workweek, their activities may vary week to week and may not reflect long term exposure risk. A long-term study would be able to pick up these details and may also be able to record the onset of foot pain. The instrumented insoles used in this study are a novel technology. While the classification of activities produced by this device is quite good, it is not perfect. This can especially be seen in activities such as standing on your toes where the device could benefit from further training data.

5.5. Future Work

This work was intended to lay the groundwork for future large population studies using an improved PDI; therefore, one of the most important directions for future work is to collect data from more participants, specifically ones with strong symptoms of foot pain such as diagnosed plantar fasciitis. It is also important to ensure a wide range of characteristics such as age, BMI, and workday duration are included in the study population for both symptomatic and healthy participants. Such a dataset will enable a much more thorough statistical analysis of factors leading to foot pain.

The FADI form used to determine a participant's foot pain was not an ideal method as it asked about only the average level of pain throughout the workday on a scale of 1-5. This provided a good overall picture, but a participant could have had severe foot pain at one instance and then decided to sit down, relieving their foot pain for the rest of the day. This would have likely resulted in a relatively low FADI score which doesn't show the complete picture of the participant's day. A more thorough method of determining foot pain would be to use the FADI form but additionally ask what the worst foot pain experienced throughout the day was on a scale of 1-10. This gives more resolution to the pain measurement and gives a better picture of how pain was experienced throughout the day. Additionally, participants should be asked if they did anything throughout the day to alleviate their foot pain.

This study excluded any participants that were currently using orthotics while at work. This was done because the participant would have to remove their orthotics from their shoes to use the PDI which may have negative impacts on their foot health. This excluded many participants that were actively managing foot pain, a group that is

important to include in this research. Future studies will need to revisit this issue and devise a method of measuring activities with orthotics still in the participant's shoes or showing that removing the orthotics while using the PDI will not have negative health implications for the participant. One method of doing this may be to integrate the PDI with a custom orthotic design that can provide the same support as the participant's existing orthotics.

Chapter 6.

Contributions and Conclusions

6.1. Contributions

This work was motivated by a need for an objective measure of workplace activities to help better understand the etiology of PF highlighted by a report commissioned by WorkSafeBC [7]. Such a device, if used in a large population study has the potential to make our workplaces safer. This research has laid the groundwork for such a study by designing a device to collect data, a method of converting that data in useable metrics, and proof that such a design can be used outside of the lab.

First, a novel, low-cost, easy to use, unobtrusive highly functioning prototype device was designed and tested in a workplace setting. While placing sensors in an insole has certainly been done before, this work optimized the sensor locations for activity classification, minimized sampling frequency therefore reducing power consumption, and proved that such a device can be used in a workplace setting.

Next, a classification algorithm capable of classifying activity data at an accuracy of 99.31% (98.3% using LOOCV) was designed. Previous research has shown that activity classification is possible using instrumented shoe insoles in a controlled lab environment with a small number of participants [30], [40], [70], [71]. In contrast, this algorithm was designed and tested using data collected from 21 participants wearing their own shoes in varying workplace environments, something that has not been done before. This is a necessary step towards showing feasibility of this device in a natural workplace environment.

The results from sensor location optimization showed that FSR-6 and FSR-7 were among the most important for activity classification. This coupled with the finding that FSRs at these locations were the least likely to break provides a valuable design finding for future revisions to the PDI design. By placing sensors at these locations, the design can be more robust while still maintaining its activity classification accuracy.

Finally, results from the 29 participants who were successfully monitored in their workplace over the course of a week show that total time spent standing and time spent standing for over 53 seconds are important factors associated with the presence of foot pain.

6.2. Limitations of the Research

Although limitations have been discussed throughout this work, a number of overarching limitations are worth mentioning. First, the data collected in the workplace setting was completely unsupervised and therefore no answers exist. While every attempt was made to interpret the data (visual inspection, recreation of activities, algorithm activity detection) there may still be incorrectly classified portions of data that may have an impact on the results found in Chapter 4 and Chapter 5. Additionally, the activities captured in the 'algorithm training' component of this research do not encompass all possible workplace activities. Training the algorithm with a larger dataset including more variety of activities could result in a more robust classification of activities. While data from more participants ($n = 21$) was used to train the activity classification algorithm than in previous work using instrumented shoe insoles for activity classification [30], [40], [70], [71], the limited number means that the algorithm may not be able to generalize to an entire population. Finally, there were no participants that experienced greater than mild foot pain throughout the course of this study. Future studies including symptomatic participants will be better equipped to conclusively determine correlation between workplace activities and PF.

6.3. Future Research Directions

While the PDI has been developed as a highly functioning prototype there are still several aspects that can be improved upon to prepare the device for future research applications. These include:

1. **Sensor longevity:** There were a number of instances where the Interlink FSR 402 sensors chosen for this device either came disconnected or degraded in sensitivity over time. While understandable in a prototype device, this must be improved upon before use in a population study. Suggestions for this improvement include investigating alternative sensors such as capacitive

sensors, integrating the wiring and sensors all into one custom flexible electronic component, or decreasing the sensor area to reduce the total pressure applied to it.

2. **Natural environment training:** The activity classification algorithm developed could potentially benefit from training data involving more natural environment activities such as standing on toes, crouching or climbing ladders.
3. **Is activity the right thing to classify?:** The results of this research have led to the question of whether classifying activities as sitting, standing or walking is an appropriate method when investigating workplace exposure in relation to foot pain. A more appropriate measure may be the total pressure applied to the foot or some other measure of tissue stress experienced in the workplace.
4. **Miniaturization of the PDI:** While participants were overall very receptive to the PDI and typically reported not noticing it by the end of the day, most did want to see something with a sleeker, less noticeable design. In particular the components housed in the box attached to the outside of the shoe could be miniaturized and moved to inside of the insole.

6.4. Significance

The work completed in this thesis has built upon previous research identifying potential locations for sensors in an instrumented insole to produce these most significant outcomes:

1. Developing the PID, a low-cost easy to use technology for objectively measuring workplace activities.
2. Designing an algorithm to accurately classify workplace activities from the data collected by the PDI.

3. Using the PDI in a 34 person out-of-lab research study showing the efficacy of the device and obtain preliminary results linking workplace standing to the presence of foot pain.

As a whole these outcomes lay a strong foundation to build upon in future population studies using the PDI to better understand the causes of foot pain.

References

- [1] R. L. Nahin, "Prevalence and Pharmaceutical Treatment of Plantar Fasciitis in United States Adults," *J. Pain*, vol. 19, no. 8, pp. 885–896, 2018.
- [2] K. B. Tong and J. Furia, "Economic burden of plantar fasciitis treatment in the United States.," *Am. J. Orthop.*, vol. 39, no. 5, pp. 227–31, May 2010.
- [3] R. A. Werner, N. Gell, M. Pt, A. Hartigan, N. Wiggerman, and W. M. Keyserling, "Risk Factors for Plantar Fasciitis Among Assembly Plant Workers," *PM&R*, vol. 2, no. 2, pp. 110–116, 2010.
- [4] D. L. Riddle, M. Pulisic, P. Pidcoe, and R. E. Johnson, "Risk factors for Plantar fasciitis: a matched case-control study," *J Bone Jt. Surg Am*, vol. 85-A, no. 5, pp. 872–877, 2003.
- [5] L. H. Gill and G. M. Kiebzak, "Outcome of Nonsurgical Treatment for Plantar Fasciitis," *Foot Ankle Int.*, vol. 17, no. 9, pp. 527–532, 1996.
- [6] J. L. Urda, B. Larouere, S. D. Verba, and J. S. Lynn, "Comparison of subjective and objective measures of office workers' sedentary time," *Prev. Med. Reports*, vol. 8, pp. 163–168, Dec. 2017.
- [7] E. R. Waclawski, J. Beach, A. Milne, E. Yacyshyn, and D. M. Dryden, "Systematic review: plantar fasciitis and prolonged weight bearing," *Occup. Med. (Chic. Ill)*., vol. 65, pp. 97–106, 2015.
- [8] S. Stock, N. Nicolakakis, H. Raïq, K. Messing, K. Lippel, and A. Turcot, "Underreporting work absences for nontraumatic work-related musculoskeletal disorders to workers' compensation: Results of a 2007-2008 survey of the Québec working population," *Am. J. Public Health*, vol. 104, no. 3, pp. 94–102, 2014.
- [9] M. E. Major and N. Vézina, "Analysis of worker strategies: A comprehensive understanding for the prevention of work related musculoskeletal disorders," *Int. J. Ind. Ergon.*, vol. 48, pp. 149–157, 2015.
- [10] Workers' Compensation Board of British Columbia and WorkSafeBC.com, "Plantar Fasciitis Due to Prolonged Weight Bearing," 2014.
- [11] D. Singh, J. Angel, G. Bentley, and S. G. Trevino, "Fortnightly Review: Plantar Fasciitis," *Br. Med. J.*, vol. 315, no. 7101, pp. 172–175, 1997.
- [12] L. Luffy, J. Grosel, R. Thomas, and E. So, "Plantar fasciitis," *J. Am. Acad. Physician Assist.*, vol. 31, no. 1, pp. 20–24, 2018.

- [13] D. Schopflocher, P. Taenzer, and R. Jovey, "The prevalence of chronic pain in Canada How Prevalent Is CP?"
- [14] P. Gautham, S. Nuhmani, and S. J. Kachanathu, "Plantar fasciitis - An update," *Bangladesh Journal of Medical Science*, vol. 14, no. 1. pp. 3–8, 2015.
- [15] M. J. Thomas, E. Roddy, W. Zhang, H. B. Menz, M. T. Hannan, and G. M. Peat, "The population prevalence of foot and ankle pain in middle and old age: A systematic review," *Pain*, vol. 152, no. 12, pp. 2870–2880, 2011.
- [16] D. Anton and D. L. Weeks, "Prevalence of work-related musculoskeletal symptoms among grocery workers," *Int. J. Ind. Ergon.*, vol. 54, pp. 139–145, Jul. 2016.
- [17] J. R. Jefferson, "The Effect of Cushioning Insoles on Back and Lower Extremity Pain in an Industrial Setting," *Workplace Health Saf.*, vol. 61, no. 10, pp. 451–457, 2013.
- [18] L. F. Reed, D. Battistutta, J. Young, and B. Newman, "Prevalence and risk factors for foot and ankle musculoskeletal disorders experienced by nurses," *BMC Musculoskelet. Disord.*, vol. 15, p. 196, 2014.
- [19] A. Sheikhzadeh, C. Gore, J. D. Zuckerman, and M. Nordin, "Perioperating nurses and technicians' perceptions of ergonomic risk factors in the surgical environment," *Appl. Ergon.*, vol. 40, no. 5, pp. 833–839, 2009.
- [20] J. Orchard, "Plantar Fasciitis," *Br. Med. J.*, vol. 345, 2012.
- [21] J. M. Labovitz, J. Yu, and C. Kim, "The Role of Hamstring Tightness in Plantar Fasciitis "," *Foot Ankle Spec.*, vol. 4, no. 3, 2011.
- [22] D. B. Irving, J. L. Cook, M. A. Young, and H. B. Menz, "Obesity and pronated foot type may increase the risk of chronic plantar heel pain: a matched case-control study," *BMC Musculoskelet. Disord.*, vol. 8, pp. 41–41, 2007.
- [23] S. J. Pedersen, C. M. Kitic, M.-L. Bird, C. P. Mainsbridge, and P. D. Cooley, "Is self-reporting workplace activity worthwhile? Validity and reliability of occupational sitting and physical activity questionnaire in desk-based workers," *BMC Public Health*, vol. 16, 2016.
- [24] C. C. Yang and Y. L. Hsu, "A review of accelerometry-based wearable motion detectors for physical activity monitoring," *Sensors*, vol. 10, no. 8, pp. 7772–7788, 2010.
- [25] O. Aziz, S. N. Robinovitch, and E. J. Park, "Identifying the number and location of body worn sensors to accurately classify walking, transferring and sedentary activities," *IEEE Trans. Inf. Technol. Biomed. Conf. IEEE Eng. Med. Biol. Soc.*, vol. 2016-Octob, pp. 5003–5006, 2016.

- [26] M. Ermes, J. Pärkkä, J. Mäntyjärvi, and I. Korhonen, "Detection of daily activities and sports with wearable sensors in controlled and uncontrolled conditions," *IEEE Trans. Inf. Technol. Biomed.*, vol. 12, no. 1, pp. 20–26, 2008.
- [27] J. A. Steeves *et al.*, "Ability of thigh-worn actigraph and activpal monitors to classify posture and motion," *Med. Sci. Sports Exerc.*, vol. 47, no. 5, pp. 952–959, 2015.
- [28] E. Fortune, V. A. Lugade, and K. R. Kaufman, "Posture and Movement Classification: The Comparison of Tri-Axial Accelerometer Numbers and Anatomical Placement," *J. Biomech. Eng.*, vol. 136, no. 5, p. 051003, 2014.
- [29] E. S. Sazonov, G. Fulk, J. Hill, Y. Schutz, and R. Browning, "Monitoring of posture allocations and activities by a shoe-based wearable sensor," *IEEE Trans. Biomed. Eng.*, vol. 58, no. 4, pp. 983–990, 2011.
- [30] N. Hegde, M. Bries, E. Melanson, and E. Sazonov, "One size fits all electronics for insole-based activity monitoring," *Proc. Annu. Int. Conf. IEEE Eng. Med. Biol. Soc. EMBS*, vol. 35487, pp. 3564–3567, 2017.
- [31] A. M. Tan, F. K. Fuss, Y. Weizman, Y. Woudstra, and O. Troynikov, "Design of Low Cost Smart Insole for Real Time Measurement of Plantar Pressure," *Procedia Technol.*, vol. 20, pp. 117–122, 2015.
- [32] C. Moufawad el Achkar, C. Lenbole-Hoskovec, A. Paraschiv-Ionescu, K. Major, C. Büla, and K. Aminian, "Classification and characterization of postural transitions using instrumented shoes," *Med. Biol. Eng. Comput.*, vol. 56, no. 8, pp. 1403–1412, 2018.
- [33] C. A. Macleod, B. A. Conway, D. B. Allan, and S. S. Galen, "Development and validation of a low-cost, portable and wireless gait assessment tool," *Med. Eng. Phys.*, vol. 36, pp. 541–546, 2014.
- [34] OpenStax, *Anatomy and Physiology*. Houston, TX: OpenStax CNX, Retrieved from: <https://openstax.org/details/books/anatomy-and-physiology>, 2013.
- [35] H. Gray and W. H. Lewis, *Anatomy of the human body*, 20th ed., by Warr... Lea & Febiger, 1924.
- [36] D. A. Winter, "Kinematic and kinetic patterns in human gait: Variability and compensating effects," *Hum. Mov. Sci.*, vol. 3, no. 1–2, pp. 51–76, 1984.
- [37] J. Perry and J. Burnfield, *Gait Analysis: Normal and Pathological Function*. Slack Incorporated, 2010.

- [38] D. M. Karantonis, M. R. Narayanan, M. Mathie, N. H. Lovell, and B. G. Celler, "Implementation of a real-time human movement classifier using a triaxial accelerometer for ambulatory monitoring," *IEEE Trans. Inf. Technol. Biomed.*, vol. 10, no. 1, pp. 156–167, 2006.
- [39] E. K. Antonsson and R. W. Mann, "The Frequency Content of Gait," *J. Biomech.*, vol. 18, no. 1, pp. 39–47, 1985.
- [40] E. Sazonov, N. Hegde, R. C. Browning, E. L. Melanson, and N. A. Sazonova, "Posture and Activity Recognition and Energy Expenditure Estimation in a Wearable Platform," *IEEE J. Biomed. Heal. Informatics*, vol. 19, no. 4, pp. 1339–1346, 2015.
- [41] M. Chen, B. Huang, K. K. Lee, and Y. Xu, "An intelligent shoe-integrated system for plantar pressure measurement," *IEEE Int. Conf. Robot. Biomimetics*, pp. 416–421, 2006.
- [42] F. Lin, A. Wang, Y. Zhuang, M. R. Tomita, and W. Xu, "Smart Insole: A Wearable Sensor Device for Unobtrusive Gait Monitoring in Daily Life," *IEEE Trans. Ind. Informatics*, vol. 12, no. 6, pp. 2281–2291, 2016.
- [43] A. M. Howell, T. Kobayashi, H. A. Hayes, K. B. Foreman, and S. J. M. Bamberg, "Kinetic gait analysis using a low-cost insole," *IEEE Trans. Biomed. Eng.*, vol. 60, no. 12, pp. 3284–3290, 2013.
- [44] "F-Scan System." [Online]. Available: <https://www.tekscan.com/products-solutions/systems/f-scan-system>. [Accessed: 23-Oct-2018].
- [45] M. Teymouri, F. Halabchi, M. Mirshahi, M. A. Mansournia, A. M. Ahranjani, and A. Sadeghi, "Comparison of plantar pressure distribution between three different shoes and three common movements in futsal," *PLoS One*, vol. 12, no. 10, p. e0187359.
- [46] E. Teh, L. F. Teng, R. Acharya U, T. P. Ha, E. Goh, and L. C. Min, "Static and frequency domain analysis of plantar pressure distribution in obese and non-obese subjects," *J. Bodyw. Mov. Ther.*, vol. 10, no. 2, pp. 127–133.
- [47] R. Periyasamy, A. Mishra, S. Anand, and A. C. Ammini, "Preliminary investigation of foot pressure distribution variation in men and women adults while standing," *Foot (Edinb)*, vol. 21, no. 3, p. 142.
- [48] M. J. Hessert, M. Vyas, J. Leach, K. Hu, L. A. Lipsitz, and V. Novak, "Foot pressure distribution during walking in young and old adults," *BMC Geriatr.*, vol. 5, no. 8, 2005.
- [49] L. A. Kelly, D. J. Farris, A. G. Cresswell, and G. A. Lichtwark, "Intrinsic foot muscles contribute to elastic energy storage and return in the human foot," *J. Appl. Physiol.*, vol. 126, no. 1, p. 231.

- [50] R. F. Ker, M. B. Bennett, S. R. Bibby, and R. C. Kester, "The spring in the arch of the human foot," *Nature*, vol. 325, pp. 147–149, 1987.
- [51] R. Puttaswamaiah and P. Chandran, "Degenerative plantar fasciitis: A review of current concepts," *Foot*, vol. 17, pp. 3–9, 2007.
- [52] D. De Garceau, D. Dean, S. M. Requejo, and D. B. Thordarson, "The Association Between Diagnosis of Plantar Fasciitis and Windlass Test Results," *Foot Ankle Int.*, vol. 24, no. 3, pp. 251–255, 2003.
- [53] R. Lucas and M. Cornwall, "Influence of foot posture on the functioning of the windlass mechanism," *Foot (Edinb.)*, vol. 30, p. 38.
- [54] L. A. Bolgla and T. R. Malone, "Plantar fasciitis and the windlass mechanism: a biomechanical link to clinical practice," *J. Athl. Train.*, vol. 39, no. 1, p. 77.
- [55] J. L. Thomas *et al.*, "The Diagnosis and Treatment of Heel Pain: A Clinical Practice Guideline," *J. Foot Ankle Surg.*, vol. 49, pp. S1–S19, 2010.
- [56] T. Wang *et al.*, "Programmable Mechanical Stimulation Influences Tendon Homeostasis in a Bioreactor System," *Biotechnol. Bioeng.*, vol. 110, pp. 1495–1507, 2013.
- [57] J. Y. Chau, H. P. Van Der Ploeg, S. Dunn, J. Kurko, and A. E. Bauman, "Validity of the occupational sitting and physical activity questionnaire," *Med. Sci. Sports Exerc.*, vol. 44, no. 1, pp. 118–125, 2012.
- [58] J. Jancey, M. Tye, S. McGann, K. Blackford, and A. H. Lee, "Application of the Occupational Sitting and Physical Activity Questionnaire (OSPAQ) to office based workers," *BMC Public Health*, vol. 14, p. 762, 2014.
- [59] N. Twomey, T. Diethe, and X. Fafoutis, "A Comprehensive Study of Activity Recognition Using Accelerometers," *Informatics*, vol. 5, no. 27, pp. 1–37, 2018.
- [60] Z. He and L. Jin, "Activity recognition from acceleration data based on discrete cosine transform and SVM," *Conf. Proc. - IEEE Int. Conf. Syst. Man Cybern.*, no. October, pp. 5041–5044, 2009.
- [61] K. Altun and B. Barshan, *Human Activity Recognition Using Inertial/Magnetic Sensor Units*. Berlin, Heidelberg: Springer, 2010.
- [62] N. Pham and T. Abdelzaher, "Robust Dynamic Human Activity Recognition Based on Relative Energy Allocation," in *Distributed Computing in Sensor Systems*, 2008, pp. 525–530.
- [63] Ó. D. Lara, A. J. Pérez, M. A. Labrador, and J. D. Posada, "Centinela: A human activity recognition system based on acceleration and vital sign data," *Pervasive Mob. Comput.*, vol. 8, no. 5, pp. 717–729, 2012.

- [64] A. M. Khan, Y. K. Lee, S. Y. Lee, and T. S. Kim, "A triaxial accelerometer-based physical-activity recognition via augmented-signal features and a hierarchical recognizer," *IEEE Trans. Inf. Technol. Biomed.*, vol. 14, no. 5, pp. 1166–1172, 2010.
- [65] A. R. Hellstrom, A. Åkerberg, M. Ekström, and M. Folke, "Walking Intensity Estimation with a Portable Pedobarography System," *Stud. Health Technol. Inform.*, vol. 224, pp. 27–32, 2016.
- [66] S. J. M. Bamberg, A. Y. Benbasat, D. M. Scarborough, D. E. Krebs, and J. a Paradiso, "Gait analysis using a shoe-integrated wireless sensor system.," *IEEE Trans. Inf. Technol. Biomed.*, vol. 12, no. 4, pp. 413–23, 2008.
- [67] S. Corbellini, C. Ramella, C. Fallauto, M. Pirola, S. Stassi, and G. Canavese, "Low-cost wearable measurement system for continuous real-time pedobarography," *2015 IEEE Int. Symp. Med. Meas. Appl. MeMeA 2015 - Proc.*, pp. 639–644, 2015.
- [68] D. A. Jacobs and D. P. Ferris, "Evaluation of a low-cost pneumatic plantar pressure insole for predicting ground contact kinetics," *J. Appl. Biomech.*, vol. 32, no. 2, pp. 215–220, 2016.
- [69] L. Shu, T. Hua, Y. Wang, Q. Qiao Li, D. D. Feng, and X. Tao, "In-shoe plantar pressure measurement and analysis system based on fabric pressure sensing array.," *IEEE Trans. Inf. Technol. Biomed.*, vol. 14, no. 3, pp. 767–775, 2010.
- [70] B. Chen, X. Wang, Y. Huang, K. Wei, and Q. Wang, "A foot-wearable interface for locomotion mode recognition based on discrete contact force distribution," *Mechatronics*, vol. 32, pp. 12–21, 2015.
- [71] F. Kawsar, M. K. Hasan, R. Love, and S. I. Ahamed, "A novel activity detection system using plantar pressure sensors and Smartphone," *Proc. - Int. Comput. Softw. Appl. Conf.*, vol. 1, pp. 44–49, 2015.
- [72] K. J. Merry, "Differentiating Common Workplace Postures through Plantar Pressure : Laying the Groundwork for a Low- Cost Instrumented Insole," Simon Fraser University, 2017.
- [73] F. El-Amrawy and M. I. Nounou, "Are Currently Available Wearable Devices for Activity Tracking and Heart Rate Monitoring Accurate, Precise, and Medically Beneficial?," *Healthc. Inform. Res.*, vol. 21, no. 4, pp. 315–320, 2015.
- [74] E. S. Sazonov, N. Hegde, and W. Tang, "Development of SmartStep: An insole-based physical activity monitor," *Proc. Annu. Int. Conf. IEEE Eng. Med. Biol. Soc. EMBS*, pp. 7209–7212, 2013.
- [75] N. Hegde and E. S. Sazonov, "SmartStep 2.0 - A completely wireless, versatile insole monitoring system," *Proc. - 2015 IEEE Int. Conf. Bioinforma. Biomed. BIBM 2015*, pp. 746–749, 2015.

- [76] J. Klenk *et al.*, “Concurrent Validity of activPAL and activPAL3 Accelerometers in Older Adults,” *J. Aging Phys. Act.*, vol. 24, pp. 444–450, 2016.
- [77] O. Aziz, S. N. Robinovitch, and E. J. Park, “Identifying the number and location of body worn sensors to accurately classify walking, transferring and sedentary activities,” *IEEE Trans. Inf. Technol. Biomed. Conf. IEEE Eng. Med. Biol. Soc.*, pp. 5003–5006, Aug. 2016.
- [78] S. Zihajehzadeh and E. J. Park, “Regression model-based walking speed estimation using wrist-worn inertial sensor,” *PLoS One*, vol. 11, no. 10, pp. 1–16, 2016.
- [79] A. Jain and V. Kanhangad, “Human Activity Classification in Smartphones Using Accelerometer and Gyroscope Sensors,” *IEEE Sens. J.*, vol. 18, no. 3, pp. 1169–1177, 2018.
- [80] J. Cheng, O. Amft, and P. Lukowicz, “Active capacitive sensing : exploring a new wearable sensing modality for activity recognition Active Capacitive Sensing : Exploring a New Wearable Sensing Modality for Activity,” *Proc. 8th Int. Conf. Pervasive Comput.*, pp. 319–336, 2010.
- [81] R. A. Lakho, Z. Yi-Fan, J. Jin-Hua, H. Cheng-Yu, and Z. Ahmed Abro, “A smart insole for monitoring plantar pressure based on the fiber Bragg grating sensing technique,” *Text. Res. J.*, vol. 89, no. 17, pp. 3433–3446, 2019.
- [82] S. Parmar, I. Khodasevych, and O. Troynikov, “Evaluation of flexible force sensors for pressure monitoring in treatment of chronic venous disorders,” *Sensors*, vol. 17, no. 8, pp. 1–18, 2017.
- [83] D. Anguita, A. Ghio, L. Oneto, X. Parra, and J. L. Reyes-Ortiz, “A Public Domain Dataset for Human Activity Recognition Using Smartphones,” in *European Symposium on Artificial Neural Networks, Computational Intelligence and Machine Learning*, 2013, pp. 437–442.
- [84] M. Morrow, W. Hurd, E. Fortune, V. Lugade, and K. Kaufman, “Accelerations of the Waist and Lower Extremities over a Range of Gait Velocities to Aid in Activity Monitor Selection for Field- Based Studies,” *J. Appl. Biomech.*, vol. 46, no. 4, pp. 564–574, 2011.
- [85] K. Merry, M. MacPherson, E. Macdonald, M. Ryan, E. J. Park, and C. Sparrey, “Differentiating Sitting, Standing and Walking Through Regional Plantar Pressure Characteristics,” *J. Biomech. Eng.*, Oct. 2019.
- [86] P. R. Cavanagh and J. S. Ulbrecht, “Clinical plantar pressure measurement in diabetes: rationale and methodology,” *Foot*, vol. 4, no. 3, pp. 123–135, 1994.
- [87] J. K. Gurney, U. G. Kersting, and D. Rosenbaum, “Between-day reliability of repeated plantar pressure distribution measurements in a normal population,” *Gait Posture*, vol. 27, pp. 706–709, 2008.

- [88] S. J. Ellis, H. Stoecklein, J. C. Yu, G. Syrkin, H. Hillstrom, and J. T. Deland, "The Accuracy of an Automasking Algorithm in Plantar Pressure Measurements," *HSS J.*, vol. 7, no. 1, pp. 57–63, 2011.
- [89] G. Giakas and V. Baltzopoulos, "Time and frequency domain analysis of ground reaction forces during walking: An investigation of variability and symmetry," *Gait Posture*, vol. 5, no. 3, pp. 189–197, 1997.
- [90] A. M. Howell and S. M. Bamberg, "Insole-based gait analysis," vol. 1509335, no. May, p. 46, 2012.
- [91] H. Sadeghi, P. Allard, F. Prince, and H. Labelle, "Symmetry and limb dominance in able-bodied gait: a review," *Gait Posture*, vol. 12, no. 1, pp. 34–45, Sep. 2000.
- [92] M. J. McGrath and C. N. Scanail, *Sensor technologies: healthcare, wellness and environmental applications*. Berkley, CA: Apress, 2013.
- [93] A. Ignatov, "Real-time human activity recognition from accelerometer data using Convolutional Neural Networks," *Appl. Soft Comput.*, vol. 62, pp. 915–922, 2018.
- [94] M. Zeng *et al.*, "Convolutional Neural Networks for Human Activity Recognition using Mobile Sensors," in *6th International Conference on Mobile Computing, Applications and Services*, 2015, pp. 197–205.
- [95] C. M. Archer, J. Lach, S. Chen, M. F. Abel, and B. C. Bennett, "Activity classification in users of ankle foot orthoses," *Gait Posture*, vol. 39, pp. 111–117, 2014.
- [96] L. Claverie, A. Ille, and P. Moretto, "Discrete sensors distribution for accurate plantar pressure analyses," *Med. Eng. Phys.*, vol. 38, pp. 1489–1494, 2016.
- [97] S. Maldonado and R. Weber, "A wrapper method for feature selection using Support Vector Machines," *Inf. Sci. (Ny)*, vol. 179, no. 13, pp. 2208–2217, Jun. 2009.
- [98] D. A. Salazar, J. Iván Vélez, and J. C. Salazar, "Comparison between SVM and Logistic Regression: Which One is Better to Discriminate?," *Rev. Colomb. Estadística*, vol. 35, no. 2, pp. 223–237, 2012.
- [99] S. Chatterjee and A. S. Hadi, *Regression analysis by example*, 5th ed. Wiley, 2012.
- [100] B. Kalantar, B. Pradhan, S. A. Naghibi, A. Motevalli, and S. Mansor, "Assessment of the effects of training data selection on the landslide susceptibility mapping: a comparison between support vector machine (SVM), logistic regression (LR) and artificial neural networks (ANN)," *Geomatics, Nat. Hazards Risk*, vol. 9, no. 1, pp. 49–69, 2018.

- [101] O. Aziz *et al.*, "Validation of accuracy of SVM-based fall detection system using real-world fall and non-fall datasets," *PLoS One*, 2017.
- [102] E. Halilaj, A. Rajagopal, M. Fiterau, J. L. Hicks, T. J. Hastie, and S. L. Delp, "Machine learning in human movement biomechanics: Best practices, common pitfalls, and new opportunities," *J. Biomech.*, vol. 81, pp. 1–11, 2018.
- [103] N. Sekiya, H. Nagasaki, H. Ito, and T. Furuna, "Optimal Walking in Terms of Variability in Step Length," *J. Orthop. Sport. Phys. Ther.*, vol. 26, pp. 266–272, 1997.
- [104] United States Bureau of Labour Statistics, "Standing or walking versus sitting on the job in 2016." .
- [105] S. J. Pedersen, C. M. Kitic, M.-L. Bird, C. P. Mainsbridge, and P. D. Cooley, "Is self-reporting workplace activity worthwhile? Validity and reliability of occupational sitting and physical activity questionnaire in desk-based workers," *BMC Public Health*, vol. 16, 2016.
- [106] C. L. Edwardson *et al.*, "A three arm cluster randomised controlled trial to test the effectiveness and cost- effectiveness of the SMART Work & Life intervention for reducing daily sitting time in office workers: study protocol," *BMC Public Health*, vol. 18, no. 1, pp. 1–13, 2018.
- [107] D. L. Scher, P. J. Belmont, R. Bear, S. B. Mountcastle, J. D. Orr, and B. D. Owens, "The Incidence of Plantar Fasciitis in the United States Military," *J. Bone Jt. Surg.*, vol. 91, no. 12, pp. 2867–2872, 2009.
- [108] K. Messing and K. Cinbiose, "Standing and very slow walking: foot pain-pressure threshold, subjective pain experience and work activity," 2001.
- [109] D. W. Hosmer, S. Lemeshow, and R. X. Sturdivant, *Applied Logistic Regression*, no. 3. Wiley, 2013.

Appendix A.

Standard Trial Procedure

Trial Procedure and Script

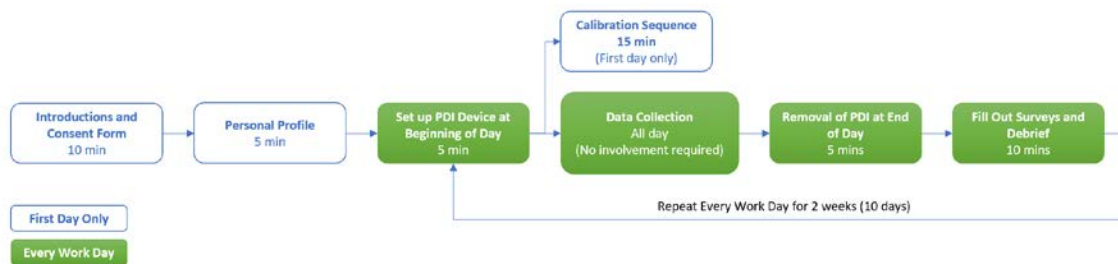
Refinement and Deployment of a Low-Cost Device to Classify Human Workplace Activities from Foot Pressure Measures

School of Mechatronic Systems Engineering
250-13450 102 Avenue, Surrey, BC, V3T 0A3

This work is funded by the Natural Sciences and Engineering Research Council (NSERC) through a Canadian Graduate Scholarships-Master's Program scholarship titled "*Development of an algorithm to accurately interpret signals from an instrumented insole to determine if a wearer is sitting, walking or standing.*" and by WorkSafeBC through grant number: WCB RS2017-IG17 titled "*Feet First: Instrumented Insoles to Examine Workplace Injury Risk.*"

Introduction

- Introduce yourself as an investigator in this study
- Explain the study purpose and rationale to the participant
- Introduce the participant to the Posture Differentiating Insole (PDI) and briefly explain how it works.
- Describe and demonstrate the procedure to be performed. (Figure below may be helpful)



- Outline the risks and benefits of the study.
- Explain how the data collected will be used, stored, shared, and destroyed
- Explain that their participation is voluntary and that they can withdraw their consent at any time without reason. They can also ask to withdraw their data from the study at any time.

Consent Forms

- Ask if they have read the Participant Information and Consent Form, if not have them read it.
- Ask if there are any questions and answer them to the best of your ability
- Ask them to thoroughly read the consent pages and if they agree, sign and date each page. Do not proceed until this is completed.
- Record the participant's unique ID number on their consent form and store it in a safe location to be immediately locked in Dr. Sparrey's office once back at SFU.

Equip Participant with the PDI

- Ask the participant to remove their shoes and take the insoles out of them if possible.
- Attach the PDI to the shoelaces using the clip.
- Insert the insole into the shoe.
- Repeat for the opposite shoe.
- Get participant to put the shoes back on and make sure that the cables etc. are sitting neatly and won't get caught on anything.
- Adjust shoelaces if necessary, to ensure the shoes are comfortable for the participant.
- Outline the potential risks of the device, particularly the battery and explain what signs the participant should look for if they believe that something isn't working correctly.
- Inform participant that the device should blink once every ~15 seconds when functioning correctly.

- Instruct the participant to immediately remove their shoe with the device on it and to call a study administrator should the device malfunction or if they have any hesitation whatsoever.
- Show the participant how to remove the device from their shoes if they need to do so throughout the day and let them know that this is okay to do if any situation should arise where they need to remove the devices.

Personal Profile

- The personal profile form is to be filled out as part of the video calibration sequence but is to be introduced prior to the sequence beginning.
- At the start of the video calibration sequence give the participant the personal profile form and introduce it as a form intended to gather personal health metrics relevant to the study and state that it will not be directly identifying.
- Note that if they feel uncomfortable or do not wish to disclose any information they are not required to do so.
- Once completed, store the form in a safe location (not in the same file as the consent form) to be immediately locked in a cabinet in the NeuroSpine lab once back at SFU.

Video Calibration Sequence

- If the participant has consented to be video recorded, ask participant if they have approximately 20 minutes to participate in the calibration sequence right away or if they would like to schedule a better time for it. (it should be completed before the end of the trial, ideally earlier on to avoid any device malfunction issues)
 - o If they cannot complete this step right now, skip to 'Data Collection Period'
 - o Note that if they would prefer they can come to our lab in Surrey or ICORD to complete this step.
- Begin by identifying a place with approximately 10m of space to walk in a straight line back and forth along with a chair and a desk or counter.
 - o Note that this area should be away from any sensitive work material or personnel so that you will not accidentally capture them on video.
- Set up the video camera in a location that will only record the participant's lower body but will still record the entire sequence involving sitting in the chair, standing and walking back and forth. Arrange the area so that the desk or counter can be reached from the chair and from a standing position near the chair with the 10m walkway starting at the chair.
 - o Note that you need to video the light on the PDI when the device turns on which may require you to temporarily move the video camera.
- Inform the participant of the procedure listed below
- Follow the procedure listed below

Procedure:

1. Turn on the video camera
2. Turn on each device (be sure to capture the light on video as each device turns on)
3. Prompt the participants to do the following activities in this order:

- a. Sit - approximately 1 minute
 - b. Stand - approximately 1 minute
 - c. Walk - approximately 1 minute (walk back and forth in area at least 10m long)
 - d. Stand - approximately 1 minute
 - e. Sit - approximately 1 minute
 - f. Walk - approximately 1 minute
 - g. Sit - approximately 1 minute
 - h. Stand with most of weight on one foot – approximately 30 seconds
 - i. Stand with most of weight on other foot – approximately 30 seconds
 - j. Walk to a counter or table
 - k. Fill out the participant information form at a table or counter while standing (distracted standing) – approximately 8-12 minutes
 - l. Walk back to chair
 - m. Sit with feet outstretched - approximately 1 minute
 - n. Sit with feet tucked under chair - approximately 1 minute
 - o. Sit while fidgeting feet, tapping toes etc. - approximately 30 seconds
 - p. Sit in their favourite position - approximately 30 seconds
- Once the above procedure is complete, turn off the video camera.
 - Turn the devices off so that the calibration sequence is captured on its own file.
 - Once they have completed the video calibration sequence ask the participant if it is okay to examine and take pictures of their feet to determine their Foot Posture Index (FPI). This involves taking off their shoes and socks and standing on a hard surface.
 - If they agree determine their FPI and record it on the Personal Profile form along with their participant ID.
 - If the participant agrees, take pictures of the back, back left, back right, front, front left, and front right (6 total pictures)
 - If the participant agrees, take pictures of their shoes. A picture of the soles and a picture of them in normal sitting position (2 total pictures)

Data Collection Period

- Turn the devices on.
- Instruct the participant to go about their normal workday, trying to pay as little attention to the devices as possible.
- Remind them that should there be any issues to please call a study administrator and make sure that they have your contact information.
- Set up a time to return to their place of work and remove the device at the end of the day.

Removal of PDI System and Questionnaires

- Return to the participants place of work at the agreed upon time.
- Ask the participant to remove their shoes.
- Turn the PDI off to finish recording for the day and remove it from the shoes, replacing the original insoles.

- Alternatively, if the participant does not need the shoes for the remainder of the evening the device can remain installed on the shoes. Just remove the battery to be charged.
- Take the device with you to be charged overnight.
- Ask the participant to complete the following three forms
 - EQ5D
 - FADI
 - End-of-Day Questionnaire
- Ask if the participant has any questions or concerns and answer them to the best of your ability.
- Set up a time to meet the participant the following morning.

Each Additional Day

- Meet the participant at the agreed upon time in the morning.
- Install the device into each shoe (or if just the battery was removed install the charged battery)
- Follow the steps outlined in 'Data Collection Period'
- Set up a time to return at the end of the day
- Return at the end of the day and follow the steps in 'Removal of PDI System and Questionnaire'
- Repeat for one week.

Final Debriefing

- If this is the last day of the trial, finish removing the devices ensuring that all parts are taken with you.
- Give the participant the \$100 reimbursement for their participation in the trial, ensuring that they sign a receipt saying that you gave them the reimbursement.
- Ask the participant if they have any outstanding questions and ensure that they have your contact information should they need to get a hold of you in the future.
- Explain that once results are available they can contact you to get results from the study.
- Thank them for their time and effort.

Appendix B.

Insole Fabrication Procedure

Device Fabrication Procedure

Refinement and Deployment of a Low-Cost Device to Classify Human Workplace Activities from Foot Pressure Measures

School of Mechatronic Systems Engineering
250-13450 102 Avenue, Surrey, BC, V3T 0A3

This work is funded by the Natural Sciences and Engineering Research Council (NSERC) through a Canadian Graduate Scholarships-Master's Program scholarship titled "*Development of an algorithm to accurately interpret signals from an instrumented insole to determine if a wearer is sitting, walking or standing.*" and by WorkSafeBC through grant number: WCB RS2017-IG17 titled "*Feet First: Instrumented Insoles to Examine Workplace Injury Risk.*"

Required Parts (per insole):

- Teensy 3.6 (Qty. 1)
- 16GB (minimum) microSD memory card (Qty. 1)
- Adafruit MMA8451 3-axis accelerometer (Qty. 1)
- CR1220 coin cell battery (Qty. 1)
- Coin cell battery holder (Qty. 1)
- Adafruit JST 2-PH battery connector w/ switch (Qty. 1)
- LP-503562 1200mAh Li-ion rechargeable battery
- 1 k Ω resistor (Qty. 1)
- Interlink FSR 402 Short (Qty. 7)
- 8-wire bus cable (~30cm)
- 26-gauge hookup wire (lots)
- Solid core wire (lots)
- 1mm diameter heat shrink cable wrap (lots)
- 3mm EVA55 foam (order from Kintec)
- 1.5mm puff foam (order from Kintec)

Required Tools:

- Soldering iron (and solder)
- Heat gun
- Tweezers
- Wire cutters
- Laser cutter (ideally)
- Hot glue gun

Procedure:

The Posture Differentiating Insole (PDI) is made up of two components, the insole and the electronics case. The instructions below outline the procedure for making these two components and assembling them together.

Electronics Case (orange box):

Using the solid core wire, solder the accelerometer, coin cell battery holder, battery connector / switch, and resistor together in the arrangement shown in the wiring diagram in Figure 1 below.

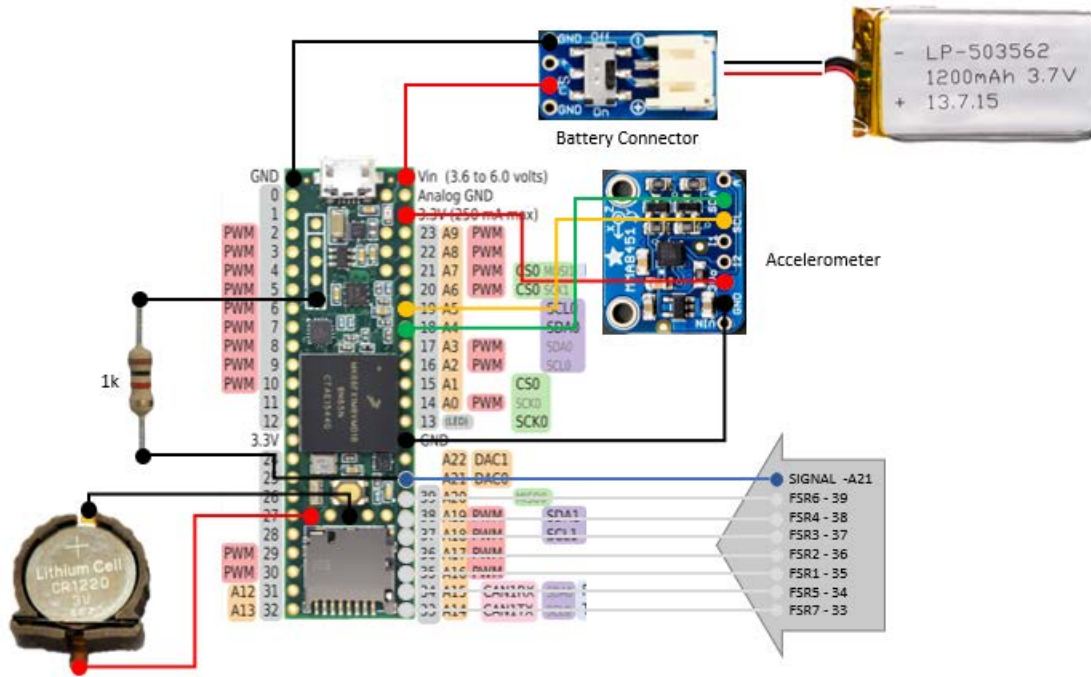


Figure 1 - Wiring Diagram for electronics case

Completed assembly can be seen in Figure 2 and Figure 3 below. Note the grey cable with 8 strands connected to the Teensy comes from the insole component that will be described in a later section.



Figure 2 - Top view of electronics case completed assembly



Figure 3 - Bottom view of electronics case completed assembly. Note the resistor is in the black heat shrink wrap to prevent accidental contact with other components

Once electronics are assembled, use the SLT, Solidworks or 3D printer files to produce a 3D printed case for the electronics. The completed case will have three parts, the case, the lid and the shoelace clip. These should look like the parts seen in Figure 4 below.



Case

Lid

Shoelace Clip

Figure 4 - 3D Printed case components

Begin assembly of the completed electronics case by inserting the li-ion battery into the case, sliding it underneath the two tabs on the right in Figure 5 (A). Next, attach the battery to the connector and insert the electronics assembly, slotting the Teensy into the four tabs on the left in Figure 5 (B), aligning them with the micro-USB port on the Teensy. The cables for the insole will fit into the slot in the case. Next align the case lid so the screw holes line up with the case and the hooks align on the left. Screw the case together using two small screws producing the final assembly seen in figure 5 (C). The shoelace connector fits onto the rounded tabs on either side of the case and is threaded through the shoelaces before attaching to the case.

Insole:

Assembly of the insole begins with cutting the insole foam into the correct shape and size. The insole foam consists of two layers, the lower white EVA foam layer with channels cut out of it to embed the wires in, and the black puff foam cover. There are Solidworks files of the white foam



Figure 5 - Electronics case assembly

for many common shoe sizes that can be used with a laser cutter to engrave the channels into the white EVA foam. You will need to play with the settings of the laser cutter to get the right depth of the channels to allow the wires to sit perfectly flush within the foam. Once you have the two pieces of foam cut, follow the below procedure to add the FSRs into the insoles.

1. If the depth of the foam is not quite correct, use box-nose cutters to cut out more foam where necessary.



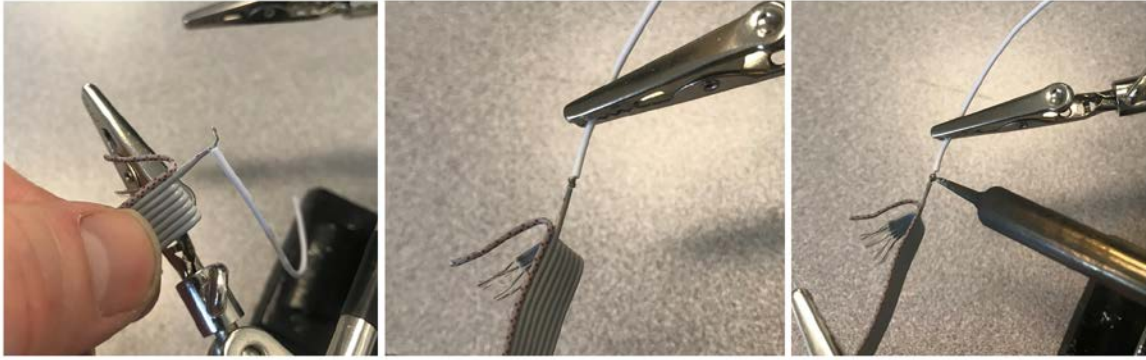
2. The foam should look something like this before you start adding wires to it.



3. Cut a ~30cm length of bus cable with 8 strands of wire.
4. Strip 7 of the wires on one end of it to look like this. Note that the wire on one side has been left longer than the others and has not yet been stripped.



5. Measure out and cut an appropriate length of layup wire to reach the FSR (if in doubt make it long) and strip one end. This will be the signal wire going to the FSR.
6. Twist the piece of layup wire together with the first strand from the bus cable, wrapping into a tight bundle, and solder together using a small solder bead (make sure it is not large or the shrink wrap will not fit).



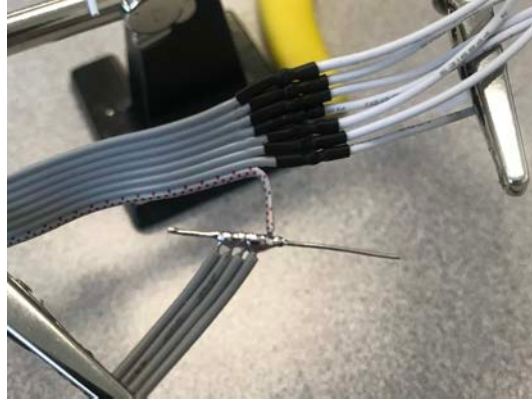
7. Cut a piece of heat shrink and slide over the soldered joint.
8. Repeat steps 5-7 for each of the remaining 6 bus cable wires.
9. Once all 7 wires have been soldered on, use a heat gut to shrink all the heat shrink pieces and strengthen the joints.



10. Next, you will create the analog receiver connection header. This gathers signal information from whichever FSR is activated and transmits it to the Teensy.
11. Cut four wires of the appropriate length (again, longer is better) and wrap them around a piece of stripped solid core wire and solder together.



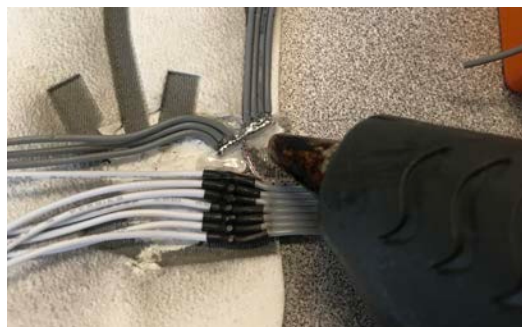
12. Next, attach the one wire that was left out of the bus cable. Be careful and solder this connection well, if this wire disconnects or breaks, none of the FSRs will work. It is important to leave some slack in this cable when attaching it to the insole to remove stress from bending etc.



13. Attach three more layup wires to the stripped solid core wire for a total of 7 wires in the arrangement seen below. Trim the ends to form a neat soldered connection.



14. Using hot glue, attach the wires to the foam insole at the location shown below. The soldered connection just created in steps 10-13 can be glued down to the insole at this point but leave the other wires free to adjust.

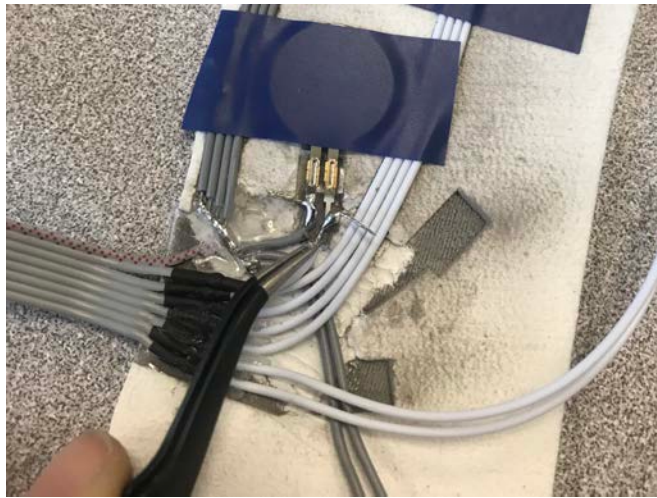


15. Tape the first FSR in place and trim and strip the layup wires to fit. There should be one wire coming from the bus cable to the FSR and then one wire returning to the analog

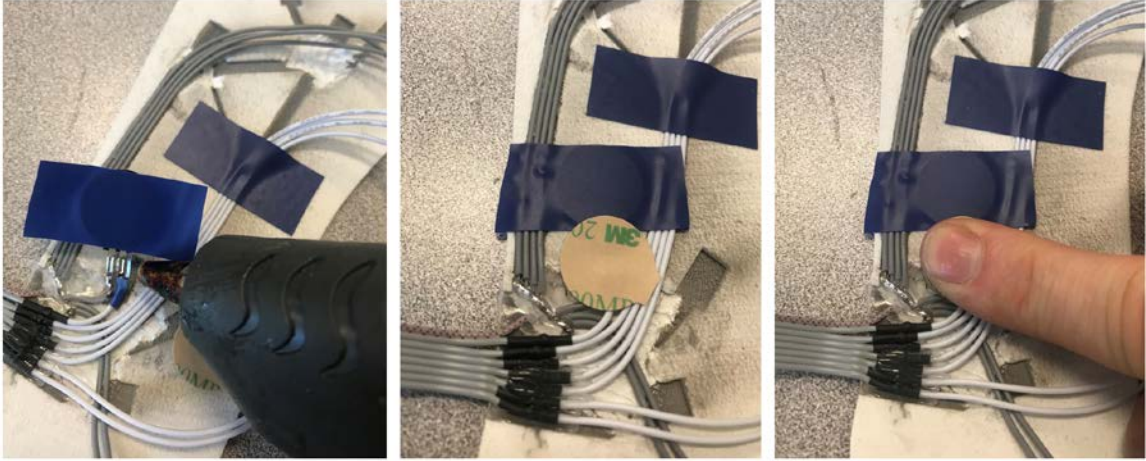
receiver connection for each FSR. Once the wires are stripped, it is easiest to twist the ends of each wire, bend a 90 degree kink in the twisted wire, then add a bead of solder to the end of the wire (seen in the image below). When doing this ensure to cover the FSRs with a piece of cardboard as pieces of solder can spray and damage the FSRs.



16. Next, use a pair of tweezers to hold the wire with a solder bead on it on top of the FSR connection while re-heating it with a soldering iron to connect the wire to the FSR connection.



17. Trim the wires and put a small piece of electrical tape around one of the connections to ensure they don't ever touch.
18. Remove sticker backing from the back of the FSR and place a dollop of hot glue under the wire connections. Place the FSR down and use a piece of parchment paper or the backing of an FSR sticker to flatten the hot glue to the insole while it is still hot. Caution this may burn your finger, timing is critical, wait until the glue has cooled enough that it won't burn your finger but not too long that you won't be able to flatten it.



19. The result should look like this:



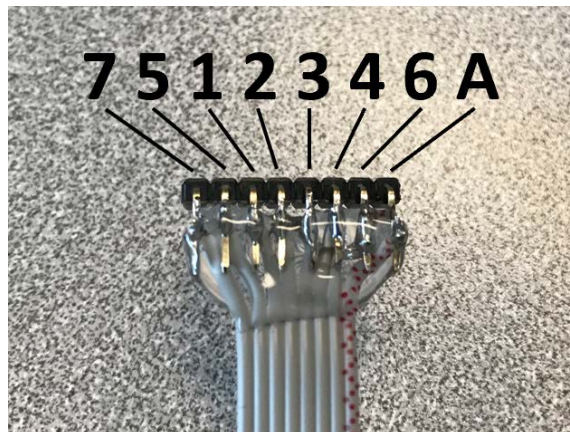
20. Repeat steps 15-18 for each of the 7 FSRs



21. Finally, glue all the wires into the cut-out channels and fill any areas where wires cross to make as close to a flat surface as possible. The result should look something like this.



22. Solder the other end of the bus cable to a 90-degree connector. Cover in hot glue to strengthen the connection. The FSR numbers are shown on the image below, assuming the same wire routing is used as in the image above.



23. Solder the 90-degree connector to the Teensy as seen in Figure 2.

24. Once you have tested that the device works correctly, use hot glue or rubber cement to attach the puff foam top sheet to the EVA foam to complete the PDI.

Once you finish this procedure, the device hardware will be complete. You will still need to program the Teensy using the appropriate data collection software ensuring that data is collecting properly and saving to the microSD card. Note that you will need to modify the code slightly for each participant to update their ID number. For details see the code description.

Appendix C.

PDI Code

```

1 /*NOTES:
2 *
3 * This code is to run the PDI
4 * Gathers data from the single 3-axis accelerometer and 7 FSRs
5 * Saves data to the built-in SD card in specific binary format
6 * Update subname below for each specific subject ID
7 *
8 */
9
10 #include <TimeLib.h>
11 #include "SdFat.h"
12 #include <SPI.h>
13 #include <Wire.h>
14 #include <Adafruit_MMA8451.h>
15 #include <Adafruit_Sensor.h>
16
17
18 //Declare accelerometer
19 Adafruit_MMA8451 mma = Adafruit_MMA8451();
20
21 //Declare the digital pins used to power the FSRs
22 const int FSR6 = 39; // 5VDC input pin number to FSR
23 const int FSR4 = 38;
24 const int FSR3 = 37;
25 const int FSR2 = 36;
26 const int FSR1 = 35;
27 const int FSR5 = 34;
28 const int FSR7 = 33;
29
30 //Declare the analog pin used to read output from an FSR
31 const int AnalogIn = A21; // Analog read pin
32
33 // Pin with LED which flashes whenever data is written to card, and does a
34 // slow blink when recording has stopped or if the device checks have not passed.
35 const int LED_PIN = 13; //built-in LED
36
37 // 16 KiB buffer.
38 const size_t BUF_DIM = 16384;
39
40 // Sampling rate
41 const uint32_t sampleIntervalMicros = 22000;
42 // 22000 us interval = approx. 45.45 Hz
43
44 // Use total of four buffer blocks.
45 const uint8_t BUFFER_BLOCK_COUNT = 4;
46
47 // Number of FSR data points per record (if you change this you need to change
48 // acquireData() to incorporate new values)
49 const uint8_t FSR_DIM = 7;
50
51 // Number of Accelerometer inputs per record (if you change this you need to change
52 // acquireData() to incorporate new values)
53 const uint8_t ACC_DIM = 3;

```

```

52
53 // Format for one data record
54 // note: should be in increments of 4 bytes since teensy stores data in 4 byte
increments.
55 struct data_t {
56 uint32_t timer; //4 bytes
57 float fsr[FSR_DIM]; //4*FSR_DIM bytes
58 float acc[ACC_DIM]; //4*ACC_DIM bytes
59 }; // total of 44 bytes per sample
60
61 // SD card declarations
62 SdFatSdio sd;
63 File file;
64
65 // Number of data records in a block.
66 const uint16_t DATA_DIM = (BUF_DIM-4)/sizeof(data_t);
67
68 // Compute number of filler bytes to insert at end of block so block size is BUF_DIM
bytes.
69 // FILL_DIM may be zero depending on number of sample bytes.
70 const uint16_t FILL_DIM = (BUF_DIM-3) - (DATA_DIM*sizeof(data_t));
71
72 // Format for one block of data
73 struct block_t {
74 data_t data[DATA_DIM];
75 byte filler[FILL_DIM]; //1 byte per FILL_DIM
76 };
77
78 // Initialize variables
79 uint16_t count = 0;
80 uint32_t nextSampleMicros = 0;
81 bool collectingData = false;
82 bool isSampling = false;
83
84 // Intialize all buffers
85 block_t block[BUFFER_BLOCK_COUNT];
86 block_t* curBlock;
87 block_t* emptyStack[BUFFER_BLOCK_COUNT];
88 uint8_t emptyTop;
89 block_t* fullQueue[BUFFER_BLOCK_COUNT];
90 uint8_t fullHead = 0;
91 uint8_t fullTail = 0;
92
93 // Variables for making a file name
94 String SubName = "L6"; //format L#
95 String DD, MM, YYYY, hh, mm, ss, fileName, SfileName;
96 char CFileName[9];
97
98 // -----
99 // Setup to setup file name, buffers, accelerometer etc.
100 void setup() {
101 pinMode(LED_PIN, OUTPUT);
102 digitalWrite(LED_PIN, HIGH);

```



```

103
104 // get date and time. if/else statemnt are to account for leading 0's that I want to
    be in file name.
105 time_t t = Teensy3Clock.get(); //time from RTC
106
107 YYYY =String(year(t));
108 if (month(t)<10){
109 MM = "0" + String(month(t));
110 }
111 else{
112 MM = String(month(t));
113 }
114 if (day(t)<10){
115 DD = "0" + String(day(t));
116 }
117 else{
118 DD = String(day(t));
119 }
120 if (hour(t)<10){
121 hh = "0" + String(hour(t));
122 }
123 else{
124 hh = String(hour(t));
125 }
126 if (minute(t)<10){
127 mm = "0" + String(minute(t));
128 }
129 else{
130 mm = String(minute(t));
131 }
132 if (second(t)<10){
133 ss = "0" + String(second(t));
134 }
135 else{
136 ss = String(second(t));
137 }
138
139 //Make file name with date and subjects initials
140 fileName = YYYY + MM + DD + "_" + hh + mm + "_" + SubName + "." + "t" + "x" + "t";
141 SfileName = DD + hh + mm + SubName + ".bin"; // short file name for name of file to
    match DOS 8.3 filename requirements
142 SfileName.toCharArray(CFileName,13); // casting file name to a char string to write
    to file name
143
144 // Put all the buffers on the empty stack.
145 for (int i = 0; i < BUFFER_BLOCK_COUNT; i++) {
146 emptyStack[i] = &block[i];
147 }
148 emptyTop = BUFFER_BLOCK_COUNT;
149
150 // Initialize accelerometer
151 if (! mma.begin()) {
152 error("accelerometer failed");

```

```

153 }
154 // Set range of accelerometer
155 mma.setRange(MMA8451_RANGE_8_G); //can be _2_G or _4_G or _8_G
156
157 if(!sd.begin()){
158 error("error with sd.begin()");
159 }
160 if (!file.open(CFileName, O_RDWR | O_CREAT | O_APPEND)) {
161 error("open failed");
162 }
163 file.close();
164
165 delay(100);
166 collectingData=true;
167 nextSampleMicros = micros(); //begin sampling right now
168
169 // Turn off light just as data begins to sample
170 // This co-ordinates the video data with the PDI data
171 digitalWrite(LED_PIN, LOW);
172 }
173
174 //-----
175 // Main loop to gather data
176 void loop() {
177 // if there is no data to write to the SD card, collect more data
178 if (fullHead == fullTail) { // full queue is empty
179 yield();// acquire data etc.
180
181 }else {
182 // There is at least one full block to write to SD
183 // Write buffer at the tail of the full queue to the SD card
184 // and return it to the top of the empty stack.
185
186 // Flash LED when data is being written
187 digitalWrite(LED_PIN, HIGH);
188
189 block_t* pBlock = fullQueue[fullTail];
190 fullTail = fullTail < (BUFFER_BLOCK_COUNT-1) ? fullTail + 1 : 0;
191
192 file.open(CFileName, O_WRITE | O_APPEND);
193 file.write(pBlock, BUF_DIM);
194 file.close();
195
196 emptyStack[emptyTop++] = pBlock; //returns block written to SD to top of emptystack
for re-use
197 digitalWrite(LED_PIN, LOW);
198 }
199 }
200
201 //-----
202 // This does the data collection. It is called whenever the teensy is not
203 // doing something else. The SdFat library will call this when it is waiting
204 // for the SD card to do its thing, and the loop() function will call this

```

```

205 // when there is nothing to be written to the SD card (most of the time).
206 void yield(){
207
208 if (!collectingData || isSampling) //disable yield() while sampling data so no
duplicate data is gathered.
209 return;
210
211 isSampling = true;
212
213 // If we don't have a buffer for data, get one from the top of the empty stack.
214 if (curBlock == 0) {
215 curBlock = getEmptyBlock();
216 }
217
218 // If it's time, record one data sample.
219 if (micros() >= nextSampleMicros) {
220 acquireData(&curBlock->data[count++]);
221 nextSampleMicros += sampleIntervalMicros;
222 }
223 if (nextSampleMicros > 4294967295){
224 nextSampleMicros = nextSampleMicros-4294967295; //resets nextSampleMicros so that
when micros() resets data will still record
225 }
226
227 // If the current buffer is full, move it to the head of the full queue. We will get
a new buffer at the beginning of the next yield() call.
228 if (count == DATA_DIM) {
229 fullQueue[fullHead] = curBlock;
230 fullHead = fullHead < (BUFFER_BLOCK_COUNT-1) ? fullHead + 1 : 0; // says
if(fillHead<BUFFER_BLOCK_COUNT) then fullHead=fullHead+1 else fullHead=0
231 curBlock = 0;
232 }
233
234 isSampling = false;
235 }
236
237 //-----
238 //Gets a block from the top of the empty stack and returns it
239 block_t* getEmptyBlock() {
240 block_t* blk;
241 if (emptyTop > 0) { // if there is a buffer in the empty stack
242 blk = emptyStack[--emptyTop]; //emptyStack is already a pointer, so assigning to
blk makes blk a pointer
243 count = 0;
244 } else { // no buffers in empty stack
245 error("All buffers in use");
246 }
247 return blk;
248 }
249
250 //-----
251 //Format for acquiring data and placing it in the data_t struct
252 void acquireData(data_t* data){

```

```

253
254 data->timer = micros();
255 data->fsr[0] = sweepFSR(1);
256 data->fsr[1] = sweepFSR(2);
257 data->fsr[2] = sweepFSR(3);
258 data->fsr[3] = sweepFSR(4);
259 data->fsr[4] = sweepFSR(5);
260 data->fsr[5] = sweepFSR(6);
261 data->fsr[6] = sweepFSR(7);
262
263 data->acc[0] = getAcceleration(1);
264 data->acc[1] = getAcceleration(2);
265 data->acc[2] = getAcceleration(3);
266 }
267
268 //-----
269 //Function that returns the current analog output from a particular FSR
270 //input is integer value of FSR to sample from.
271 float sweepFSR(int FSRnum){
272
273 float sensor = 999.0;
274 switch (FSRnum) {
275 case 1:
276 allFloat();
277 pinMode(FSR1, OUTPUT);
278 digitalWrite(FSR1, HIGH);
279 sensor = analogRead(AnalogIn);
280 break;
281
282 case 2:
283 allFloat();
284 pinMode(FSR2, OUTPUT);
285 digitalWrite(FSR2, HIGH);
286 sensor = analogRead(AnalogIn);
287 break;
288
289 case 3:
290 allFloat();
291 pinMode(FSR3, OUTPUT);
292 digitalWrite(FSR3, HIGH);
293 sensor = analogRead(AnalogIn);
294 break;
295
296 case 4:
297 allFloat();
298 pinMode(FSR4, OUTPUT);
299 digitalWrite(FSR4, HIGH);
300 sensor = analogRead(AnalogIn);
301 break;
302
303 case 5:
304 allFloat();
305 pinMode(FSR5, OUTPUT);

```

```

306 digitalWrite(FSR5, HIGH);
307 sensor = analogRead(AnalogIn);
308 break;
309
310 case 6:
311 allFloat();
312 pinMode(FSR6, OUTPUT);
313 digitalWrite(FSR6, HIGH);
314 sensor = analogRead(AnalogIn);
315 break;
316
317 case 7:
318 allFloat();
319 pinMode(FSR7, OUTPUT);
320 digitalWrite(FSR7, HIGH);
321 sensor = analogRead(AnalogIn);
322 break;
323
324 default:
325 allFloat();
326 }
327
328 // Want 1 to be the lowest value.
329 // This removes noise that happens between 0 and 1
330 if (sensor == 0){
331 sensor = 1.0;
332 }
333 return sensor;
334 }
335
336 //-----
337 //sets all FSR pins to float so there is no interference when sampling
338 void allFloat (){
339
340 digitalWrite(FSR1, LOW);
341 digitalWrite(FSR2, LOW);
342 digitalWrite(FSR3, LOW);
343 digitalWrite(FSR4, LOW);
344 digitalWrite(FSR5, LOW);
345 digitalWrite(FSR6, LOW);
346 digitalWrite(FSR7, LOW);
347
348 pinMode(FSR1, INPUT);
349 pinMode(FSR2, INPUT);
350 pinMode(FSR3, INPUT);
351 pinMode(FSR4, INPUT);
352 pinMode(FSR5, INPUT);
353 pinMode(FSR6, INPUT);
354 pinMode(FSR7, INPUT);
355
356 return;
357 }
358

```

```

359 //-----
360 //Function that gets the acceleration of an axis depending on the integer value passed
to it
361 // X = 1
362 // Y = 2
363 // Z = 3
364 float getAcceleration(int accNum){
365
366 // Read the 'raw' data in 14-bit counts
367 mma.read();
368
369 /* Get a new sensor event */
370 sensors_event_t event;
371 mma.getEvent(&event);
372
373 float acc = 99.99;
374
375 switch (accNum) {
376 case 1:
377 acc = event.acceleration.x;
378 break;
379
380 case 2:
381 acc = event.acceleration.y;
382 break;
383
384 case 3:
385 acc = event.acceleration.z;
386 break;
387 }
388
389 //dont want any zero values to make data processing easier.
390 if(acc == 0){
391 acc = 0.01;
392 }
393
394 return acc;
395 }
396
397 //-----
398 //not currently using the string capability of this, but if debugging can turn
399 //on Serial and this will print an error code produced from wherever you call error
400 void error(String msg) {
401 blinkForever();
402 }
403
404 //-----
405 //blinks light in a neverending loop
406 void blinkForever() {
407 while (1) {
408 digitalWrite(LED_PIN, HIGH);
409 delay(1000);
410 digitalWrite(LED_PIN, LOW);

```

```
411 delay(1000);  
412 }  
413 }
```

Appendix D.

FADI Form

Please answer every question with one response that most closely describes your condition within the past week by placing an X in the appropriate box. If the activity in question is limited by something other than your foot or ankle, mark N/A

	No difficulty at all	Slight difficulty	Moderate difficulty	Extreme difficulty	Unable to do
1. Standing					
2. Walking on even ground					
3. Walking on even ground without shoes					
4. Walking up hills					
5. Walking down hills					
6. Going up stairs					
7. Going down stairs					
8. Walking on uneven ground					
9. Stepping up and down curves					
10. Squatting					
11. Sleeping					
12. Coming up to your toes					
13. Walking initially					
14. Walking 5 minutes or less					
15. Walking approximately 10 minutes					
16. Walking 15 minutes or longer					
17. Home responsibilities					
18. Activities of daily living					
19. Personal care					
20. Light to moderate work (standing, walking)					
21. Heavy work (push/pulling, climbing, carrying)					
22. Recreational activities					
	No pain	Mild	Moderate	Severe	Unbearable
23. General level of pain					
24. Pain at rest					
25. Pain during your normal activity					
26. Pain first thing in the morning					

Administrator Use Only: Score: ____/104 points

Reference for Score: Martin, R. L., Burdett, R. G., Irrgang, J. J. (1999). Development of the Foot and Ankle Disability Index (FADI). J Orthop Sports Phys Ther. 1999; 29: A32-33

Version 1—July 23rd, 2018
Study Number: 2018s0321

Appendix E.

Participant Questionnaire

The following profile collects personal health information along with selected information about your background as it is relevant to the study. Please fill out the following to the best of your abilities. If you have any questions, please consult the test administrator. If you are not comfortable answering a question, please leave it blank.

Age (years): _____ Weight (lbs): _____ Height: _____(ft) _____(in)

Gender: M F Other

Dominant Foot: R L

Shoe Size: _____

--HEALTH INFO--

Have you had foot or ankle pain in the last 12 months that has caused you to modify your activities in any way? If so on the image provided below, please indicate the areas where you have felt pain.



Images taken from http://lookfordiagnosis.com/mesh_info.php?term=foot&lang=1 (Left) and <http://oppositelock.kinja.com/feet-the-oppo-review-1665703006> (Right)

--OCCUPATIONAL INFO--

Occupation: _____

Choose the type of floor that best describes your *primary* work environment (i.e. the place you spend the most time during an average work day):

- | | | |
|-----------------------------------|---------------------------------|---------------------------------------|
| <input type="checkbox"/> Wood | <input type="checkbox"/> Tile | <input type="checkbox"/> Sand |
| <input type="checkbox"/> Concrete | <input type="checkbox"/> Brick | <input type="checkbox"/> Grass |
| <input type="checkbox"/> Laminate | <input type="checkbox"/> Carpet | <input type="checkbox"/> Other: _____ |

For an average workday, approximately how long (in hours) do you spend in each of the following postures: (Note: the times should add up to the total length of your typical work day)

Sitting	Standing	Walking	Other (please indicate)

Do you constantly maintain one posture while at work for most of the time? Or do you frequently switch postures (ie. Several times an hour)? Please Describe.

Is there any additional information that you would like to provide that you feel would be relevant to this study regarding your occupational demands/circumstances?

You have completed the survey. Please inform your test administrator. We thank you for your participation.

The following section is to be completed by the study investigator.

Foot Posture Index (FPI): _____